
Theses and Dissertations

Summer 2010

Studies of proliferating cell nuclear antigen and its role in translesion synthesis

Bret D. Freudenthal
University of Iowa

Copyright 2010 Bret D Freudenthal

This dissertation is available at Iowa Research Online: <http://ir.uiowa.edu/etd/668>

Recommended Citation

Freudenthal, Bret D.. "Studies of proliferating cell nuclear antigen and its role in translesion synthesis." PhD (Doctor of Philosophy) thesis, University of Iowa, 2010.
<http://ir.uiowa.edu/etd/668>.

Follow this and additional works at: <http://ir.uiowa.edu/etd>



Part of the [Biochemistry Commons](#)

**STUDIES OF PROLIFERATING CELL NUCLEAR ANTIGEN AND ITS ROLE
IN TRANSLESION SYNTHESIS**

by

Bret D. Freudenthal

An Abstract

Of a thesis submitted in partial fulfillment of the requirements for the Doctor of
Philosophy degree in Biochemistry in the Graduate College of
The University of Iowa

July 2010

Thesis Supervisor: Associate Professor M. Todd Washington

ABSTRACT

DNA damage on the template strand blocks replication by classical DNA polymerases. One major pathway to overcome these replication blocks is translesion synthesis, which is the replicative bypass of DNA damage by non-classical polymerases. For the cell to utilize translesion synthesis, the non-classical DNA polymerase must be recruited to sites of DNA damage and a polymerase switch must occur between the stalled classical polymerase and the incoming non-classical polymerase. This switching event is believed to be mediated by the replication accessory factor proliferating cell nuclear antigen (PCNA). *In vivo* studies have shown that interactions between PCNA and the non-classical polymerase are required for translesion synthesis. However the regions of PCNA important for the protein-protein interactions between the non-classical polymerase and PCNA are largely unknown. Moreover, in response to DNA damage PCNA is monoubiquitinated at Lys-164. This monoubiquitinated form of PCNA (Ub-PCNA) is required for translesion synthesis. However, the function of monoubiquitinated PCNA in translesion synthesis remains unknown. This is partly because of the difficulty in obtaining sufficient quantities of monoubiquitinated PCNA for biochemical and biophysical studies.

To better understand the role of PCNA during translesion synthesis, I biochemically and structurally characterized two PCNA mutant proteins that are deficient in translesion synthesis: the G178S and E113G PCNA mutant proteins. The structures of both mutant proteins were determined crystallographically and revealed that an extended loop, called loop J, has shifted its position relative to that in the wild type PCNA structure. Steady-state kinetic studies showed that, in contrast to wild type PCNA, which stimulates the non-classical polymerases, the two PCNA mutant proteins failed to stimulate the activity of the non-classical polymerase pol η . These results indicate that loop J in PCNA plays an essential role in facilitating translesion synthesis.

During the structural studies of the E113G PCNA mutant protein, I observed a unique PCNA structure that failed to form the characteristic PCNA ring shaped structure, through traditional intersubunit interactions of domain A and domain B on neighboring subunits. Instead this non-trimeric PCNA structure formed A-A and B-B intersubunit interactions. The B-B interface is structurally similar to the A-B interface observed for the trimeric ring shaped form. In contrast, the A-A interface is stabilized by hydrophobic interactions. The location of the E113G substitution is directly within this hydrophobic surface and would not be favorable in the wild type protein. This suggests that the side chain of Glu-113 promotes trimer formation by destabilizing these possible alternate subunit interactions.

To better understand the role of Ub-PCNA during translesion synthesis, I developed an Ub-PCNA analog by splitting the protein into two self-assembling polypeptides. This analog supports cell growth and translesion synthesis *in vivo*. Steady state kinetics studies showed that the Ub-PCNA analog stimulates the catalytic activity of pol η *in vitro*. The X-ray crystal structure of this Ub-PCNA analog showed that the ubiquitin moieties are located on the back face of PCNA and interact with it via their canonical hydrophobic surface. Surprisingly, the attachment of ubiquitin does not change the conformation of PCNA. This implies that ubiquitination does not cause an allosteric change in PCNA, and instead facilitates non-classical polymerase recruitment to the back of PCNA by forming a new binding surface for the non-classical polymerases. This is consistent with a “tool belt” model of DNA polymerase exchange, whereby both classical and non-classical polymerases bind to Ub-PCNA simultaneously.

Abstract Approved: _____
Thesis Supervisor

Title and Department

Date

**STUDIES OF PROLIFERATING CELL NUCLEAR ANTIGEN AND ITS ROLE
IN TRANSLESION SYNTHESIS**

by

Bret D. Freudenthal

A thesis submitted in partial fulfillment of the requirements for the Doctor of
Philosophy degree in Biochemistry in the Graduate College of
The University of Iowa

July 2010

Thesis Supervisor: Associate Professor M. Todd Washington

Copyright by
BRET D. FREUDENTHAL
2010
All Rights Reserved

Graduate College
The University of Iowa
Iowa City, Iowa

CERTIFICATE OF APPROVAL

PH.D. THESIS

This is to certify that the Ph.D. thesis of

Bret D. Freudenthal

has been approved by the Examining Committee
for the thesis requirement for the Doctor of Philosophy
degree in Biochemistry at the July 2010 graduation.

Thesis Committee: _____
Madeline Shea, Thesis Chairman

S. Ramaswamy

Marc Wold

Ernesto Fuentes

Michael Feiss

To Jean and my Parents

TABLE OF CONTENTS

LIST OF TABLES	vi
LIST OF FIGURES	vii
LIST OF ABBREVIATIONS.....	ix
CHAPTER 1 INTRODUCTION	1
DNA Metabolism.....	1
DNA replication, mutagenesis and cancer	1
DNA damage and Repair.....	2
DNA damage tolerance and translesion synthesis.....	4
DNA Polymerases	6
Overview	6
Classical Polymerases	7
Non-Classical Polymerases	9
DNA Polymerase ϵ	9
Proliferating Cell Nuclear Antigen.....	12
Overview and Structural Studies.....	12
Protein interactions and cellular roles of PCNA	14
PCNA modifications	17
Un-modified PCNA and translesion synthesis.....	18
Ubiquitinated PCNA.....	19
Cellular and genetic studies.....	19
Biochemical studies.....	21
Interactions at the replication fork.....	23
Polymerase Switch.....	24
Ubiquitination induced switch: Is it Allosteric?.....	25
Tool Belt model.....	26
PCNA Mutants defective in translesion synthesis.....	27
Thesis Overview	28
CHAPTER 2 STRUCTURE OF A MUTANT FORM OF PROLIFERATING CELL NUCLEAR ANTIGEN THAT BLOCKS TRANSLESION DNA SYNTHESIS.....	41
Abstract.....	41
Introduction.....	42
Materials and Methods	44
Protein Expression and Purification	44
Crystallization of the PCNA G178S mutant protein	45
Data Collection and Structural Determination	45
DNA substrates.....	46
Polymerase activity assays	46
Results.....	47
Overview of the PCNA G178S protein structure.....	47
Loop J in the wild type and Mutant Protein Structures.....	48
Comparison of the two PCNA Domains	49
Impact of the mutant PCNA Protein on the Activity of Pol η	49
Discussion.....	51

CHAPTER 3 A CHARGED RESIDUE AT THE SUBUNIT INTERFACE OF PCNA PROMOTES TRIMER FORMATION BY DESTABILIZING ALTERNATE SUBUNIT INTERACTIONS	71
Abstract.....	71
Introduction.....	72
Materials and Methods	73
Protein Expression and Purification.....	73
Crystallization of the E113G mutant PCNA protein.....	74
Data Collection and Structural Determination.....	74
Size-exclusion Chromatography.....	75
Results.....	76
Overview of the structures of two forms of the E113G mutant PCNA protein.....	76
Subunit interactions of the nontrimeric form of the E113G mutant PCNA protein.....	78
Comparison of the domains of the trimeric and nontrimeric forms of the E113G mutant PCNA protein	79
Stability of the trimeric form of the E113G-mutant PCNA protein.....	79
Discussion.....	80
CHAPTER 4 STRUCTURE OF MONOUBIQUITINATED PCNA AND IMPLICATIONS FOR TRANSLESION SYNTHESIS AND THE POLYMERASE EXCHANGE.....	96
Abstract.....	96
Introduction.....	96
Materials and Methods	98
Protein Expression and Purification.....	98
Crystallization of Split PCNA and Ub-PCNA	100
Data Collection and Structural Determination.....	101
DNA substrates.....	103
Polymerase Activity Assay.....	103
Genetic Complementation Assay	104
Results.....	105
Production of Split PCNA and Ub-PCNA	105
Effect of split PCNA and Ub-PCNA on DNA pol η activity.....	106
Effect of split PCNA and Ub-PCNA on cell growth and UV sensitivity.....	107
Structure of Split PCNA.....	108
Structure of Ub-PCNA	109
Discussion.....	110
CHAPTER 5 DISCUSSION.....	143
Role of PCNA loop J in translesion synthesis.....	144
Preliminary and ongoing PCNA loop J studies.....	144
Non-trimeric form of PCNA.....	146
Ub-PCNA and the Polymerase switch.....	148
Implications for the field and future studies.....	151
Structural studies of Ub-PCNA co-complexes.....	152
Polyubiquitination of PCNA	153
Sumolyated PCNA	154
Recruitment Studies.....	155

Concluding Remarks and Implications for the field.....	156
REFERENCES	163

LIST OF TABLES

Table 2.1 Data collection and refinement statistics for the G178S PCNA mutant protein.....	69
Table 2.2 Steady state kinetic parameters of pol η catalyzed nucleotide incorporation.....	70
Table 3.1 Data collection and refinement statistics for the E113G PCNA mutant proteins.	95
Table 4.1 Steady state kinetic parameters of nucleotide incorporation opposite an abasic site by pol η	141
Table 4.2 Data collection and refinement statistics for split and Ub-PCNA	142
Table 5.1 Steady state kinetic parameters of pol η catalyzed nucleotide incorporation.....	162

LIST OF FIGURES

Figure 1.1 Model of the DNA replication fork.....	31
Figure 1.2 Common types of DNA damage..	32
Figure 1.3 Major sites of damage in DNA.....	33
Figure 1.4 The polymerase switch model.....	34
Figure 1.5 X-ray crystal structure of polymerase η	35
Figure 1.6 The crystal structures of polymerase η and the T7 DNA polymerase.....	36
Figure 1.7 X-ray Crystal Structure of wild type PCNA.....	37
Figure 1.8 NMR solution structure of the (A) UBZ motif and the X-ray crystal structure of (B) ubiquitin.....	39
Figure 1.9 Polymerase switch with Ub-PCNA.....	40
Figure 2.1 Structure of the PCNA G178S mutant protein	57
Figure 2.2 G178S subunit interface	58
Figure 2.3 Conformation of loop J in the wild type and mutant structure.....	59
Figure 2.4 Close up view of loop J.	60
Figure 2.5 Crystal Packing of the G178S PCNA mutant protein	61
Figure 2.6 Superimposition of the PCNA monomer backbone of wild type and mutant PCNA proteins.	62
Figure 2.7 Running start experiment with pol η on an abasic site.....	64
Figure 2.8 Steady state kinetics of pol η on an abasic site.....	65
Figure 2.9 Steady state kinetics of pol η on non-damaged DNA	66
Figure 2.10 The position of loop J in the trimeric E113G mutant PCNA protein.....	67
Figure 2.11 Kinetic and structural studies of the E113G PCNA mutant protein.....	68
Figure 3.1 Structures of the trimeric E113G PCNA mutant protein.....	84
Figure 3.2 Structure of the non-trimeric E113G PCNA mutant protein.....	85
Figure 3.3 Subunit interfaces of the trimeric and non-trimeric forms of the E113G mutant PCNA protein.....	86
Figure 3.4 The B-B interface of the non-trimeric form of the E113G PCNA protein.....	88

Figure 3.5 The A-A interface of the non-trimeric form of the E113G PCNA protein	90
Figure 3.6 Overlay of the trimeric and non-trimer PCNA	92
Figure 3.7 Stability of the the wild type and E113G PCNA proteins	93
Figure 3.8 PCNA homotrimer formation	94
Figure 4.1 Schematic of Split and Ub-PCNA	115
Figure 4.2 Purification of Ub-PCNA	117
Figure 4.3 Stimulation of pol η activity by split PCNA and Ub-PCNA	119
Figure 4.4 Steady state kinetics of pol η on an abasic site	120
Figure 4.5 Viability and UV sensitivity of yeast cells expressing split PCNA and Ub-PCNA	121
Figure 4.6 Structure of the split PCNA trimer	122
Figure 4.7 The monomeric subunit of split PCNA	123
Figure 4.8 Comparison of split PCNA with non-split PCNA	125
Figure 4.9 Overlay of the two preferred positions of the ubiquitin moiety	127
Figure 4.10 Stereo images of the electron density of the ubiquitin moiety	128
Figure 4.11 Structure of the Ub-PCNA trimer	129
Figure 4.12 Side view of the Ub-PCNA trimer	130
Figure 4.13 Overlay of the Ub-PCNA with non-split PCNA	131
Figure 4.14 Interactions between ubiquitin and PCNA within Ub-PCNA	132
Figure 4.15 Ligplots for the ubiquitin PCNA interactions	134
Figure 4.16 Model of the complex between Ub-PCNA and pol η	135
Figure 4.17 The tool-belt model	137
Figure 4.18 Electron density of the ubiquitin moiety at different stages of analysis	138
Figure 5.1 Running start experiment with pol η on an abasic site	157
Figure 5.2 Close up view of loop J	158
Figure 5.3 Eukaryotic (PCNA) and viral (UL44) processivity factors	159
Figure 5.4 Generation of polyubiquitinated PCNA	161

LIST OF ABBREVIATIONS

UV – ultraviolet radiation

MMS – methyl methanesulfonate

MMR – mismatch repair

BER – base excision repair

NER – nucleotide excision repair

CPD – cyclobutane pyrimidine dimers

8-oxo-G – 7,8-dihydro-8-oxoguanine

Pol – polymerase

α - alpha

β - beta

γ - gamma

δ - delta

ε - epsilon

η - eta

ι - iota

κ - kappa

ζ – zeta

PCNA – proliferating cell nuclear antigen

Ub-PCNA – ubiquitinated proliferating cell nuclear antigen

RFC – replication factor C

PIP – PCNA-interacting peptide motif

IDCL – interdomain connecting loop

RPA – replication protein A

DUB – de-ubiquitinating enzyme

UBZ – ubiquitin-binding zinc motif

CHAPTER 1

INTRODUCTION

DNA Metabolism

DNA replication, mutagenesis and cancer

All living organisms store their hereditary information in the form of DNA. During cellular division, a complete copy of this DNA must be generated and passed to the daughter cell¹. This process of replicating the DNA is accomplished by a complex assembly of multiple enzymes and proteins. Figure 1.1 shows a simplified model of DNA replication. The proteins involved in this process include helicases, single stranded DNA binding proteins, DNA polymerases, sliding clamps, and clamp loaders². The helicase uses ATP hydrolysis to separate the DNA strands as it moves along the DNA³. The single stranded DNA binding protein binds ssDNA exposed by the helicase⁴. The DNA polymerases synthesize the new daughter strand using the parental strand as a template⁵. The sliding clamp encircles the DNA and enhances the processivity of the DNA polymerases⁶. The clamp loader uses ATP hydrolysis to open the sliding clamp and load it onto the DNA⁷. These are only a few of the factors involved in DNA replication, but they highlight the complexity of the process.

Accurate DNA replication is essential to the survival of the daughter cell and, in the case of higher eukaryotes, the organism as a whole. When the DNA is replicated inaccurately, it leads to mutations, which can be harmful depending on where in the genome they occur. Most mutations likely occur in regions of the genome that do not affect protein function or expression levels and these are likely neutral. Some mutations, however, could occur in regions of the genome that lead to protein dysfunction, and these could be harmful. Particularly harmful mutations can lead to the death of the cell or the improper functioning of a cell in a multicellular organism. A clear example of the latter is

carcinogenesis, which often results from mutations in proto-oncogenes and tumor suppressor genes. These mutations are often the result of DNA damage.

DNA damage and repair

DNA damage (also called DNA lesions) results from both exogenous and endogenous sources (Figure 1.2). Exogenous sources include ultraviolet radiation (UV), ionizing radiation, and chemical agents. UV radiation, such as that found in sunlight, is the most extensively studied exogenous DNA-damaging agent. Cyclobutane pyrimidine (CPD) dimers are the most frequent type of UV-induced lesion, with thymine-thymine dimers accounting for about 70% of CPD dimers^{8,9}. If left unrepaired, this lesion is a major block to DNA replication because of the distortion it places on the DNA backbone¹⁰. Ionizing radiation also damages the DNA by creating oxygen free radicals that can react with either the DNA backbone or the bases¹¹. This results in both single and double stranded breaks, as well as many types of base lesions. These DNA breaks are a major block to DNA replication and, if left unrepaired, can ultimately lead to genomic rearrangement or cell death.

Endogenous sources are the predominate means by which DNA is damaged in the cell under normal conditions. Endogenously generated lesions are mainly produced through hydrolytic and oxidative reactions, which are the consequences of the cellular environment and byproducts of cellular processes. Figure 1.3 shows the major sites of DNA that are susceptible to hydrolytic and oxidative damage. An example of a hydrolytic reaction is the generation of an abasic site resulting in the loss of a base that leaves the sugar phosphate backbone intact (Figure 1.2). It has been estimated that human cells generate 10,000 abasic sites a day, which can result in mutations or stalling of the replication fork if left unrepaired¹²⁻¹⁴. Oxidative reactions are caused by reactive oxygen species (ROS) often generated by oxidative phosphorylation in the mitochondria. These ROS are highly reactive with DNA and can result in various types of DNA lesions, such

as 8-oxo-guanines (8-oxo-G), which occur 1000-2000 times per day in a single cell¹⁴. An 8-oxo-G prefers to form a base pair with an adenine residue in the active sites of DNA polymerases, and this can give rise to transversion mutations if these lesions are replicated^{15,16}. These are only a few examples of various types of DNA lesions, but they give an idea of the scale to which DNA damage occurs daily in any given cell.

With so many types of DNA lesions occurring at such a high frequency, the cell has developed multiple biological responses to DNA damage. These processes can be divided into two main categories: DNA repair and DNA damage tolerance. DNA repair is a cellular response to DNA damage that results in the restoration of the normal nucleotide sequence and DNA structure. This occurs by either the direct reversal of the DNA damage or the excision of the damaged elements. The direct reversal of DNA damage is a lesion-specific reaction and does not require a DNA template or breakage of the phosphodiester bond. An example is the direct reversal of thymine dimers using the enzyme photolyase. Photolyase uses visible light to catalyze the breakage of the pyrimidine dimer^{17,18}. Photolyases are found in both prokaryotes and eukaryotes, but are not found in humans or the great apes¹⁹.

In contrast to the direct reversal of DNA damage, DNA repair through the excision of the damaged elements requires breakage of the phosphodiester backbone. Two examples of this are: (1) base excision repair and (2) nucleotide excision repair. Base excision repair removes small non-helix distorting lesions²⁰. In base excision repair the damaged base is recognized and removed by DNA glycosylases, resulting in an abasic site²¹⁻²³. The abasic site is then removed by AP endonucleases resulting in a single nucleotide gap that is filled in by a DNA polymerase^{24,25}. The remaining nick is then sealed by a DNA ligase²⁶. Nucleotide excision repair removes large DNA distorting lesions²⁰. These distortions are identified by a recognition complex that recruits helicases to unwind the DNA around the lesion²⁷. Nucleases then make incisions 3' and 5' to the lesion on the damaged strand, resulting in a single stranded gap of about 25-30

nucleotides. This gap is then filled in by a DNA polymerase and sealed by a DNA ligase²⁸.

Other types of DNA repair include mismatch repair, non-homologous end joining, and recombination repair. Mismatch repair involves mismatch recognition proteins that scan DNA looking for mismatches^{27,29}. Following mismatch recognition the DNA is nicked on the newly synthesized daughter strand near the mismatch, and a helicase unwinds the DNA generating ssDNA. This ssDNA contains the incorrectly incorporated nucleotide which is digested by an exonuclease. The resulting single stranded gap is then repaired by the normal DNA synthesis machinery. Non-homologous end joining involves the recognition of double stranded breaks and subsequent ligation of the DNA ends by a DNA ligase³⁰. Any gaps generated during this process are filled in by a DNA polymerase. Recombination repair can also be utilized to repair double stranded breaks, although the process is not well understood at present. The general mechanism involves the resection of the double stranded break at each 5' end. This generates 3' overhangs that undergo strand invasion, at a similar sequence on the sister chromatid, generating a D-loop. A polymerase then extends the invading strand making the Holliday junction. The Holliday junction is then resolved resulting in an exchange between the two sister chromatids and repair of the double stranded break³¹.

DNA damage tolerance and translesion synthesis

Even with multiple pathways to repair DNA damage there will persist some amount of damage that must be tolerated during DNA replication. This process of coping with DNA damage is referred to as the DNA damage tolerance pathway. This pathway is as biologically important as the DNA repair pathways. During DNA damage tolerance, the lesion is bypassed and left unrepaired in hopes of it being fixed in subsequent stages of the cell cycle by the DNA repair machinery described above³². This temporary bypass

and tolerance of a DNA lesion often comes at a cost. There is an increased mutation rate at the lesion site due to the error-prone nature of this process³³.

The predominant mechanism of DNA damage tolerance is translesion synthesis. Translesion synthesis is the replicative bypass of DNA damage by non-classical DNA polymerases in both prokaryotes and eukaryotes. This process involves the direct incorporation of nucleotides across from a DNA lesion, which blocks DNA replication by classical polymerases that are unable to accommodate the lesion in their active site. This process is error-prone because the polymerases responsible for translesion synthesis have a reduced fidelity of nucleotide incorporation, a property that allows them to accommodate the structural distortions caused by various types of DNA lesions³⁴. In fact, replication errors associated with translesion synthesis are believed to be responsible for almost all DNA damage-induced mutations³⁵. The focus of this thesis is understanding the process of translesion synthesis and the role of replication associated factors during translesion synthesis.

The non-classical polymerases involved in translesion synthesis in eukaryotes are polymerase η , polymerase ι , polymerase ζ , polymerase κ , and the Rev1 protein. *In vitro* studies have provided valuable insight into the mechanisms of each of these polymerases.³⁶ These studies have shown that each of these polymerases bypass DNA lesions in a unique manner, but each polymerase has a reduced fidelity compared to classical polymerases^{33,36}. To employ these non-classical polymerases, the stalled classical polymerase at the site of DNA damage must be exchanged for a non-classical polymerase, as shown in Figure 1.4. The non-classical polymerase will then bypass the damage and a second exchange will occur between the non-classical and the classical polymerase. This switching event is believed to be mediated by replication accessory factors at the replication fork^{37,38}. However, little is known about the switching event and the role replication accessory factors play in bypassing damaged DNA. Multiple models

have been proposed and are discussed in further detail in the *Polymerase Switch* section of this chapter.

DNA Polymerases

Overview

The essential functions of DNA replication, repair, and recombination are carried out by a large set of enzymes and proteins. While the mechanism and interactions of these protein complexes remains an active area of research, the central player in each of these processes remains the DNA polymerase. The eukaryotic cell utilizes 14 to 16 polymerases to conduct the various pathways of DNA metabolism. There are currently six major families of DNA polymerases based on amino acid sequence similarity: A, B, C, D, X, and Y.³⁹ The A family is composed of prokaryotic polymerases involved in both DNA replication (T7 polymerase) and repair (*E. coli* pol I)⁴⁰. The B family is composed of the major eukaryotic replicative polymerases, pol α , pol ϵ , and pol δ ². The B family also contains polymerase ζ which is involved in lesion bypass synthesis and primer extension⁴¹. The C family is composed of prokaryotic replicative polymerases (*E. coli* pol III)⁴⁰. The D family is composed of the Archea replicative polymerases. The X family is composed of polymerases involved in base excision repair (polymerase β) and non-homologous end joining (polymerase μ and λ)⁴². The Y family is composed of polymerases that are unique in their low fidelity and their ability to replicate through DNA lesions³⁵. With the exception of pol ζ , the polymerases involved in translesion synthesis are all members of the Y family.

While these polymerase families are largely unrelated in terms of sequence homology, their catalytic domains are similar in overall architecture. Figure 1.6 shows the T7 polymerase as an example of the overall architecture of the catalytic domain⁴³. To date there are X-ray crystal structures of at least one, if not multiple, members of the A, B, X, and Y families⁴⁴⁻⁵⁰. They all have a catalytic or polymerase domain that resembles a

right hand with fingers, palm, and thumb sub-domains. The fingers and thumb sub-domains vary in size among polymerase families but largely retain a similar function between families. The fingers sub-domain is involved in aligning the incoming dNTP and the thumb sub-domain binds the DNA double helix. The palm sub-domain is the catalytic center of the polymerase and is strikingly similar across polymerase families. This sub-domain contains the three conserved aspartic acid residues that coordinate the two divalent ions required for catalysis⁵¹. While the catalytic domains of different polymerases are similar, there are additional domains that are particular to a family depending on the given function of the polymerase or the protein-protein interactions it requires at the replication fork. For example, B family polymerases involved in bulk genome replication often contain a proofreading domain possessing a 3' to 5' exonuclease activity to enhance their DNA fidelity⁵².

Classical Polymerases

Classical polymerases are those that replicate through normal non-damaged DNA and are involved in bulk genome replication and repair. In eukaryotes, the three DNA polymerases responsible for bulk genome replication belong to the B family and are pol α , pol δ , and pol ϵ . These polymerases are all thought to act together during DNA fork progression with the other accessory proteins (Figure 1.1)². Perhaps the best understood of all these polymerases is pol α . Pol α is an essential protein and unique among the B family because it couples the primase and DNA polymerase activities into a single four subunit complex⁵³. The primase activity initiates DNA replication by forming a short RNA primer that is extended by approximately 20 nucleotides by the DNA polymerase activity of pol α . The resulting primer-template can then be elongated by either pol δ or pol ϵ ⁵⁴. In yeast, pol δ is composed of three subunits and is responsible for lagging strand synthesis and Okazaki fragment maturation^{5,55}. In contrast, pol ϵ is responsible for the leading strand synthesis^{5,56}. Both pol δ and pol ϵ contain a 3' to 5' proofreading

exonuclease activity that enhances their fidelity by 10-60 fold³³. This exonuclease domain detects and removes any incorrect nucleotides allowing a correct one to be subsequently incorporated.

A hallmark characteristic of classical DNA polymerases is their inherently high fidelity, even in the absence of the proofreading exonuclease domain. This was shown with both *in vitro* kinetic studies and *in vivo* mutagenesis assays³³. X-ray crystal structure of the classical polymerases, most recently pol δ , have shown that the high fidelity is achieved by the active site pocket accommodating only the correct Watson-Crick base pair⁵⁷. This is referred to as geometric selection, where the geometry of the correct base pair is favored through interactions by amino acids from both the fingers and palm subdomains of the polymerase making specific contacts with the minor groove and base stacking with the incipient base pair. High resolution X-ray crystal structure of all 12 possible mismatches in the active site of the high fidelity prokaryotic DNA pol I also support the geometric selection model⁵⁸. These structures illustrated that mismatches stall polymerases through unfavorable interactions between the mismatch and the polymerase active site. These structures highlight the constrained nature of the polymerase active site and the mechanism of geometric selection that ensures an inherent high fidelity of the classical polymerase.

Geometric selection is also the basis for why classical polymerases stalling at sites of DNA damage. The stalling is a result of geometric distortions in the damaged DNA being unable to fit into the active site and undergo correct Watson-Crick base pairing. High resolution structures of high fidelity classical polymerases bound to DNA damage have determined that smaller lesions do not fit well in the active site and thus form unfavorable interactions in a similar manner as do mismatches⁵⁹⁻⁶¹. Furthermore, large bulky adducts like CPD dimers are completely excluded from the active site^{59,62}. Depending on the type of DNA damage the polymerase can either inefficiently misincorporate or will completely stall at the lesion^{59,62-64}.

Non-Classical Polymerases

Non-classical polymerases are those that are able to efficiently bypass damaged DNA. These polymerases are not involved in bulk genome replication and are utilized specifically during translesion synthesis to bypass lesions that block classical polymerases. The eukaryotic non-classical polymerases involved in translesion synthesis are polymerase ζ , polymerase η , polymerase ι , polymerase κ , and the Rev1 protein³⁴. These polymerases are all members of the Y family, except pol ζ which is a B family member. Pol η is able to bypass UV photoproducts and is discussed in the subsequent section. Pol ι and Rev1 both function as inserters, incorporating directly across from a DNA lesion, such as abasic sites and 8-oxo-guanines⁶⁵⁻⁶⁷. Pol κ is believed to be involved in bypassing adducts on the N² position of guanine, such as benzo[a]pyrene guanine⁶⁸⁻⁷⁰. Furthermore, pol κ and pol ζ are efficient extenders from DNA lesions^{65,71-74}.

The major characteristic of these non-classical polymerases is their reduced fidelity compared to the classical polymerases and the lack of a proofreading domain^{75,76}. Structural studies have shown that the lowered fidelity for the Y family polymerases comes from a reduced geometric selectivity at the active site^{50,67,77,78}. This results from the active site being more open and solvent accessible than the more accurate classical polymerases. This open active site is the basis for the ability of these non-classical polymerases to bypass DNA damage, because the active site can accommodate both the DNA lesion and any distortion to helix geometry. While this is beneficial for lesion bypass it also leads to an increase in the error rate³⁶. Therefore, the non-classical DNA polymerases are generally considered to be error-prone.

DNA Polymerase eta

DNA polymerase eta (pol η) is the prototypical member of the Y-family polymerases and is perhaps the most thoroughly characterized translesion synthesis polymerase (Figure 1.5). Pol η is encoded by the RAD30 gene and can efficiently and

accurately bypass UV-induced DNA lesions, such as thymine-thymine dimers^{75,79-82}. The loss of pol η in humans results in the genetic disorder xeroderma pigmentosum variant form (XPV), which is characterized by an increased sensitivity to UV radiation and susceptibility to skin cancers^{83,84}. The increase in mutagenesis is believed to occur because the absence of pol η allows for the other even more mutagenic non-classical polymerases, pol ζ and pol ι , to bypass the UV lesions. Similar results were also observed in yeast with the loss of pol η resulting in a greater sensitivity to UV irradiation and an increase in mutagenesis^{81,82}. Furthermore, it was shown that the Rad30 transcript is induced ~ 3.5 -fold in response to DNA damage by UV-irradiation in higher eukaryotes^{85,86}. UV-induced lesions are not the only type of DNA damage pol η has been implicated in bypassing. Work in human cells has shown that pol η accurately bypasses 8-oxo-guanine (8-oxo-G) lesions and cisplatin GpG adducts^{87,88}. Together these *in vivo* studies indicate an important role of pol η in the replicative bypass of various DNA lesions.

Biochemical studies have shown that purified pol η utilizes the inherent Watson-Crick base pairing ability of DNA lesions and bypasses them with a lower fidelity compared to classical polymerases. Using steady state and pre-steady state kinetics it was shown that pol η incorporates the correct nucleotides opposite 8-oxo-G and thymine dimers with the same catalytic efficiency as it does opposite an undamaged guanine or thymine residue^{75,80,89,90}. This indicates that these DNA lesions provide no kinetic barrier to pol η . By comparison, the catalytic efficiency for pol η is significantly reduced when the DNA lesions cannot form Watson-Crick base pairs. This occurs at abasic sites, (6-4) photoproducts, and bulky N²-adducted guanine residues⁹¹⁻⁹³. These results highlight the ability of pol η to accommodate any geometric distortion caused by the DNA lesion in the active site and utilize the inherent Watson-Crick hydrogen bonding interactions. This is in direct contrast to the classical polymerases which rely on the geometric selection of

the active site for correct nucleotide pairing and are not as dependent on the Watson-Crick base pairing⁹⁴.

Our understanding of the structural basis for the ability of pol η to accommodate DNA lesions came from the X-ray crystal structure of pol η bound to DNA⁵⁰. The pol η protein used to determine the structure lacked the last 115 amino acids at the C-terminus, but retained full catalytic activity⁹⁵. The pol η structure was similar to classical polymerases containing a palm, finger, and thumb sub-domain (Figure 1.5). In addition pol η has a polymerase associated domain (PAD) that is found in all Y family polymerases and increases the potential DNA binding surface area. The palm region is the most similar to the classical polymerases and contains the conserved acidic residues required for catalysis and coordination of the divalent ions. The fingers of pol η are shorter in comparison to the classical polymerase. The stubby nature is due to pol η lacking the two main helices “O” and “O1”, which play a central role in restricting the active site of classical polymerases. This results in the characteristic open active site of pol η (Figure 1.6). This open active site of pol η is able to accommodate the geometric distortions caused by DNA damage that would result in a steric clash in the active site of classical polymerases. For example, it is able to accommodate both bases of the thymine dimers allowing for the accurate bypass of this UV-induced lesion.

The regulation of pol η at the replication fork is predominantly through protein-protein interactions located at the C-terminus of the protein. While the X-ray crystal structure of the catalytic core provided insight into the polymerase mechanism, the C-terminal domain was deleted in this form of the protein. Interestingly, it was shown that the C-terminal domain is not required for the catalytic *in vitro* function of pol η by itself, but is essential for the *in vivo* function of pol η ⁹⁶. The C-terminal domain of pol η contains two functional motifs involved in protein-protein interactions that are conserved between yeast and humans. These are the PCNA-interacting peptide motif (PIP) and the

ubiquitin-binding zinc motif (UBZ) (Figure 1.5)^{96,97}. Both of these motifs are further discussed below.

Proliferating Cell Nuclear Antigen

Overview and Structural Studies

Proliferating cell nuclear antigen (PCNA) is a member of the sliding clamp family of proteins which contains members that are found in eubacteria, archeobacteria, and eukaryotes⁹⁸. While there is almost no sequence homology between the various clamps, from these three domains of life, crystallographic studies have shown they are all structurally similar to each other. Each clamp forms a ring shaped structure with a large central cavity that can accommodate B form DNA. In bacteria, the β clamp is a homodimer and is a component of the pol III holoenzyme⁹⁹. In archaea, the sliding clamp consists of three subunits that form a trimeric ring structure (either homo or hetero) and is believed to interact with multiple DNA replication proteins simultaneously^{100,101}. In eukaryotes, the sliding clamp PCNA exists as a homotrimer with a three-fold symmetry^{102,103}. Interestingly, all of these sliding clamps perform similar functions as scaffolding proteins, processivity factors, regulatory centers, and docking stations during multiple cellular processes¹⁰⁴. The focus of this section will be predominantly on the eukaryotic sliding clamp PCNA.

The eukaryotic sliding clamp PCNA was originally identified 30 years ago as an antigen for autoimmune disease in systemic lupus erythematosus patients¹⁰⁵. Around this time PCNA was shown to be differently expressed during the cell cycle, peaking during S-phase, and co-localizing with bromodeoxyuridine labeled DNA¹⁰⁶. *In vitro* studies confirmed its role in DNA replication as an essential factor for SV-40 DNA replication^{107,108}. Cellular studies have determined that PCNA is present in a pool of about 500,000 monomers/cell (200/1 actin/PCNA ratio and 1/10 RPA/PCNA ratio)^{109,110}. This pool is required because PCNA is essential to multiple processes other than DNA

replication, such as DNA repair, chromosome remodeling and assembly, chromatid cohesion, and regulating cell cycle checkpoints¹⁰⁴. While PCNA has no enzymatic activity, its role as a scaffolding protein or docking station in all these processes is mediated through protein-protein interactions that remain an active area of research.

Perhaps the largest breakthrough in understanding the role of PCNA was the determination of its X-ray crystal structure (Figure 1.7)¹⁰³. The crystal structure of PCNA revealed it to be a closed circular homotrimeric ring with a pseudo-six-fold symmetry. Each monomeric subunit of the PCNA homotrimer consists of two independent domains, with the N-terminal domain referred to as Domain A and the C-terminal domain referred to as Domain B. These independent domains are joined together firmly by forming an extended β sheet across the interdomain boundary. Each domain is further connected through a long flexible linker, called the interdomain connector loop (IDCL), that acts as a binding site for various replication associated proteins¹¹¹⁻¹¹³. To form the final ring structure, three monomeric subunits organize in a head-to-tail manner with domain A of one subunit interacting with domain B on an adjacent subunit. In eukaryotes this interaction is stabilized through eight backbone hydrogen bonds within an anti-parallel β sheet composed of strands from domain A and strands from domain B on adjacent subunits. There are three of these intersubunit β -sheets per trimer, one for each subunit interface. The formation of this final ring structure results in an outer layer of β sheets composing the circular collar and a layer of α helices lining the inner surface of the ring (Figure 1.7). While the overall electrostatic potential of PCNA is negative, the inner surface is positively charged due to the presence of many lysine and arginine residues. These localized positive charges facilitate the passage of the negatively charged DNA through PCNA and allow for the subsequent sliding of the clamp along the DNA.

In order to function in DNA metabolism, the PCNA ring must be opened and loaded around DNA by replication factor C (RFC) in an ATP-dependent manner^{7,114}. RFC is composed of five proteins that are responsible for binding and loading PCNA at

the primer-template DNA near the 3' end of the primer strand¹¹⁵. It has been shown that the binding of ATP to RFC is required for RFC-PCNA interactions, while the subsequent hydrolysis of ATP facilitates the binding of RFC to the DNA and the release of the sliding clamp¹¹⁶. Molecular simulations and FRET studies indicate that RFC opens the PCNA clamp out of the plane of the rings to form a right-handed helix (similar to a lock washer) that is loaded onto the DNA and subsequently closed around the DNA¹¹⁷⁻¹¹⁹. This opening and closing of PCNA occurs between the monomeric subunits of PCNA. Importantly, RFC only loads PCNA near the primer terminus in one orientation. This ensures that the face of PCNA-interacting with the DNA polymerase is oriented towards the growing end of the DNA.

Protein interactions and cellular roles of PCNA

PCNA has a distinct front and back face (Figure 1.7). The front face of PCNA is involved in protein-protein interactions and contains the interdomain connecting loop (IDCL)^{98,120}. The cellular function of PCNA is completely dependent on the protein-protein interactions at the front face of PCNA and there is an ever growing list of PCNA-binding proteins^{121,122}. This list includes proteins involved in DNA replication, repair, cell cycle control, chromatin remodeling, epigenetic inheritance, chromatid cohesion, and transcription. PCNA interacts with nearly all of these proteins through a hydrophobic groove located on the front side of PCNA at the IDCL. This hydrophobic pocket is composed of a center loop, the C-terminal tail, and the IDCL. It is important to mention that each monomer of PCNA contains an equivalent binding site and this allows for as many as three proteins to bind the PCNA trimer simultaneously.

Analysis of PCNA-binding proteins has revealed a conserved PCNA-interacting peptide motif (PIP motif) that is defined as Qxx(M/L/I)xxF(Y/F) where x is any residue. This PIP motif folds into a 3_{10} helix and acts as a hydrophobic plug by binding within a hydrophobic pocket on PCNA at the IDCL^{98,104}. The PIP motif is often at the C-terminus

or in a flexible region of the PCNA-interacting partner. This allows the protein to have a stable tether to PCNA, but does not restrict its movement allowing for some flexibility regarding its orientation with respect to the PCNA ring. Mutations in the conserved PIP motifs of several proteins result in a loss of their function *in vivo*, highlighting the importance of PIP-PCNA interactions^{96,102,112,123-128}. Currently, it is thought that the binding of target proteins to PCNA occurs in a competitive manner and is dependent on the local protein concentrations and the affinities of the PIP motifs of the various proteins for PCNA. It has been shown that the affinity between PIP motifs can be impacted by the flanking sequences and varies by as much as 1000-fold between different PCNA-interacting proteins¹¹².

Perhaps the most studied role of PCNA is during the multi-step process of DNA replication (Figure 1.1). At a basic level, PCNA serves as a moving platform sliding along the DNA and interacting with DNA replication proteins¹²². This mechanism allows for multiple proteins to interact at the replication fork and remain bound to and slide along the DNA. The classic example is the enhanced processivity observed for pol ϵ and pol δ in the presence of PCNA^{2,6,129,130}. This occurs because the polymerase-PCNA interactions tether the polymerase to the DNA preventing it from falling off the DNA during replication. Similarly, PCNA interacts with topoisomerases I and II and behaves as a moving platform for these enzymes as they relax the DNA¹³¹. PCNA has also been implicated in orchestrating the replication fork events in both leading and lagging strand synthesis. In synthesis of the leading and lagging strand, the switch from the primase (pol α) to a replicative polymerase requires PCNA be loaded at the primer terminus^{122,132}. PCNA also helps orchestrate Okazaki fragment maturation in the lagging strand by recruiting the flap endonuclease (FEN-1) and DNA ligase 1 through PIP-PCNA interactions^{120,133,134}. PCNA can also stimulate the catalytic activity of DNA replication associated proteins. Structural and kinetic studies with FEN-1 and DNA ligase 1 indicate that the catalytic functions of these proteins are stimulated by conformational changes

induced by their binding to PCNA loaded on the DNA^{135,136}. Together these examples highlight the role PCNA plays during DNA replication by enhancing both the processivity and catalytic activity of these enzymes while helping to orchestrate the processes at the replication fork through protein interactions.

Similar to its role in DNA replication, PCNA also facilitates DNA repair through scaffolding, regulatory, and stimulatory functions. In mismatch repair (MMR), PCNA loaded onto the DNA has been shown to interact with almost all MMR proteins through PIP motif interactions¹³⁷⁻¹³⁹. This interaction is believed to aid in the identification of the newly synthesized strand needing repaired, which is an important aspect of MMR called strand discrimination. Similar to MMR, the base excision and nucleotide excision repair (BER and NER) pathways require PCNA for scaffolding and stimulatory roles. During BER almost all proteins involved interact with PCNA both prior to and during the repair DNA synthesis step. Specifically, DNA glycosylases and DNA polymerases involved in BER have been shown to localize, interact with, and be enzymatically stimulated through interactions with PCNA¹⁴⁰⁻¹⁴². PCNA is also required for NER during the removal of the damage and the subsequent repair synthesis step. The endonuclease XPG has been shown to contain a PIP motif in the C-terminus required for PCNA-binding and functional NER *in vivo*¹⁴³. PCNA is also heavily involved in the DNA damage tolerance pathway of translesion synthesis and will be discussed in more detail below.

With PCNA being involved in both the replication and repair of DNA, it would be expected that its regulation would drastically impact the cell cycle. This is in fact the case and is most clearly illustrated with the classic cell cycle regulatory protein p21. In eukaryotes p21 is a crucial regulator of PCNA through its PIP motif located at the C-terminus^{144,145}. Both *in vitro* and *in vivo* experiments have shown that the binding of p21's PIP motif to PCNA inhibits DNA replication by blocking the surface required for polymerase binding^{144,146}. In fact, of all the tested PIP motifs, p21 has the highest affinity for PCNA and is able to out compete any known PCNA-interacting proteins.

Additionally, p21 has been shown to down regulate the translesion synthesis polymerases by both restricting their access to PCNA and preventing the ubiquitination of PCNA¹⁴⁷. The ability of p21 to prevent all replication illustrates the importance of the protein-protein interactions between PCNA and proteins involved in DNA metabolism.

PCNA modifications

With so many processes utilizing PCNA, the cell has developed additional methods of regulation through modifications of PCNA. These include acetylation, sumoylation, monoubiquitination, and polyubiquitination. For the sake of clarity, I will describe PCNA monoubiquitination and polyubiquitination in a separate section. The acetylation of PCNA was recently identified and is currently the least understood of all PCNA modifications. It was shown that PCNA is both acetylated and deacetylated at varying stages of the cell cycle by the transcription factor p300 and HDAC1 respectively¹⁴⁸. Using binding and DNA polymerization assays, it was also determined that the deacetylated form of PCNA has a reduced affinity for pol β and pol δ than the acetylated form and the polymerization activity of these proteins is lowered with the deacetylated form of PCNA¹⁴⁸. The authors concluded that the acetylation of PCNA is associated with DNA replication, whereas the non-acetylated form is believed to prevent DNA replication by decreasing the affinity of PCNA to the DNA polymerases.

The sumoylation of PCNA occurs predominantly at Lys-164 and to a lesser extent on Lys-127^{149,150}. Lys-127 lies directly in the PIP binding box of PCNA and its sumoylation prevents the binding of proteins utilizing PIP motifs. This is believed to act as a reset button displacing PIP box proteins in a similar manner to p21 in higher eukaryotes¹⁵¹. Sumoylation at Lys-164 is more complicated because this is also the site of PCNA ubiquitination. One function of the sumoylation at Lys-164 is to recruit the Srs2 helicase-like enzyme that will strip the recombinase Rad51 off the DNA¹⁵². This helps to prevent any unwanted homologous recombination during S phase. The second function of

Lys-164 sumoylation has been postulated to act as a switch between DNA replication and DNA damage tolerance. When the cell is in S phase there is an increase in the sumoylation of PCNA and it is believed that upon DNA damage there is a switch from sumoylation to ubiquitination, promoting the DNA damage tolerance pathway^{150,153,154}. This hypothesis is largely speculative and has been difficult to test using traditional genetic techniques.

Un-modified PCNA and translesion synthesis

Early studies of translesion synthesis indicated an important role of PCNA in regulating and stimulating the non-classical polymerases. These studies were predominantly performed using unmodified PCNA because of the difficulty in obtaining significant amounts of ubiquitinated PCNA. Therefore, this section will be devoted to describing studies to determine the cellular role of unmodified PCNA in translesion synthesis. All non-classical polymerases interact with PCNA during translesion synthesis, and these interactions have similar effects on the recruitment and catalytic activity of the non-classical polymerases^{34,113,155}. Since pol η is the best studied, I will highlight studies utilizing pol η . However, similar trends have been observed for all non-classical polymerases.

Located at the extreme C-terminus of pol η is the PIP motif, which acts as a flexible linker attaching pol η to the DNA via interactions with PCNA¹⁵⁶. The importance of the PIP motif is evident in some XP-V cells, where the PIP motif of pol η is missing leading to a complete loss of pol η in these cells¹²⁵. In yeast, mutations within the hydrophobic regions of the PIP motif results in a complete loss of pol η function *in vivo*, however the *in vitro* catalytic activity in the absence of PCNA is unaffected⁹⁶. *In vivo* colocalization studies determined that the ability of pol η to be recruited to replication forks following UV irradiation is dependent on an intact PIP motif^{156,157}. Further, yeast two-hybrid studies and pull-down assays determined that the PIP motif is required for protein

interactions between pol η and PCNA^{96,125}. Together these studies highlight the cellular importance of the pol η - PCNA interaction mediated through the PIP motif.

Additional *in vitro* kinetic studies have shown that PCNA enhances the ability of pol η to replicate past DNA damage^{96,125,158}. This phenomenon is best observed by using DNA containing an abasic site, which pol η is unable to efficiently bypass by itself. Using steady state kinetics it was shown that the ability of pol η to bypass an abasic site was enhanced by the loading of PCNA onto the DNA. Utilizing pol η mutants lacking a PIP motif, it was shown that the stimulation is dependent on protein interactions between pol η and PCNA. Studies with human pol η show that this stimulation is not lesion specific, because the replication of undamaged DNA, 8-oxo-G lesions, and T-T dimers by pol η is similarly stimulated by interactions with PCNA¹⁵⁹. Interestingly, PCNA has been shown to have no appreciable impact on the processivity of pol η , which is able to only incorporate 1-10 nucleotides per binding event⁹⁶. This is in direct contrast to the traditional role of PCNA as a processivity factor during DNA replication. The likely reason for the inability of PCNA to enhance the processivity of pol η is because these non-classical polymerases are highly mutagenic and have evolved to have a limited number of incorporation events. Combined these studies illustrate the role of PCNA as both a scaffolding protein and stimulatory factor for the non-classical polymerases during translesion synthesis.

Ubiquitinated PCNA

Cellular and genetic studies

The ubiquitination of proteins occurs in three steps: (1) ATP-dependent activation of the ubiquitin moiety and attachment to the E1 protein, (2) transfer of the ubiquitin from the E1 to a cysteine residue of the ubiquitin conjugating E2 enzyme, (3) binding of the E2 enzyme to the ubiquitin E3 ligase and subsequent transfer of the ubiquitin moiety to a lysine residue on the targeted protein¹⁶⁰. The E3 enzymes confer specificity by

binding to and bringing both the ubiquitin target and E2 enzyme together. While this ubiquitination modification has long been appreciated to be involved in targeting proteins for proteosomal degradation, there is clear evidence that ubiquitin modifications are involved in other essential cellular functions. These include controlling protein stability, function, localization, and the regulation of pathways¹⁶¹.

The broader role of ubiquitin modifications is clearly apparent in the DNA damage tolerance pathway, which requires the ubiquitination of PCNA¹⁶². In eukaryotes, cells treated with DNA-damaging agents were shown to undergo either mono or polyubiquitination of PCNA at Lys-164. Monoubiquitination of PCNA (Ub-PCNA) is catalyzed by the Rad6/Rad18 (E2/E3) ubiquitinating complex^{150,154,163}. In yeast this ubiquitination was shown to occur during S-phase and in response to DNA-damaging agents such as UV light or methyl methanesulfonate (MMS)¹⁵⁰. Genetic studies determined that yeast lacking the Rad6 or Rad18 protein are defective in UV-induced mutagenesis, and are extremely sensitive to UV and MMS¹⁵⁴. Mutational analysis using PCNA mutants that lack specific lysine residues showed that the ubiquitination of PCNA needed for induced mutagenesis is at Lys-164. Genetic studies showed that yeast containing a K164R PCNA mutation are epistatic to mutants deficient in the non-classical polymerases pol η (RAD30) and pol ζ (REV3). Together these genetic studies highlight the connection between DNA damage, Rad6/Rad18, Lys-164 linked Ub-PCNA, and translesion synthesis.

The polyubiquitination of PCNA also occurs at Lys-164 and promotes the error free pathway of DNA damage tolerance^{150,154}. This pathway is dependent on the Rad5 (E2) and Mms2-Ubc13 (E3) complex catalyzing the formation of polyubiquitin chains through Lys-63 linkages on ubiquitin¹⁶⁴⁻¹⁶⁶. The error-free pathway is not well understood and is believed to use the undamaged sister duplex as the template to bypass the DNA lesion. Discussions of ubiquitinated PCNA will refer to the monoubiquitinated form, unless otherwise indicated.

The control of PCNA ubiquitination is an active area of research and is currently not well understood. The current model is that Ub-PCNA results from replication fork stalling. This is because treatment with hydroxyurea which results in the halting of fork progression by depleting the cell of deoxyribonucleotides triggers the ubiquitination of PCNA^{167,168}. In contrast, ionizing radiation which does not cause the slowing or stalling of replication forks does not trigger ubiquitination of PCNA. It has been suggested that replication blocks allow the helicase to keep moving in front of the replication fork and expose long regions of ssDNA. The ssDNA region is then bound by Rad18 which interacts with both ssDNA and replication protein A (RPA), the ssDNA binding protein¹⁶⁹. Rad18 then interacts with Rad6 and ubiquitinates PCNA³⁸. Currently it remains unknown whether all three monomeric subunits of PCNA must be monoubiquitinated to support translesion synthesis. *In vivo* studies determined that the ubiquitinated form of PCNA that is found associated with pol η following DNA damage has all three monomers ubiquitinated¹⁶⁷. However a more thorough analysis will require future experimental studies to determine if only one PCNA monomer is sufficient to support translesion synthesis.

The de-ubiquitination of PCNA is also not well understood and only the mammalian de-ubiquitinating enzyme (DUB) USP1 has been identified¹⁷⁰. It was shown that in response to UV light USP1 is degraded and there is an increase in Ub-PCNA. Using siRNA to USP1 resulted in an increase in Ub-PCNA amounts during all stages of the cell cycle and an increase in hypermutability. These results suggest a model by which the DUB keeps Ub-PCNA at low levels in undamaged cells to prevent the unwanted employment of translesion synthesis polymerases.

Biochemical studies

Compared to the unmodified form of PCNA, Ub-PCNA is considerably less studied *in vitro*. This is because of the difficulty in obtaining significant amounts of Ub-

PCNA. The enzymatic generation of Ub-PCNA *in vitro* is a multistep process and requires at least 5 proteins (Uba1, Rad6, Rad18, RFC, and ubiquitin). Following the reaction, the Ub-PCNA must be purified from the other components, and this results in only sub-microgram quantities of Ub-PCNA. To overcome this problem, one group utilized Ub-PCNA analogs generated by cross-linking reactions using dichloroacetone¹⁷¹. This requires that Lys-164 of PCNA and the C-terminal glycine of ubiquitin be mutated to cysteine residues. Another group generated linear fusions of PCNA with ubiquitin at either the N-terminus or the C-terminus¹⁷². This fusion allowed for adequate *in vitro* binding studies, but failed to restore UV resistance when expressed in yeast. In Chapter 4 I describe the generation and utilization of a novel Ub-PCNA mimic that functions *in vivo* and *in vitro*.

Recently two separate labs used steady state kinetic studies to examine the effect Ub-PCNA has on the activity of pol η , pol ζ , and Rev1^{173,174}. Both papers enzymatically mono-ubiquitinated PCNA using the Rad6/Rad18 complex and loaded Ub-PCNA onto the DNA. The groups then looked at the ability of the non-classical polymerases to incorporate nucleotides across from abasic sites on a DNA substrate containing PCNA or Ub-PCNA. The groups had conflicting results on the effect Ub-PCNA has on the activity of non-classical polymerases. One group showed an enhanced activity of the non-classical polymerases pol η and Rev1 upon mono-ubiquitination of PCNA and no impact on the catalytic activity of pol ζ ¹⁷³. The other group showed no stimulation in the activity of all the tested polymerases (pol ζ , pol η , and Rev1) following mono-ubiquitination of PCNA¹⁷⁴. The reason for the discrepancy between these groups remains unknown, but is likely due to the fact that any such stimulation is very minor making it difficult to observe.

The impact the ubiquitination of PCNA has on the other traditional replicative functions of PCNA were also assessed *in vitro* by both groups. In these studies, both groups obtained identical results. The first group determined that Ub-PCNA has the same

replicative functions as unmodified PCNA. Specifically, Ub-PCNA can be loaded onto the DNA by RFC and can support Okazaki fragment maturation by the coordinated actions of DNA polymerase δ , FEN1, and DNA ligase 1¹⁷³. The second group showed that the ubiquitination of PCNA has no impact on the catalytic activity of pol δ *in vitro*¹⁷⁴. Together these results indicate that ubiquitination does not disrupt the binding of replication proteins to PCNA or their catalytic activity. Prior to my work these were the only *in vitro* biochemical studies performed looking at the impact Ub-PCNA has on the catalytic properties of replication associated factors.

Interactions at the replication fork

All non-classical polymerases have been shown to interact with Ub-PCNA at stalled replication forks during translesion synthesis. This interaction is dependent on at least two interactions: (1) the non-classical polymerase PIP motif to the IDCL of PCNA, and (2) the ubiquitin-binding domain of the non-classical polymerase to the ubiquitin moiety on PCNA. The PIP motif is believed to provide a basal binding affinity between PCNA and the non-classical polymerases and is essential for the PCNA-polymerase interaction, as discussed above. The ubiquitin-binding domains are located in almost all non-classical polymerases and are involved in recognizing the ubiquitinated form of PCNA and facilitating the polymerase switch during translesion synthesis⁹⁷. To date the best studied ubiquitin-binding motif is the pol η UBZ motif located at the C-terminus, (Figure 1.5).

The pol η UBZ motif is a C₂H₂ ubiquitin-binding zinc finger located between the catalytic domain of pol η and the PIP motif at the extreme C-terminus. The UBZ motif structure was recently determined by nuclear magnetic resonance (NMR) (Figure 1.8)¹⁷⁵. Using NMR titrations the binding interface between the UBZ motif and ubiquitin were determined to be between the α -helix of the UBZ motif and the canonical hydrophobic surface of ubiquitin defined by residues L8, I44, and V70. This interaction had a binding

affinity of 73uM as measured by NMR and 81uM as measured by isothermal titration calorimetry. *In vivo* studies determined that the UBZ motif is required for pol η recruitment to replication factories and UV survivability⁹⁷. Further localization studies determined that pol η localizes to these replication factories specifically with Ub-PCNA and this localization is enhanced by the UBZ motif^{172,176}. Subsequent studies also determined that the UBZ motif is required for pol η bypass of 8-oxo-G lesions *in vivo*¹⁷⁷. Additional cellular pull down assays showed pol η co-immunoprecipitated specifically with Ub-PCNA and not unmodified PCNA¹⁶⁷. This co-immunoprecipitation was further enhanced by treating the cell with UV radiation and is dependent on the C-terminal domain of pol η . Together these results highlight the importance of the non-catalytic UBZ structural element involved in the pol η and Ub-PCNA interaction.

Polymerase Switch

Almost all DNA repair and DNA damage tolerance pathways require the actions of multiple polymerases that must switch places to gain access to the DNA template. The nature of this switch is currently an active area of research and debate, especially with respect to translesion synthesis (Figure 1.4). During translesion synthesis the high fidelity classical DNA polymerases are unable to bypass DNA damage and stall upon encountering the DNA damage. This stalling results in the ubiquitination of PCNA and the subsequent recruitment of the low fidelity, non-classical polymerase. Following ubiquitination of PCNA there is a switch between the classical and non-classical DNA polymerase. The non-classical polymerase then replicatively bypasses the DNA lesion. Following bypass of the lesion there is a second exchange between the non-classical and classical DNA polymerase, allowing traditional DNA replication to continue.

Due to the error-prone nature of the non-classical polymerases this switch is believed to be highly regulated and controlled. One study that provided some insight into the polymerase switch mechanism utilized an *in vitro* polymerase exchange assay¹⁷⁸. It

was determined that pol η requires its C-terminus (PIP and UBZ motifs) and the ubiquitination of PCNA to undergo the polymerase exchange with pol δ . This exchange was also shown to be dependent on the stalling of the replication fork. In contrast, pol η was unable to exchange with pol δ in the presence of unmodified PCNA even when the replication fork was stalled. Together these studies indicate that pol η is only able to replace pol δ following the ubiquitination of PCNA at stalled replication forks.

Ubiquitination induced switch: Is it Allosteric?

Genetic studies have determined that PCNA and its mono-ubiquitination are required for translesion synthesis to occur *in vivo*. This observation has led to multiple models involving ubiquitination as a key player in the polymerase switch mechanism. There are two commonly discussed models for the role ubiquitin plays in the polymerase switch: (1) ubiquitination of PCNA induces an allosteric change to PCNA promoting the polymerase switch and (2) the ubiquitin moiety does not induce an allosteric change and only provides an additional binding site for the non-classical polymerases.

One of the earliest models of polymerase exchange was the attachment of ubiquitin to PCNA causing a conformational change, thus facilitating the switch from the classical to non-classical polymerase. In this model the ubiquitination would either increase the affinity between PCNA and the non-classical polymerase or decrease the affinity between PCNA and the classical polymerase. Currently there is no direct evidence to support this model during translesion synthesis and to my knowledge there is no reported allosteric change to PCNA following any post-translation modifications. Evidence against the ubiquitination of PCNA causing a decrease in the affinity for the classical polymerase has been shown with enzymatically generated Ub-PCNA. *In vitro* biochemical assays determined that Ub-PCNA does not impact the stability of the pol δ holoenzyme on the DNA or its enzymatic activity¹⁷⁸. This result indicates that PCNA does not undergo an allosteric change following ubiquitination that facilitates the switch

by destabilizing interactions with classical polymerases. Prior to my work, there was no evidence either way with respect to an allosteric model favoring the binding of the non-classical polymerases. My work described in Chapter 4 argues that neither type of allosteric model is very likely.

The second model is that the ubiquitin moiety on PCNA provides an added binding site and does not induce an allosteric change in PCNA. This model is based on the presence of an ubiquitin-binding motif in the non-classical polymerases and these motifs providing additional interaction sites for the non-classical polymerases to Ub-PCNA. Since the classical polymerases lack these ubiquitin-binding motifs, the non-classical polymerases would have a competitive advantage for access to PCNA at the primer terminus following PCNA ubiquitination. Prior to my work there was no direct evidence for this model; only the lack of evidence for an allosteric change to PCNA following ubiquitination.

Tool Belt model

One of the most popular models currently discussed regarding the polymerase switch is the tool belt model (Figure 1.9). This model postulates that multiple polymerases can bind a single clamp with each polymerase interacting with a different monomeric subunit of the clamp. In the case of PCNA (the belt) this would allow up to three polymerases (the tools) to bind simultaneously. In this model PCNA would be able to quickly utilize a specific polymerase as needed by engaging a specific polymerase at the primer terminus. It is tempting to think that ubiquitination of PCNA may establish a tool belt. One could imagine that during times of DNA damage, PCNA is ubiquitinated and would only then exist as a tool belt allowing it to quickly switch between translesion synthesis and classical replication as needed. In comparison, when low levels of DNA damage are present, PCNA would remain un-modified and only bind to the classical polymerases. While this model is very attractive and exciting, it remains largely untested.

Support for the tool belt model came from prokaryotic studies using the β clamp, the classical DNA polymerase III (pol III), and non-classical DNA polymerase IV (pol IV)¹⁷⁹. Using fluorescence based binding studies, it was determined that pol III and pol IV can bind the β clamp simultaneously. The ability of pol IV to gain access to the primer terminus is dependent on the stalling of pol III, and immediately after the stall is relieved, pol III regains control of the primer terminus back from pol IV. Our understanding of the structural basis of the ability of pol IV to bind the β clamp and ride “piggy back” while not impacting DNA replication by pol III comes from the X-ray crystal structural of the pol IV C-terminal domain bound to the β clamp¹⁸⁰. The extreme C-terminal domain binds to the front of the clamp on one subunit (similar to the PIP interaction in eukaryotes) and additional contacts of the C-terminal domain are made at the subunit interface and angled away from the DNA. These contacts would prevent the polymerase from contacting the DNA and therefore would be a means of carrying the polymerase along without interfering with pol III function. Together these studies provide evidence for a tool belt model in prokaryotes.

PCNA Mutants defective in translesion synthesis

More than 30 years ago, seven mutants were isolated in yeast that had a reduced frequency of induced mutations and the genes responsible for this phenotype were designated as REV¹⁸¹. These genes are now widely appreciated as being involved in the DNA damage tolerance pathway. For example, the REV1, REV3, and REV7 genes were all shown to encode non-classical polymerases involved in translesion synthesis in the early 90's¹⁸²⁻¹⁸⁵. In 2006, the REV6 gene was shown to be the same as the POL30 gene, which encodes PCNA¹⁸⁶. Yeast containing the *rev6-1* allele of this gene are completely defective in translesion synthesis and have an increased sensitivity to DNA-damaging agents, similar to a K164R PCNA mutant. After cloning and sequencing the *rev6-1* allele it was shown to encode a mutant form of PCNA in which a G178S substitution has

occurred¹⁸⁶. This allele was therefore renamed the *pol30-178* allele. Gly-178 is located at the monomer-monomer interface of the trimeric PCNA. Further *in vivo* studies determined this mutant form of PCNA functions normally in all respects except that it is unable to support translesion synthesis¹⁸⁶. In fact, yeast strains containing the G178S PCNA mutant and yeast strains lacking pol η have a very similar reduced ability to bypass DNA damage. Prior to my work, nothing was known about how this substitution in PCNA leads to a loss of translesion synthesis

Another mutation at the monomer-monomer interface of PCNA resulting in a loss of translesion synthesis is the *pol30-113* PCNA mutant, which is an E113G substitution¹⁸⁷. Glu-113 is located directly across from Gly-178 on the adjacent monomeric subunit. Interestingly, the E113G substitution is phenotypically similar to the G178S and K164R PCNA mutants. Yeast harboring the E113G mutant have a complete loss in translesion synthesis and an increased sensitivity to DNA damage, while normal DNA replication and general cell growth are unaffected¹⁸⁷. Additional *in vivo* yeast studies determined that the E113G PCNA mutant protein can be monoubiquitinated in response to DNA damage¹⁸⁷. This result shows the loss of translesion synthesis in yeast harboring the E113G substitution is not due to the inability of the PCNA mutant to be ubiquitinated, as seen in the K164R PCNA mutant. This finding also illustrates that ubiquitination, although necessary, is not sufficient to support translesion synthesis alone. Further *in vitro* studies showed the E113G PCNA mutant protein is unable to stimulate the activity of the non-classical polymerases¹⁸⁷. However, the reason for the inability of the E113G to stimulate the catalytic activity remains unknown. My work described in Chapter 2 addresses how these mutant proteins fail to support translesion synthesis.

Thesis Overview

Chapter 2 is about the biochemical and structural characterization of two PCNA mutant proteins that are defective in translesion synthesis, the G178S (encoded by the

rev6-1 allele) and the E113G (encoded by the *pol30-113* allele) PCNA mutant proteins. I chose to study these two proteins to gain a better understanding of the interactions between PCNA and the non-classical polymerases that are specific to translesion synthesis. The X-ray crystal structure of the G178S PCNA mutant protein showed a 6.5Å shift in an extended loop, called loop J, compared to the wild type PCNA structure. Steady state kinetic studies determined that, in contrast to wild type PCNA which stimulates pol η , the G178S substitution actually inhibits the activity of pol η . Similar results were also observed for the E113G PCNA mutant protein, albeit to a lesser extent. The E113G mutant protein structure had a 3Å shift in loop J and failed to stimulate the activity of pol η , but it did not inhibit it. Combined these results indicate that the position of loop J in PCNA plays an essential role in facilitating translesion synthesis.

Chapter 3 is about a distinct X-ray crystal structure of the E113G PCNA mutant protein that I observed while performing my structural studies described in Chapter 2. This unique PCNA structure failed to form the expected ring-shaped structure through the traditional intersubunit interactions of domain A and domain B of neighboring subunits. Instead this structure was a non-trimeric form of the protein that formed A-A and B-B intersubunit interactions. Upon analysis, I determined that the B-B interface is stabilized by an anti-parallel β sheet that appears structurally similar to the A-B interface observed for the trimeric ring shaped form. In contrast the A-A interface is stabilized by hydrophobic interactions. The location of the E113G substitution is directly within this hydrophobic surface and would not be favorable in the wild type protein. This suggests that the side chain of Glu-113 promotes trimer formation by destabilizing these possible alternate subunit interactions.

Chapter 4 is about the characterization and generation of an Ub-PCNA analog for structural and biochemical studies. A major difficulty with studying Ub-PCNA has been the ability to obtain significant amounts of it to perform structural and biochemical studies. In this Chapter, I describe a novel means of generating large amounts of Ub-

PCNA by splitting the protein into two self-assembling polypeptides. Using yeast genetics, I determined that the analog supports cell growth, viability, and translesion synthesis *in vivo*. Using steady state kinetics, I determined that the Ub-PCNA analog is stably loaded onto the DNA and stimulates the catalytic activity of pol η *in vitro*. I also determined the X-ray crystal structure of Ub-PCNA and found that the ubiquitin moieties are located on the back face of PCNA and interact with it via their canonical hydrophobic surface. Surprisingly, the attachment of ubiquitin does not change PCNA's conformation. This implies that PCNA ubiquitination does not cause an allosteric change to PCNA, and instead facilitates non-classical polymerase recruitment to the back of PCNA by forming a new binding surface for the non-classical polymerases. This is consistent with a "tool belt" model of the polymerase exchange, whereby classical and non-classical polymerases simultaneously bind Ub-PCNA.

Chapter 5 discusses further biochemical and structural work testing the role of loop J in translesion synthesis, as discussed in Chapter 2. The chapter also discusses the implications of the conclusions from each chapter and the future directions and applications of the Ub-PCNA analog.

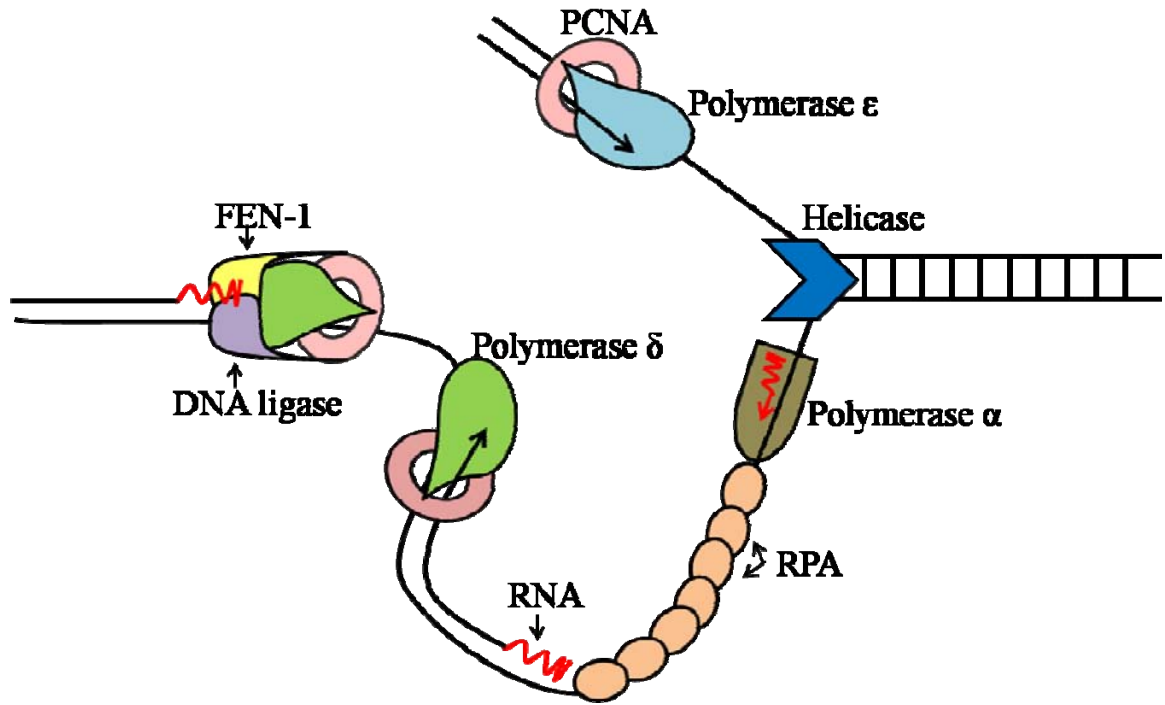


Figure 1.1 Model of the DNA replication fork. Both leading and lagging strand replication is shown with the key factors indicated and labeled. This figure was adapted from Garg et al.²

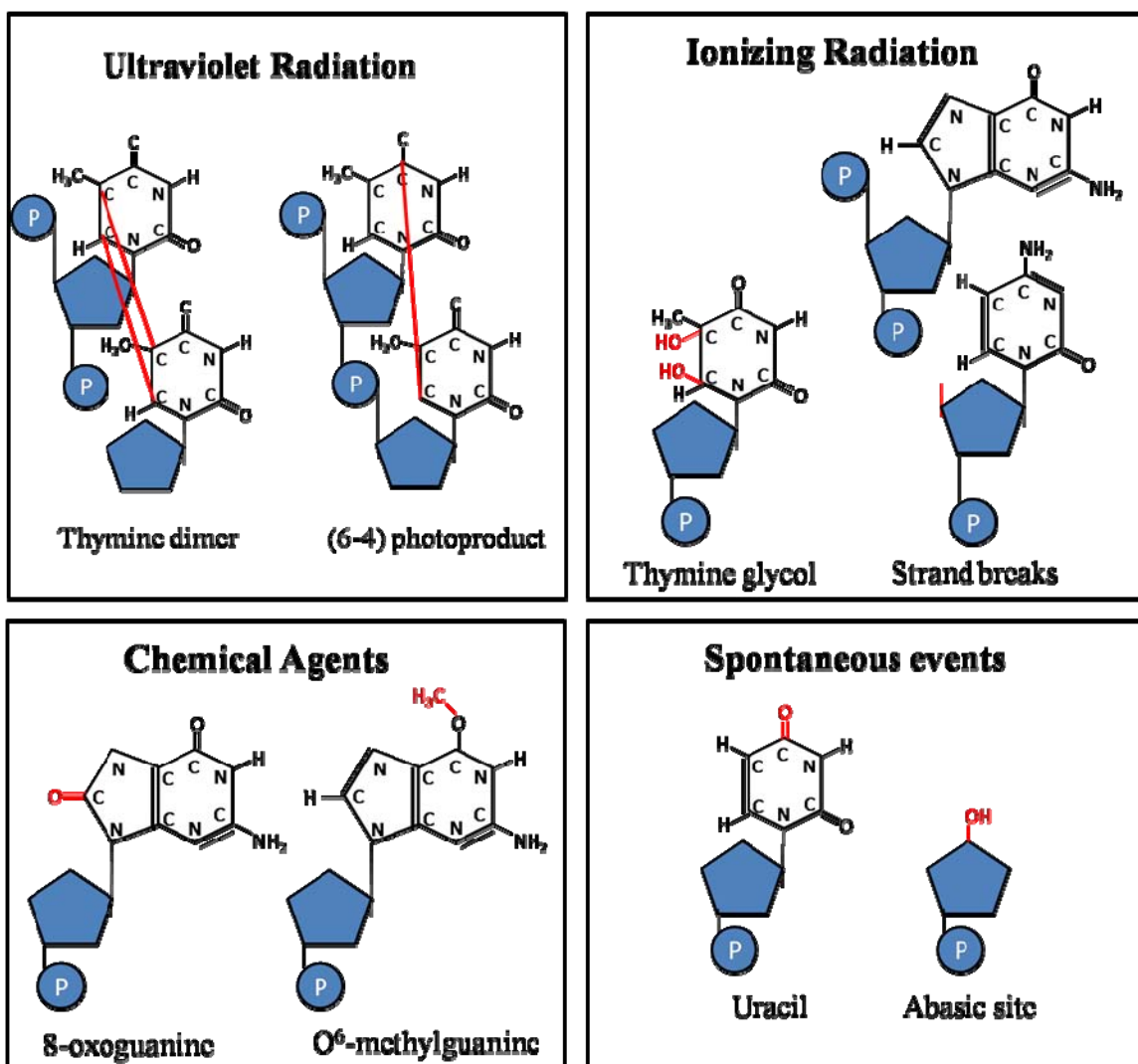


Figure 1.2 Common types of DNA damage. The structures of common DNA lesions are shown with the damage promoting factors in black above the structures. The modification is shown in red.

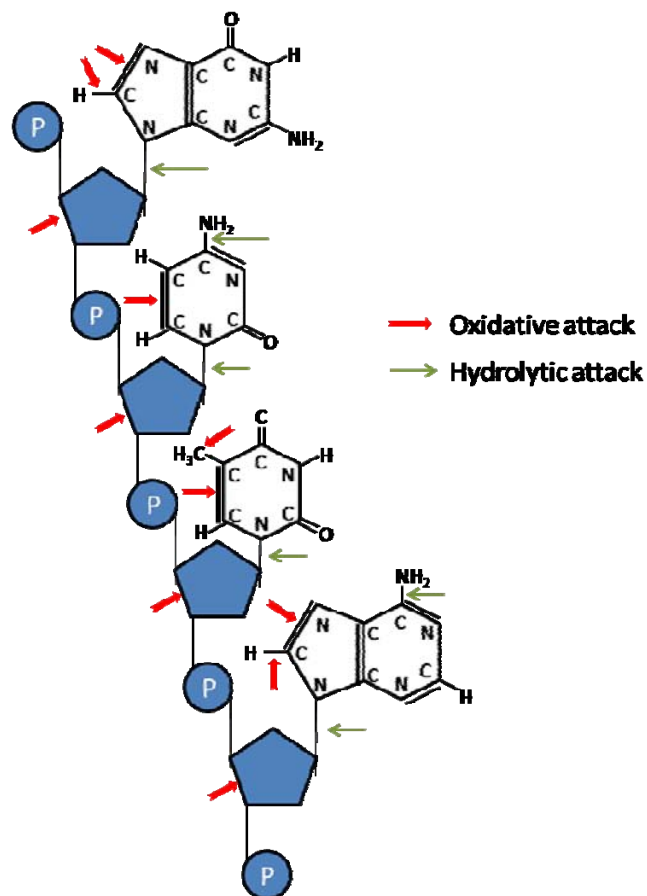


Figure 1.3 Major sites of damage in DNA. A short sequence of DNA is shown with the major sites of damage indicated as described in the key. Figure adapted from Lindahl et al.¹²

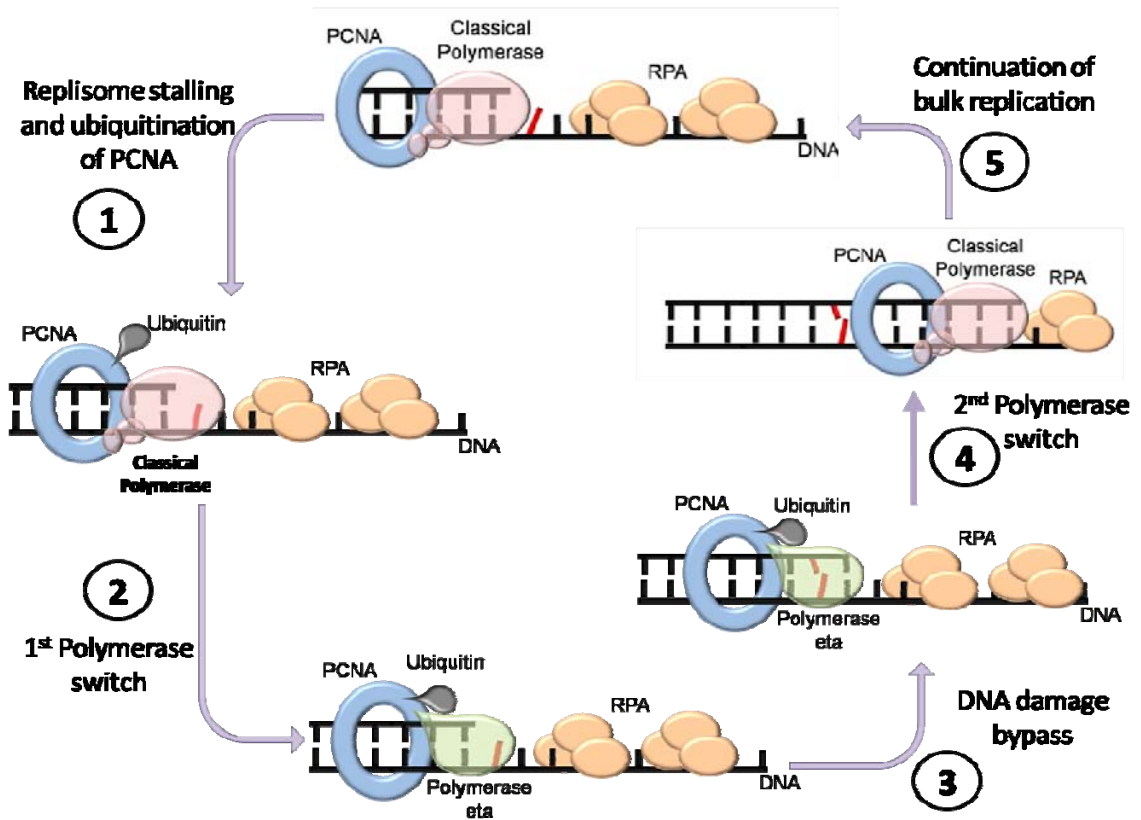


Figure 1.4 The polymerase switch model. The classical polymerase (pink) stalls at the site of DNA damage (red dash) and PCNA is ubiquitinated. The classical polymerase comes off the template strand and the non-classical polymerase eta (green) then binds to the primer template and bypasses the DNA damage (steps 2 and 3). There is then a second switch to replace the non-classical polymerase with the classical polymerase which continues replication of the daughter strand (steps 4 and 5).

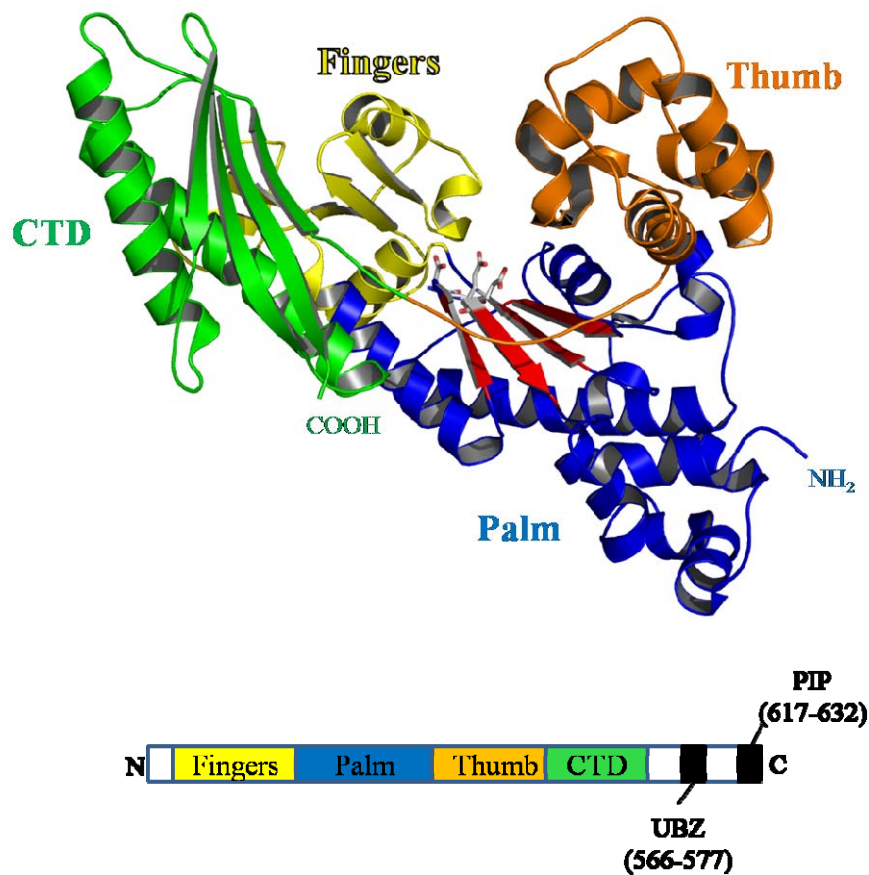


Figure 1.5 X-ray crystal structure of polymerase η . The X-ray crystal structure of pol η is shown with the three key active site residues shown in stick format. Below the structure is a schematic of the complete DNA polymerase η structure with the ubiquitin-binding motif (UBZ) and PCNA-interacting peptide motif (PIP) indicated. (PDB ID: 1JIH)

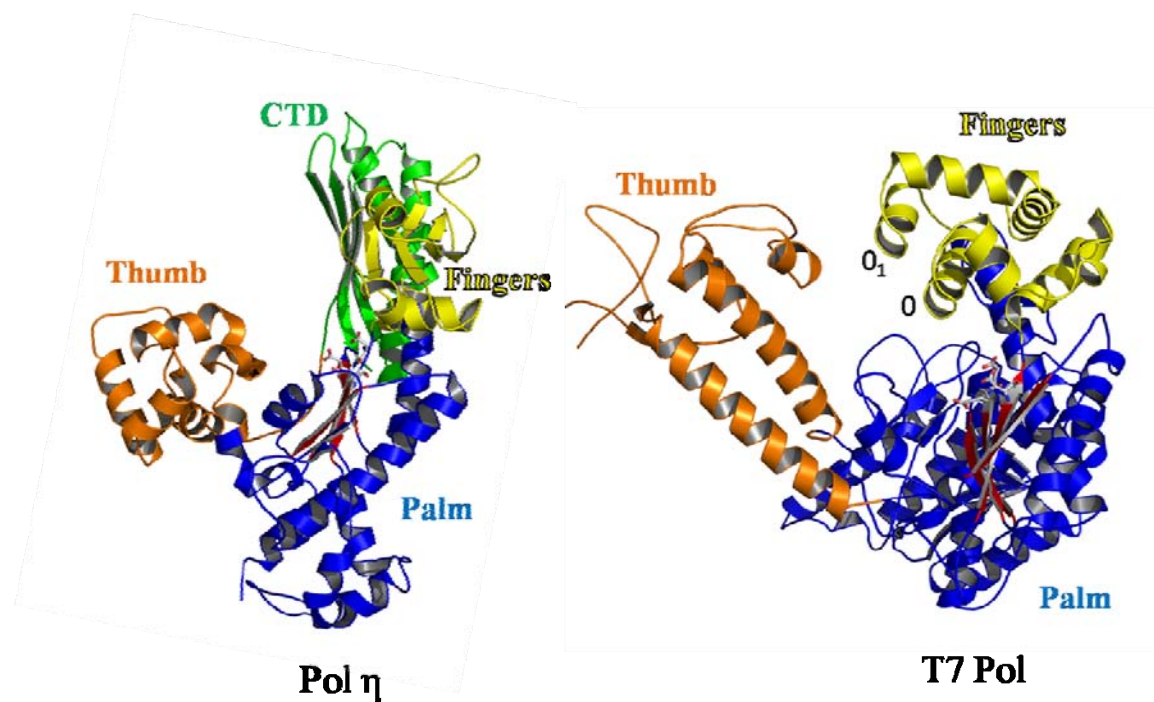


Figure 1. 6 The crystal structures of polymerase η and the T7 DNA polymerase. The characteristic fingers, palm, and thumb domains are indicated. Polymerase η lacks the O₁ and O helices of the finger domain in the T7 polymerase that restricts the active site. This allows polymerase η to have a more “open” active site than the T7 polymerase. (PDB ID: 1JIH and 1T7P)

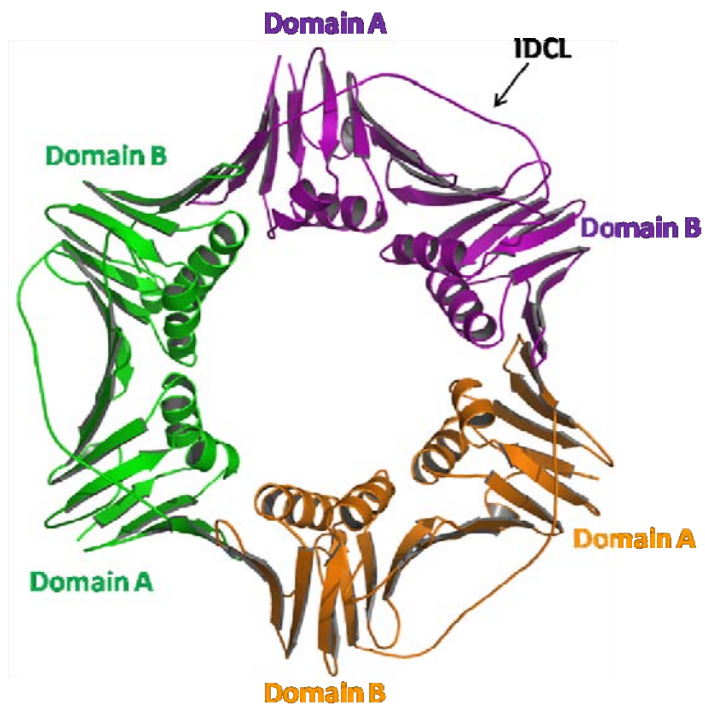
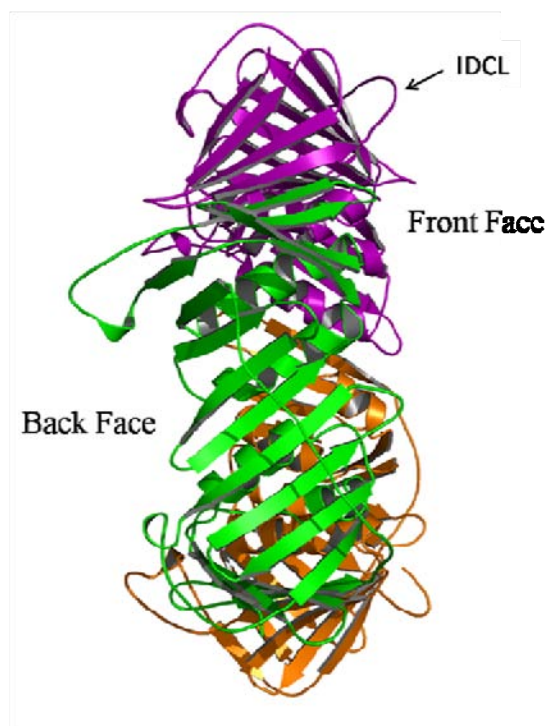
A**B**

Figure 1.7 X-ray Crystal Structure of wild type PCNA

Figure 1.7 continued. X-ray crystal structure of wild type yeast PCNA from the (A) front and (B) side view. Each monomeric subunit is shown in purple, green, and orange. Domain A and domain B of each monomeric subunit are indicated. The interdomain connecting loop is indicated for the purple subunit. The front and back faces are indicated in the side view. (PDB ID: 1PLQ)

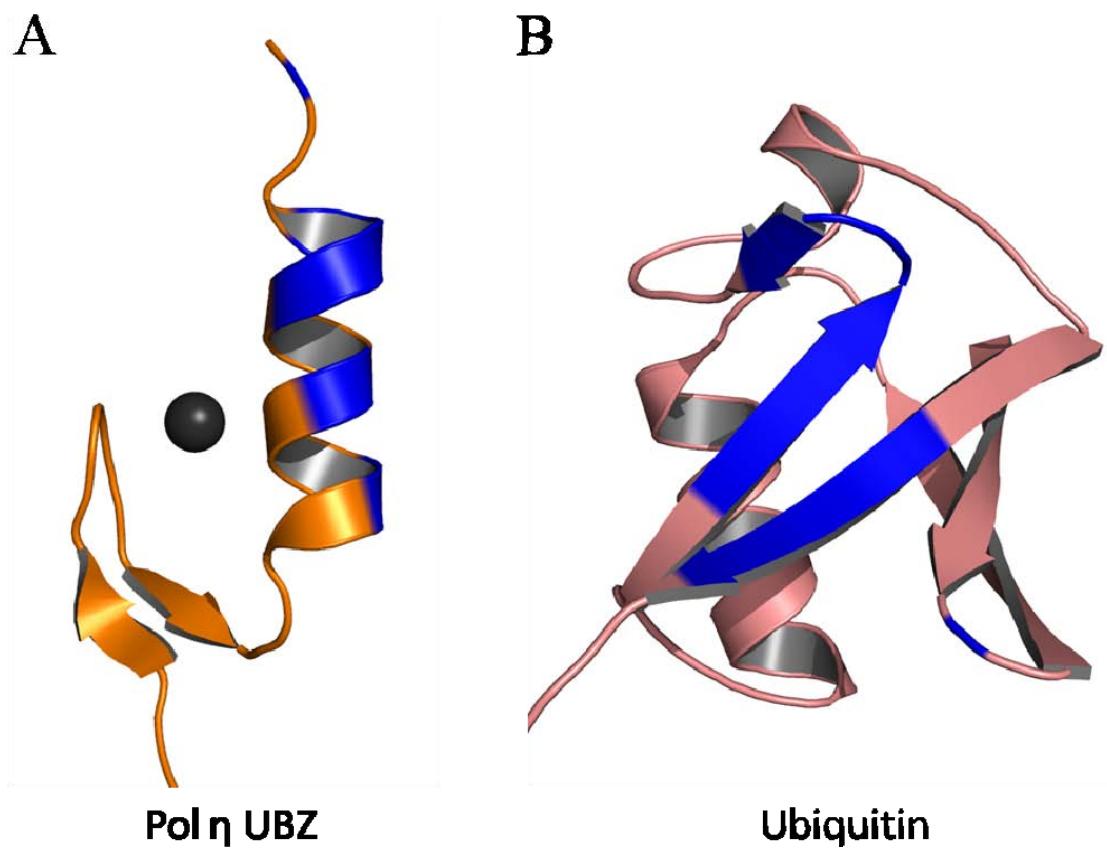


Figure 1.8 (A) NMR solution structure of the UBZ motif and (B) the X-ray crystal structure of ubiquitin. The regions of interaction between the UBZ and ubiquitin motifs are shown in blue. The zinc ion of the UBZ motif is shown in grey. (PDB ID: 2I50 and 1UBQ)

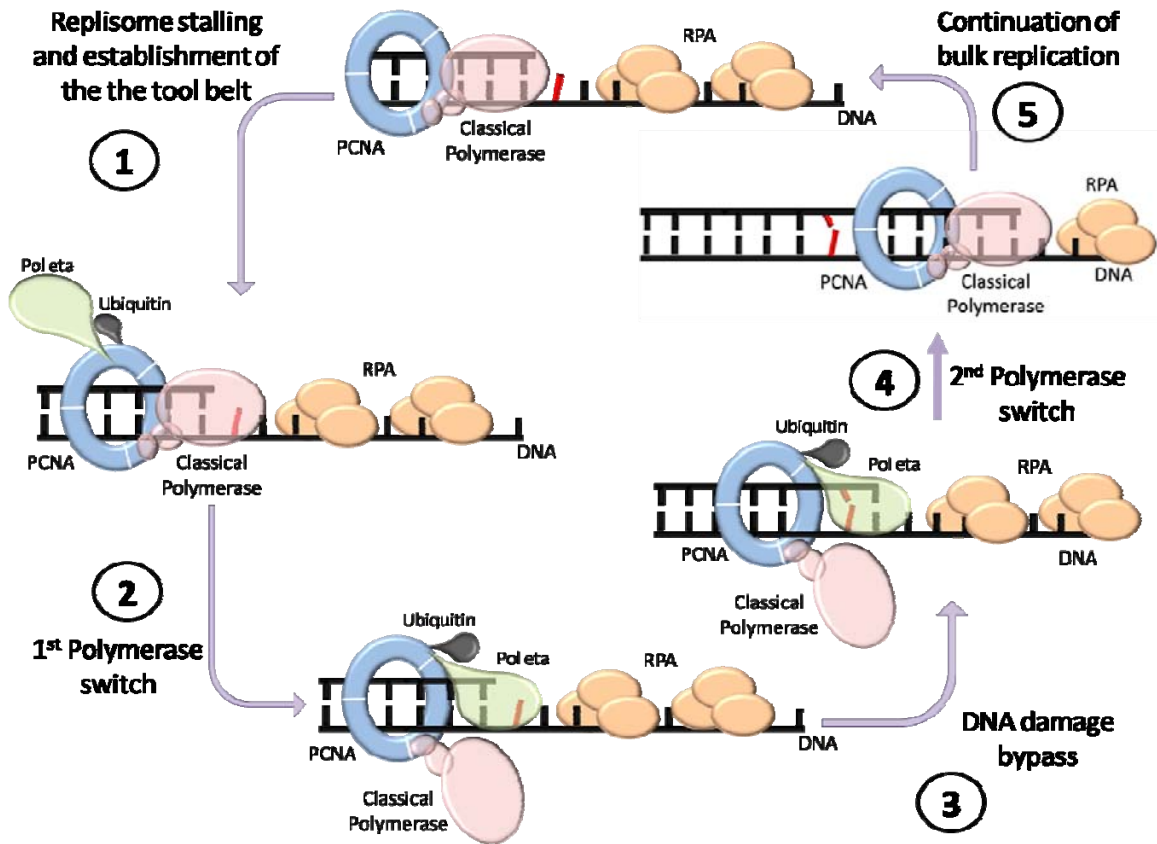


Figure 1.9 The tool belt model. The tool belt model with PCNA being ubiquitinated and establishing the “belt” that is able to bind multiple polymerases simultaneously. The steps of lesion bypass during translesion synthesis are the same as shown in Figure 1.4.

CHAPTER 2
STRUCTURE OF A MUTANT FORM OF PROLIFERATING
CELL NUCLEAR ANTIGEN THAT BLOCKS TRANSLESION
DNA SYNTHESIS

Abstract

Proliferating cell nuclear antigen (PCNA) is a homotrimeric protein that functions as a sliding clamp during DNA replication. Several mutant forms of PCNA that block translesion DNA synthesis have been identified in genetic studies in yeast. One such mutant protein (encoded by the *rev6-1* allele) is a glycine to serine substitution at residue 178, located at the subunit interface of PCNA. To better understand how this substitution interferes with translesion synthesis, I have determined the X-ray crystal structure of the G178S PCNA mutant protein. This substitution has little effect on the structure of the domain in which the substitution occurs. Instead, significant, local structural changes are observed in the adjacent subunit. The most notable difference between mutant and wild type structures is in a single, extended loop (comprising amino acid residues 105-110), which I call loop J. In the mutant protein structure, loop J adopts a very different conformation in which the atoms of the protein backbone have moved by as much as 6.5 Å from their positions in the wild type structure. To better understand the functional consequences of this structural change, I have examined the ability of this mutant protein to stimulate nucleotide incorporation by DNA polymerase eta (pol η). Steady state kinetic studies show that while wild type PCNA stimulates incorporation by pol η opposite an abasic site, the mutant PCNA protein actually inhibits incorporation opposite this DNA lesion. These results show that the position of loop J in PCNA plays an essential role in facilitating translesion synthesis. (The work described in this chapter was published in Freudenthal et al. (2008) *Biochemistry* **47**, 13354-13361.)

Introduction

DNA damage in the template strand blocks replication by classical DNA polymerases, which are involved in normal DNA replication and repair. In order to overcome these replication blocks, cells employ several non-classical DNA polymerases that are capable of replicating through template DNA lesions in a process called translesion DNA synthesis^{34,188,189}. One such enzyme is eukaryotic DNA polymerase eta (pol η), which is a 71-kDa monomeric protein encoded by the *RAD30* gene in yeast⁸⁰. Pol η functions in the replication of a few types of DNA lesions, including thymine dimers^{75,80,190} and 8-oxoguanines^{89,90}. Deletion of the *RAD30* gene in yeast leads to an increase in ultraviolet (UV) radiation-induced mutagenesis^{81,82,191}, and in humans, inactivation of pol η is responsible for the variant form of xeroderma pigmentosum (XPV)^{83,84}, which results in greater cancer susceptibility. Another non-classical DNA polymerase in eukaryotes is DNA polymerase zeta (pol ζ), which is comprised of a 173-kDa catalytic subunit and a 29-kDa accessory subunit encoded in yeast by the *REV3* and *REV7* genes, respectively^{183,192}. Pol ζ functions in the error-prone replication of a wide range of DNA lesions, and disruptions of the *REV3* and *REV7* genes result in a drastic decrease in the frequency of DNA damage-induced mutations in yeast^{193,194}. Moreover, expression of anti-sense RNA to pol ζ leads to a reduction in the frequency of UV radiation-induced mutations in human cells¹⁹⁵.

A key factor in translesion synthesis is proliferation cell nuclear antigen (PCNA). PCNA, encoded in yeast by the *POL30* gene, is a ring-shaped, homotrimeric protein that acts as a sliding clamp for classical DNA polymerases^{6,103}. Many protein factors involved in DNA replication and repair interact with PCNA via their PCNA-interacting peptide (PIP) motifs that bind along the inter-domain connector loop of PCNA¹⁹⁶. Pol η binds to PCNA in this manner, and this interaction is necessary for pol η function *in vivo*^{96,125}. Moreover, this interaction stimulates the enzymatic activity of pol η *in vitro*⁹⁶. Pol ζ ,

although lacking a PIP motif, also interacts with PCNA, and its enzymatic activity is stimulated by PCNA¹⁹⁷.

Several PCNA mutant proteins in yeast have been identified that interfere with translesion synthesis *in vivo*^{107,186,187}. One of these is encoded by the *pol30-178* allele (formerly called the *rev6-1* allele); it encodes a mutant form of PCNA in which Gly-178 is substituted with a serine¹⁸⁶. This amino acid substitution is at the subunit interface of PCNA, and genetic studies have shown that translesion synthesis by both pol η and pol ζ is completely blocked in cells expressing only this mutant form of PCNA¹⁸⁶. All other aspects of DNA replication and repair appear to occur normally in cells expressing this PCNA mutant protein¹⁸⁶. Another PCNA mutant protein that blocks translesion synthesis, but supports normal cell growth is encoded by the *pol30-113* allele¹⁸⁷. In this mutant protein, Glu-113 is substituted with a glycine. Interestingly, Glu-113 is also located at the subunit interface of PCNA directly opposite from Gly-178 on the neighboring subunit. Based on the fact that these mutant proteins block translesion synthesis without interfering with normal DNA replication, the structural changes resulting from these amino acid substitutions are likely subtle.

To understand the structural and mechanistic basis of the defect in the PCNA G178S mutant protein's ability to support translesion synthesis, I determined the X-ray crystal structure of this mutant protein to a resolution of 2.9 Å. I found that the substituted serine side chain forms a new hydrogen bond with the backbone carbonyl of Glu-113 on the adjacent subunit. This contact results in an extended loop on the adjacent subunit (comprising amino acid residues 105-110, which I refer to as loop J) changing its conformation and moving it into an aberrant position that deviates as much as 6.5 Å from its position in the wild type structure. I have examined the biochemical relevance of this structure by carrying out steady state kinetic studies with a model non-classical polymerase, pol η , in the presence of the wild type and mutant PCNA proteins. I found that while wild type PCNA stimulates incorporation by pol η opposite an abasic site, the

mutant PCNA protein inhibits incorporation opposite this DNA lesion. These findings suggest that the proper conformation of loop J is essential for translesion DNA synthesis.

Materials and Methods

Protein Expression and Purification

Wild-type and mutant PCNA proteins from *Saccharomyces cerevisiae* were over-expressed in *E. coli* Rosetta-2 (DE3) cells harboring pET-11a vectors into which wild type or mutant PCNA genes were cloned using BamHI and NdeI restriction sites. PCNA proteins were N-terminally FLAG tagged for rapid purification during PCR. Transformed cells were grown at 37°C in Overnight Express Instant TB Medium (Novagen) for 12 hrs. Cells were lysed in 50mM TrisCl, pH 7.5, 150mM NaCl, 1mM PMSF, 1mg/ml lysozyme, with a Complete Mini Protease Inhibitor Cocktail tablet (Roche). Following ultracentrifugation, the crude extract was loaded onto a 15 ml resin bed of Anti-FLAG M2 Affinity Gel (Sigma) by gravity flow for at least three successive passes. The resin was then washed with ten column volumes of a high salt wash consisting of 1M NaCl and 50mM TrisCl, pH 7.5. Next a low salt wash was performed with 10 column volumes of 150mM NaCl and 50mM TrisCl, pH 7.5. Following the washes the protein was eluted by three column volumes of a FLAG peptide solution at 100 µg/ml in the low salt wash. The eluted PCNA protein was then concentrated to 1ml and run on a Superdex G-75 column equilibrated with 20mM TrisCl, pH 7.5, 1mM DTT, and 250mM NaCl. Yeast pol η was over-expressed and purified as previously described¹⁹⁸. Briefly, pol η was over-expressed in yeast strain BJ5464 as a GST-fusion and the tag was removed using PreScission protease. Replication factor C (RFC) was provided by Manju M. Hingorani (Wesleyan University). All purified proteins were stored in aliquots at -80 °C.

Crystallization of the PCNA G178S mutant protein

Crystallization of the G178S PCNA mutant protein was performed manually using the hanging drop method with 4 μ l drops. To identify ideal crystallization conditions, an initial screen utilized conditions similar to those which produce wild type PCNA crystals¹⁰³. The formation of protein crystals was enhanced by utilizing a fresh protein prep and trays being set up immediately after gel filtration. Optimally diffracting crystals were generated by combining an equal volume of protein at (20 mg/ml monomer concentration) with a reservoir solution containing 2.06 M ammonium sulfate and 0.1 M sodium citrate, pH 5.8. Cubic crystals formed within 16 h at 18°C.

Data Collection and Structural Determination

G178S PCNA protein crystals were presoaked in a mother liquor containing 10% (v/v) glycerol prior to being flash frozen at 100 K. Mounted crystals were subsequently used for data collection at 100 K at the 4.2.2 synchrotron beamline at the Advanced Light Source in the Ernest Orlando Lawrence Berkeley National Laboratory. The data were collected with a crystal to detector distance of 150 mm. The data were analyzed and scaled using d*trek¹⁹⁹ to a resolution of 2.9 Å and the space group was determined to be P2₁3, which is the same space group into which the wild type PCNA protein crystallizes¹⁰³.

We carried out molecular replacement using the known structure of wild type PCNA (1PLQ) and the PHASER program²⁰⁰ to produce a model with the P2₁3 space group. To remove any structural bias, simulated annealing was performed using the PHENIX program²⁰¹ prior to any refinement. Further structural refinement was executed using PHENIX and REFMAC5 from the CCP4 package²⁰⁰. Model building was carried out using Coot and O²⁰². The O program was used to build loop J in baton mode with the aid of Dr. S. Ramaswamy. The coordinates have been deposited in the PDB with ID number 3F1W.

DNA substrates

For DNA polymerase activity assays, a synthetic 68-mer oligodeoxynucleotide with the sequence 5'-Biotin-GAC GGC ATT GGA TCG ACC TCX AGT TGG TTG GAC GGG TGC GAG GCT GGC TAC CTG CGA TGA GGA CTA GC-Biotin, was used as the template strand where X is an abasic site or a non-damaged guanine. For the running start abasic bypass assays, a synthetic 31-mer oligodeoxynucleotide with the sequence 5'- TCG CAG GTA GCC AGC CTC GCA CCC GTC CAA C was used as a primer. For the steady state kinetic studies, a synthetic 31-mer oligodeoxynucleotide with the sequence 5'-GGT AGC CAG CCT CGC ACC CGT CCA ACC AAC T, was used as a primer. Primer strands were 5'-³²P-end-labeled using T4 polynucleotide kinase (New England Biolabs) and (³²P- γ)ATP (PerkinElmer) at 37°C for one hour. Labeled primer strands were separated from unreacted (³²P- γ)ATP with a Sephadex G-25 spin column (GE Healthcare). Template strands and labeled primer strands (1 μ M each) were annealed in 25 mM Tris-Cl, pH 7.5, 100 mM NaCl by heating to 90°C for 8 min and slow cooling to 22°C over night. Labeled and annealed DNA substrates were stored at 4°C for up to 2 weeks.

Polymerase activity assays

All experiments were carried out in 40 mM TrisCl pH 7.5, 8mM MgCl₂, 150mM NaCl, 1mM DTT, and 100 μ g/ml bovine serum albumin. Reactions also contained a 10-fold molar excess of streptavidin over DNA to block the ends of the DNA to prevent PCNA dissociation. The wild type or mutant PCNA proteins were loaded onto the DNA substrates by incubating 90 nM PCNA (trimer concentration), 20 nM DNA, 25 nM RFC, and 500 μ M ATP for 5 minutes at 22°C. Reactions also contained various concentrations of dGTP (0 to 100 μ M for the abasic site template) or dCTP (0 to 5 μ M for the non-damaged template). Each dNTP was obtained from New England Biolabs. Reactions were initiated by adding 1 nM pol η and were quenched after 10 min by the addition of

10 volumes of formamide loading buffer (80% deionized formamide; 10 mM EDTA, pH 8.0; 1 mg/ml xylene cyanol; 1 mg/ml bromophenol blue). Extended primers (the product) and unextended primers (the substrate) were separated on a 15% polyacrylamide sequencing gel containing 8 M urea. The intensities of the labeled gel bands were determined using the InstantImager (Packard). Each experiment was repeated several times to ensure reproducibility and the rates were all in close agreement. The rate of product formation was graphed as a function of dNTP concentration, and the data were fit to the hyperbolic equation using SigmaPlot 10.0. The V_{\max} and K_m values were obtained from the best fit of the data to the Michaelis–Menten equation.

The running start abasic site bypass assay was performed under identical conditions as the steady state kinetic studies except that 20 μ M of each dNTP was used. Reactions were quenched after 5, 10, and 15 min by the addition of 10 volumes of formamide loading buffer, and reaction products were visualized on a 15% polyacrylamide sequencing gel containing 8 M urea.

Results

Overview of the PCNA G178S protein structure

I determined the X-ray crystal structure of the PCNA G178S mutant protein to a resolution of 2.9 Å, statistics are shown in Table 2.1. Figure 2.1 shows an overview of the structure of the PCNA G178S mutant protein trimer. Each subunit is comprised of two domains arranged in the trimeric ring in a head-to-tail fashion with domain A (residues 1-118) of one subunit interacting with domain B (residues 135-240) of its neighbor. Within each subunit, domains A and B are linked by the inter-domain connector loop (residues 119-134). No large-scale differences in the structure of the PCNA G178S mutant protein and the wild type PCNA protein are detectible.

Figure 2.2A shows a closer view of the subunit interface of the PCNA mutant protein. The G178S substitution is located in β strand D₂ of domain B of the upper

subunit. The side chain hydroxyl group of the substituted serine forms a new hydrogen bond with the backbone carbonyl of Glu-113 on the adjacent subunit. The two oxygen atoms are 2.6 Å apart, which is typical for a hydroxyl group-carbonyl group hydrogen bond. Glu-113 is in β strand I_1 , which forms an anti-parallel β sheet with strand H_1 . In the mutant protein structure, the new hydrogen bond between Ser-178 and Glu-113 alters the trajectory of this anti-parallel β sheet. This is most clearly seen by superimposition of the structures of the wild type and mutant PCNA proteins, as shown in Figures 2.2B and 2.3.

Loop J in the wild type and Mutant Protein Structures

Altering the trajectory of the H_1 and I_1 anti-parallel β sheet results in structural changes in the extended loop between strands H_1 and I_1 (residues 105-110), which I refer to as loop J, as shown in Figure 2.3. In the mutant protein structure, this loop adopts a very different conformation in which the atoms of the protein backbone have moved significantly from their positions in the wild type structure. For example, the α carbon of Lys-107 has moved 6.5 Å from its position in the wild type protein structure. Figure 2.4 shows the protein backbone and electron density of loop J in its aberrant conformation in the mutant protein structure overlaid with the protein backbone of loop J in its usual conformation in the wild type protein structure. Based on the clear electron density of loop J in both the wild type and mutant protein structures, it is important to note that loop J is not merely becoming more flexible and disordered in the mutant protein structure. Instead this loop has shifted from one stable configuration in the wild type structure to another stable configuration in the mutant protein structure.

It should also be pointed out that the shift in loop J in this structure is not the result of crystal packing. The space group and unit cell dimensions of our crystals are the same as those of reported for the wild type protein¹⁰³, so observed structural differences cannot be attributed to crystal packing. Moreover, in the crystal lattice, loop J does not

contact any proteins from neighboring asymmetric units; rather, it sticks out into solvent-filled spaces of the crystal lattice (Figure 2.5).

Comparison of the two PCNA Domains

To gain insight into global structural changes occurring to PCNA as a result of the G178S substitution beyond the affected loop J, I superimposed the protein backbone of the structures of the wild type and mutant subunits (Figure 2.6). Domain B which contains the G178S substitution is structurally identical to the wild type form of PCNA. By contrast, domain A is affected by the G178S mutation due to the G178S substitution on the adjacent monomer. To quantify the degree of structural differences between the wild type and mutant forms of PCNA, I calculated RMSD values between the backbone of the wild type and mutant forms of PCNA for each domain independently. The backbone RMSD value for the domain which contains the G178S mutation (domain B) is 0.50 Å. The RMSD value for the domain without the mutation (domain A) is three times as large at 1.3 Å. Thus, these results show that the G178S mutation is affecting the structure of PCNA by acting in *trans* to alter the structure of the neighboring monomer's domain A.

In summary, the only notable structural difference between the wild type and mutant forms of PCNA is in domain A with the largest change being in the position of loop J. Thus it is highly likely that the aberrant conformation of loop J is responsible for the effect of this mutation on translesion DNA synthesis.

Impact of the mutant PCNA Protein on the Activity of Pol η

Previous genetic studies have shown that this mutant protein blocks translesion DNA synthesis¹⁸⁶. To better understand how the structural changes described here interfere with translesion DNA synthesis, I have directly measured the enzymatic activity of the non-classical DNA polymerase pol η in the presence and absence of the wild type and mutant PCNA protein. Similar studies have previously shown that wild type PCNA

enhances the ability of pol η to incorporate nucleotides opposite an abasic site⁹⁶. Figure 2.7 shows the incorporation of pol η opposite an abasic site in a running start assay in the absence of PCNA and in the presence of either the wild type or mutant form of PCNA. The presence of wild type PCNA stimulates the ability of pol η to incorporate a nucleotide opposite the abasic site compared to pol η alone. By contrast, the mutant protein appears to have no ability to stimulate incorporation opposite the abasic site.

To quantify the effects of wild type and mutant PCNA proteins on the enzymatic activity of pol η , I measured the kinetics of dGTP (the preferred incoming dNTP) incorporation opposite the abasic site under steady state conditions. The rate of incorporation was plotted as a function of dGTP concentration (Figure 2.8) the V_{\max} and K_m steady state kinetic parameters were obtained from the best fit of the data to the Michaelis-Menten equation, and these parameters are provided in Table 2.2. The catalytic efficiency (V_{\max}/K_m) of incorporation opposite the abasic site by pol η was reproducibly 2 to 4-fold greater in the presence of wild type PCNA than in the absence of PCNA, and this was due mainly to a decrease in the K_m for nucleotide incorporation as has been previously reported. By contrast, the catalytic efficiency was not greater in the presence of the G178S PCNA mutant protein than in its absence. In fact, the catalytic efficiency was reproducibly 2 to 4-fold lower in the presence of the mutant PCNA than in its absence. It should be noted that like wild type PCNA, the mutant PCNA protein also decreased the K_m for nucleotide incorporation in this context. The V_{\max} for incorporation in the presence of the mutant form of PCNA, however, was ~10-fold lower than incorporation in its absence. Thus the mutant form of PCNA actually inhibits the ability of pol η to incorporate nucleotides opposite abasic sites.

The inhibitory effect observed with the mutant PCNA protein requires the mutant protein to be loaded onto the primer-template DNA. I showed this by omitting either replication factor C (RFC, the ATP-dependent PCNA-loading protein) or ATP from the reaction so that the mutant PCNA protein would not be loaded onto the DNA. In these

experiments, the efficiencies of nucleotide incorporation by pol η were exactly the same as those measured when no PCNA was present. For example, when I omitted ATP, the catalytic efficiency of incorporation opposite the abasic site in the presence of the unloaded mutant PCNA protein was 0.028, which is identical to the catalytic efficiency of 0.029 determined in the absence of PCNA (Table 2.2). Thus I observed no inhibition of pol η -catalyzed nucleotide incorporation opposite abasic sites when the mutant form of PCNA was not loaded on the DNA substrate.

To determine whether the inhibition by this mutant PCNA protein is specific to abasic sites, I used steady state kinetics to examine if the mutant form of PCNA could inhibit the incorporation of nucleotides opposite non-damaged DNA. Figure 2.9 shows the rate of dCTP incorporation opposite a non-damaged G by pol η as a function of nucleotide concentration. Here again the catalytic efficiency of incorporation opposite the non-damaged template was reproducibly 2 to 4-fold greater in the presence of wild type PCNA than that in its absence (Table 2.2). In this case, the increased catalytic efficiency in the presence of wild type PCNA was due to both an increase in the V_{\max} and a decrease in the K_m for nucleotide incorporation in the presence of wild type PCNA. The mutant PCNA protein inhibited the ability of pol η to incorporate opposite the non-damaged DNA to a 2 to 4-fold lower level of activity than pol η alone, and this was mainly due to an increase in the K_m for nucleotide incorporation. Thus this mutant protein inhibits nucleotide incorporation by pol η opposite both damaged and non-damaged templates.

Discussion

Interactions between PCNA and non-classical polymerases have been shown to be essential for translesion synthesis. Pol η possesses a PCNA-interacting peptide (PIP) motif at its extreme C-terminus (residues 621-628). While a pol η mutant protein truncated at position 624 shows activity *in vitro*, yeast expressing this truncated version of pol η have the same defect in translesion synthesis as yeast completely lacking pol η ⁹⁶.

Thus the interaction between PCNA and pol η is essential to pol η 's function *in vivo*. This may be because the interaction between PCNA and pol η leads to an increase in the catalytic efficiency (V_{\max}/K_m) of nucleotide incorporation by pol η opposite damaged and non-damaged templates *in vitro*⁹⁶. Similarly, PCNA increases the DNA synthesis activity of pol ζ , which lacks a PIP motif, on both non-damaged DNA and UV-treated DNA¹⁹⁷. Incidentally, this also shows that there are functionally important interactions between non-classical polymerases and PCNA that are not mediated solely by PIP motifs.

Translesion synthesis by both pol η and pol ζ is severely defective in yeast expressing the G178S mutant form of PCNA. This was clearly demonstrated by experiments in which plasmids containing specific DNA lesions were transformed into various yeast strains such that the transformation efficiency indicated the efficiency of DNA damage bypass¹⁸⁶. The *rev6-1* strain (expressing the G178S mutant form of PCNA) bypasses both abasic sites and *cis-syn* thymine dimers at ~1 % efficiency compared to wild type¹⁸⁶. The *rev3 Δ* strain (lacking pol ζ) bypasses thymine dimers at ~94 % efficiency compared to wild type; abasic sites are bypassed at ~5 % efficiency¹⁸⁶. The *rad30 Δ* strain (lacking pol η) bypasses abasic sites at ~80 % efficiency compared to wild type; *cis-syn* thymine dimers are bypassed at ~15 % efficiency¹⁸⁶. Only in the *rad30 Δ rev3 Δ* strain are the efficiencies of bypassing either of these lesions as low as they are in the *rev6-1* strain¹⁸⁶.

To better understand why the G178S substitution in PCNA leads to a loss of function of both pol η and pol ζ , but no other discernable effects on DNA replication and cell growth, I determined the X-ray crystal structure of the mutant form of PCNA to a resolution of 2.9 Å. I found that while the global structures of the wild type and mutant protein are the same, there is a significant difference in the structure of a small region of PCNA near the subunit interface. The substituted Ser-178 side chain forms a new hydrogen bond with the backbone carbonyl of Glu-113 on the neighboring subunit. This new hydrogen bonds alters the trajectory the β sheet comprised of strands H₁ and I₁

(containing Glu-113). This has the effect of moving loop J as much as 6.5 Å in the structure of the mutant protein from its location in the structure of the wild type protein, Figure 2.3 and 2.4.

Since the alteration in loop J is the only significant difference between the wild type and mutant protein structures, I concluded that the proper positioning of loop J is critical for supporting translesion synthesis by both pol η and pol ζ. Further support for this notion comes from our structural studies of the E113G mutant form of PCNA, which leads to a similar defect in translesion synthesis as does the G178S mutant PCNA protein¹⁸⁷. Glu-113 is at the subunit interface directly across from Gly-178, and the side chain hydroxyl group on the G178S substitution forms a hydrogen bond with the backbone carbonyl of this residue. I have obtained crystals of the E113G mutant form of PCNA and collected X-ray diffraction data to a resolution of 3.8 Å. Comparisons of the electron densities at this resolution of the wild type, G178S mutant, and E113G mutant proteins show that loop J is also in an aberrant configuration in the structure of the E113G mutant protein as it is in the structure of the G178S protein (see Figures 2.10 and 2.11). Taken together, these data favor the hypothesis that loop J of PCNA makes an important direct contact with non-classical polymerases and that when loop J adopts an aberrant conformation in the case of these two mutant proteins, this contact is disrupted.

Additional evidence for the importance of loop J comes from previous structure-function studies of PCNA. These studies have shown that several substitutions in and around loop J (residues 105-110) have been found to lead to increased sensitivity to UV radiation and the DNA-damaging agent methyl methanesulfonate (MMS)¹⁰⁷. Cells expressing the E104A,D105A double mutant have a severe defect in the ability to grow following UV or MMS treatment¹⁰⁷. Cells expressing the K108A,D109A double mutant have a minor defect in the ability to survive MMS treatment¹⁰⁷. Cells expressing the D109A,R110A double mutant have a minor defect in the ability to survive UV and MMS

treatment¹⁰⁷. These studies provide additional compelling evidence that loop J of PCNA is critical for translesion DNA synthesis.

As described above, previous studies have shown that the interaction between PCNA and pol η that is mediated by the PIP motif of the polymerase is essential for translesion synthesis⁹⁶. It is important to note that the binding site for the PIP motif is located on the opposite face of the PCNA ring from loop J. The PIP motif binds to a hydrophobic pocket in domain B near the inter-domain connector loop. Incidentally, I observe no significant structural differences between the wild type and G178S mutant PCNA proteins in the regions of domain B or the inter-domain connector loop that bind the PIP motif. Loop J is located at the subunit interface and extends out from the opposite face of the PCNA ring. These observations imply that pol η can simultaneously interact with both faces of the PCNA ring. The feasibility of this model is supported by a structure of a complex containing the “little fingers” domain of *E. coli* pol IV, which is a Y-family polymerase related to pol η , and the β -clamp processivity factor, which is structurally similar to PCNA. The C-terminal peptide of pol IV (analogous to the pol η PIP motif) binds in a pocket on one face of the β -clamp ring, and the “little fingers” domain of pol IV binds at the subunit interface¹⁸⁰.

To gain further understanding of how the altered conformation of loop J of PCNA affects the function of pol η , I compared the impact of the wild type and mutant PCNA proteins on pol η 's activity. I found that this mutant protein fails to stimulate the activity of pol η on both abasic sites and non-damaged templates. Not only does it fail to stimulate pol η , this mutant form of PCNA actually inhibits the activity of pol η to levels 2 to 4-fold lower than that of pol η in the absence of PCNA. As a result, the activity of pol η in the presence of the G178S PCNA mutant protein is approximately 10-fold lower than its activity in the presence of wild type PCNA protein. To our knowledge, this is the first amino acid substitution in PCNA that inhibits the activity of a non-classical DNA polymerase. It should be pointed out that the E113G mutant proteins also failed to

stimulate the ability of pol η to incorporate nucleotides opposite an abasic site, although no inhibition was observed with this mutant protein (Figure 2.11A). It is unclear why the G178S mutant protein inhibits pol η and the E113G protein does not. One possibility is that subtle differences in the positions of loop J between these two mutant proteins accounts for this difference in function. While the position of loop J is aberrant in the structures of both mutant proteins, the position of the loop is closer to that of the wild type protein in the E113G protein structure (Figure 2.11B).

It should be noted that if RFC or ATP is omitted from the reaction, no inhibition of pol η is observed with the G178S PCNA mutant protein. This shows that the inhibition requires that the mutant PCNA protein be loaded onto the DNA substrate. The precise mechanism by which the G178S mutant form of PCNA inhibits the catalytic activity of pol η is unclear, and this awaits a more detailed understanding of precisely how wild type PCNA impacts the kinetic mechanism of nucleotide incorporation by pol η . However, one straightforward possibility is that without the requisite interaction between pol η and loop J of PCNA, the presence of PCNA on the DNA sterically interferes with the proper binding and positioning of pol η . This would prevent the formation of a productive polymerase-PCNA complex on the DNA, which may be responsible for the defect in translesion synthesis observed in cells expressing this mutant form of PCNA.

Finally, it had been suggested that the G178S substitution might block translesion synthesis by interfering with PCNA mono-ubiquitination¹⁸⁶, which is required for translesion synthesis¹⁵⁰. This is unlikely to be the case for several reasons. First, the site of mono-ubiquitination, Lys-164, is located in domain B of PCNA, which I have shown here to have the same structure in both the mutant and wild type proteins. Second, it has previously been shown that the E113G mutant form of PCNA, which appears to block translesion synthesis by the same mechanism as does the G178S mutant protein, is capable of being mono-ubiquitinated *in vitro* by the Rad6-Rad18 complex¹⁸⁷. It should be pointed out, however, that any ability or inability of the G178S mutant protein to be

mono-ubiquitinated is likely not relevant to understanding the mechanism by which this mutant protein blocks translesion synthesis. This is because the data presented here show that this mutant PCNA protein, even in the absence of mono-ubiquitination, inhibits the catalytic activity of pol η . This implies that the defect in translesion synthesis caused by this mutant protein is independent of its mono-ubiquitination state.

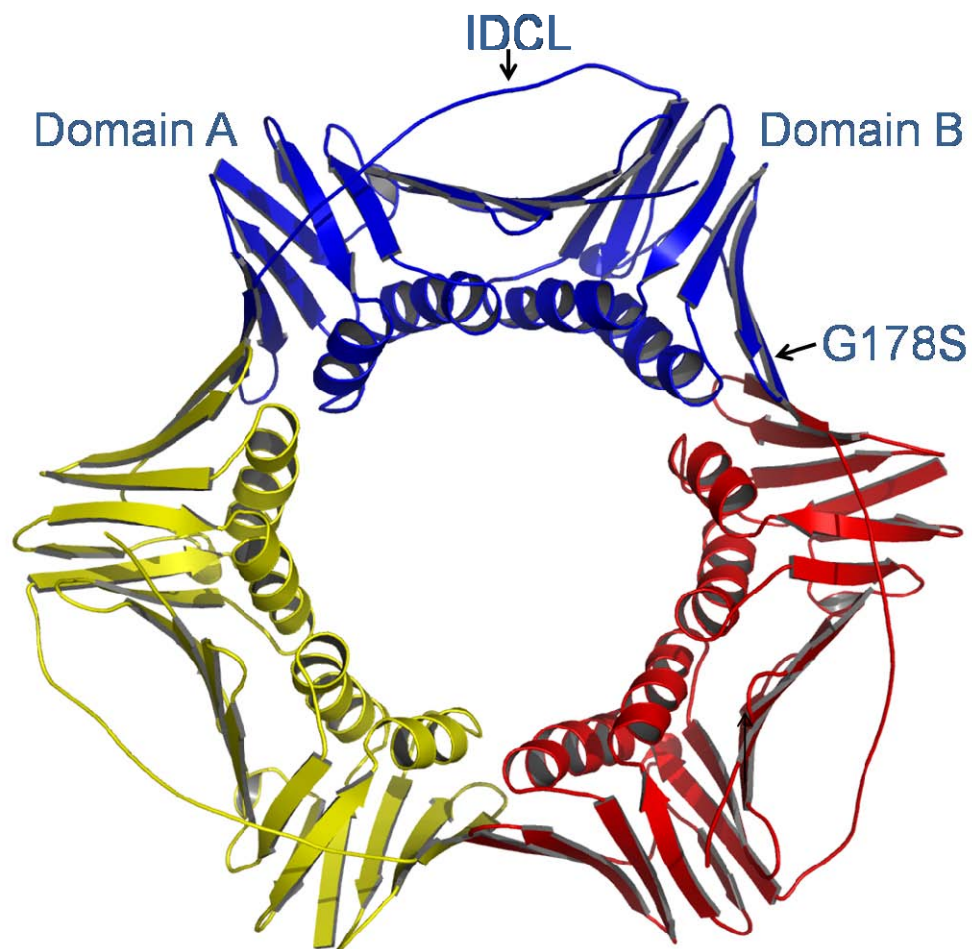


Figure 2.1 Structure of the PCNA G178S mutant protein. The trimeric form of the protein is shown with monomeric subunits in red, yellow, and blue. The inter-domain connecting loop (IDCL), domains A and B, and the G178S substitution are indicated on one of the subunits.

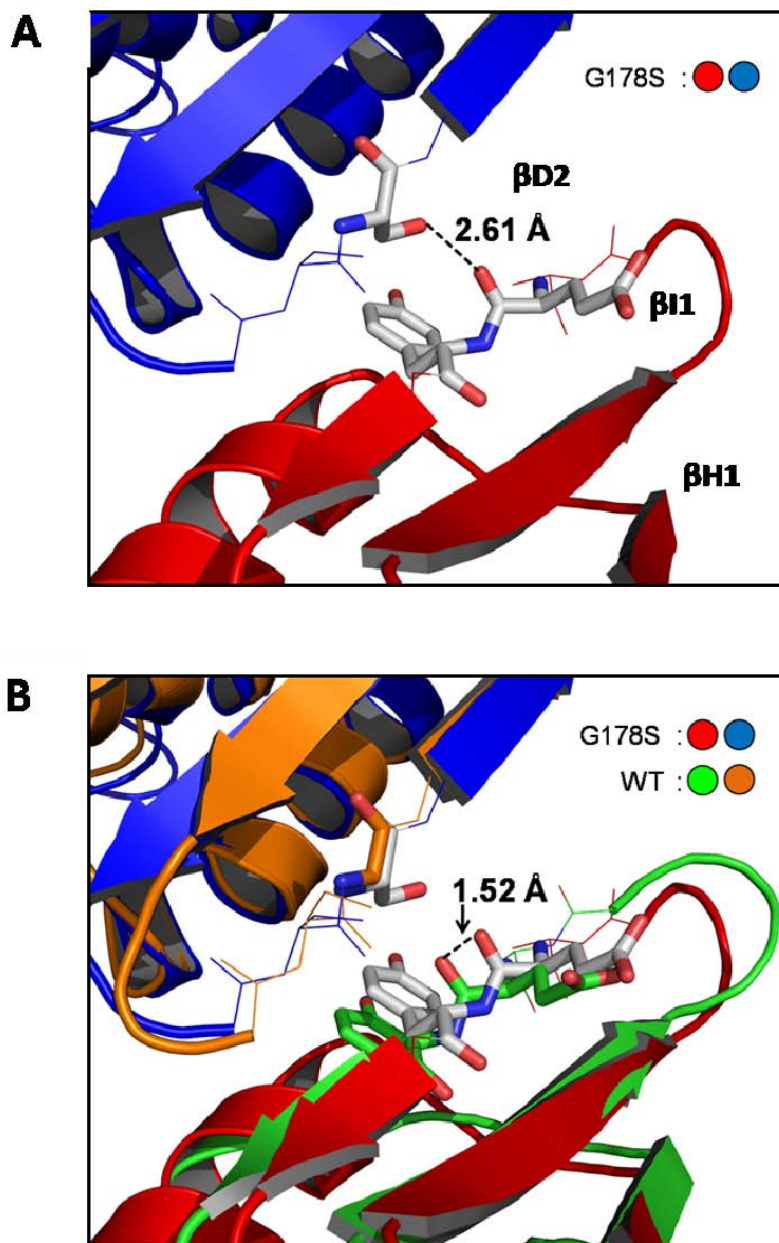


Figure 2.2 G178S subunit interface. (A) Close up, side view of the subunit interface with the Ser-178 substitution of the blue monomer and Tyr-114 and Glu-113 of the red monomer shown in stick format. The distance between the hydroxyl of Ser-178 and the backbone carbonyl of Glu-113 is indicated. (B) The superimposition of the structures of the G178S PCNA mutant protein and wild type PCNA (1PLQ). The distance between backbone carbonyl of Glu-113 in the wild type and mutant PCNA structures is indicated.

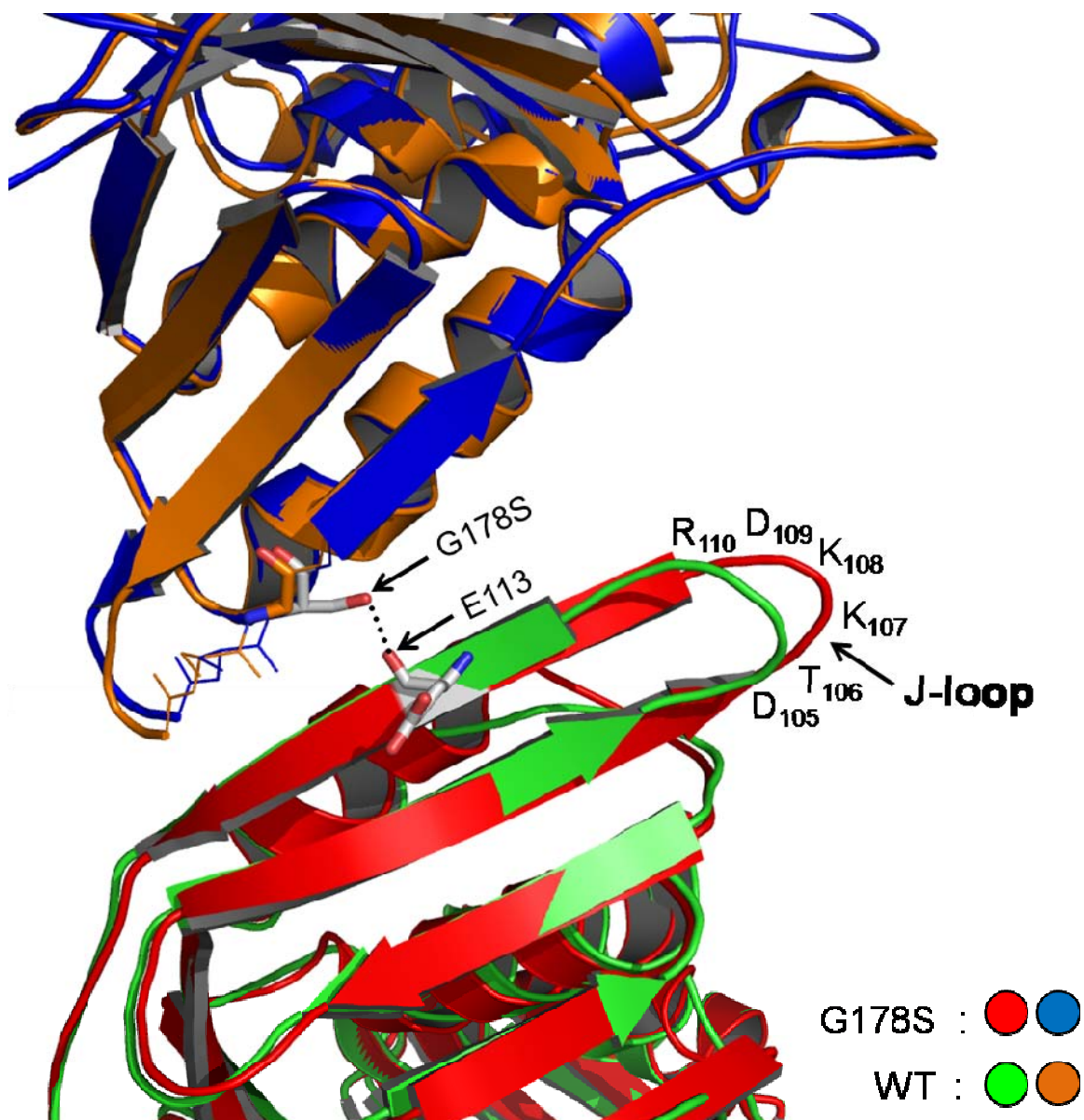


Figure 2.3 Conformation of loop J in the wild type and mutant structure. Superimposition of the wild type and G178S PCNA mutant protein structures is shown with the Ser-178 substitution and Glu-113 represented in stick format and the hydrogen bond between them shown as black dots. The amino acid residues of loop J are indicated.

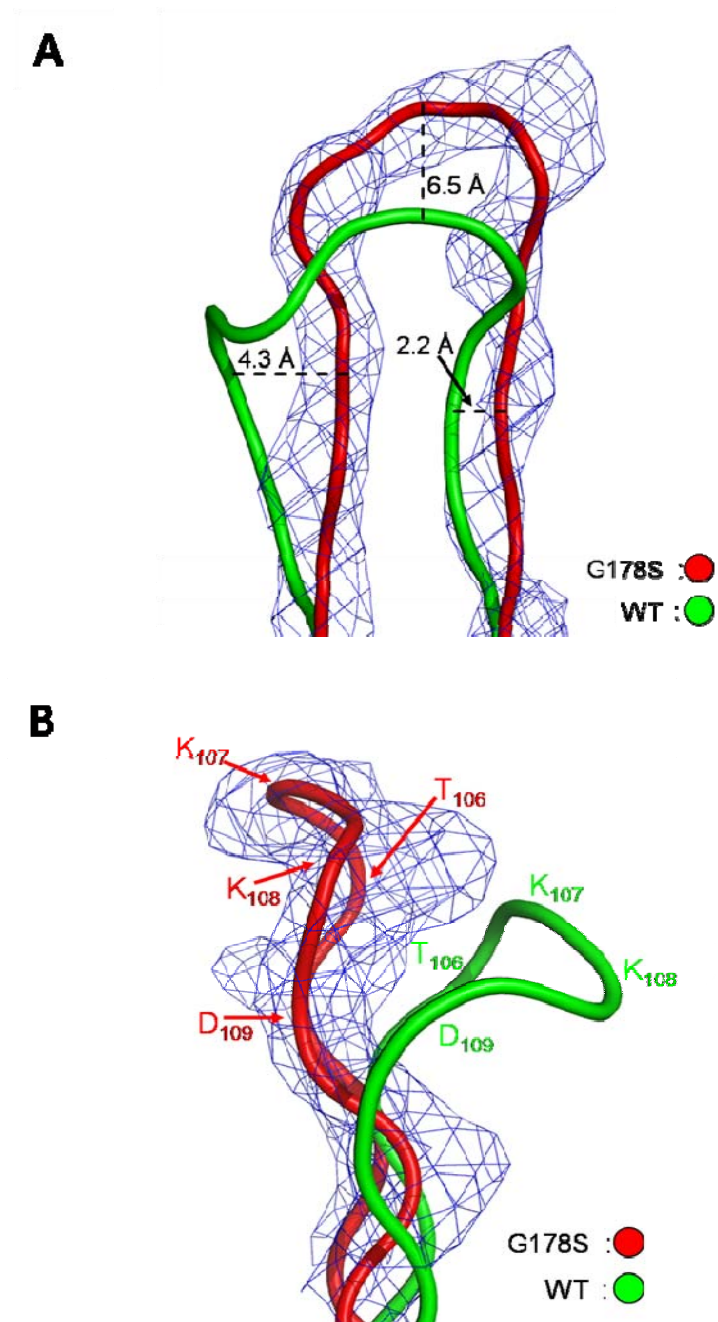


Figure 2.4 Close up view of loop J. (A) Electron density (level=2.0) for the G178S PCNA mutant protein and the backbone of the wild type and mutant proteins in ribbon representation. The distances between the wild type and mutant protein backbone are specified. (B) Side view of loop J with the position of the amino acid residues indicated.

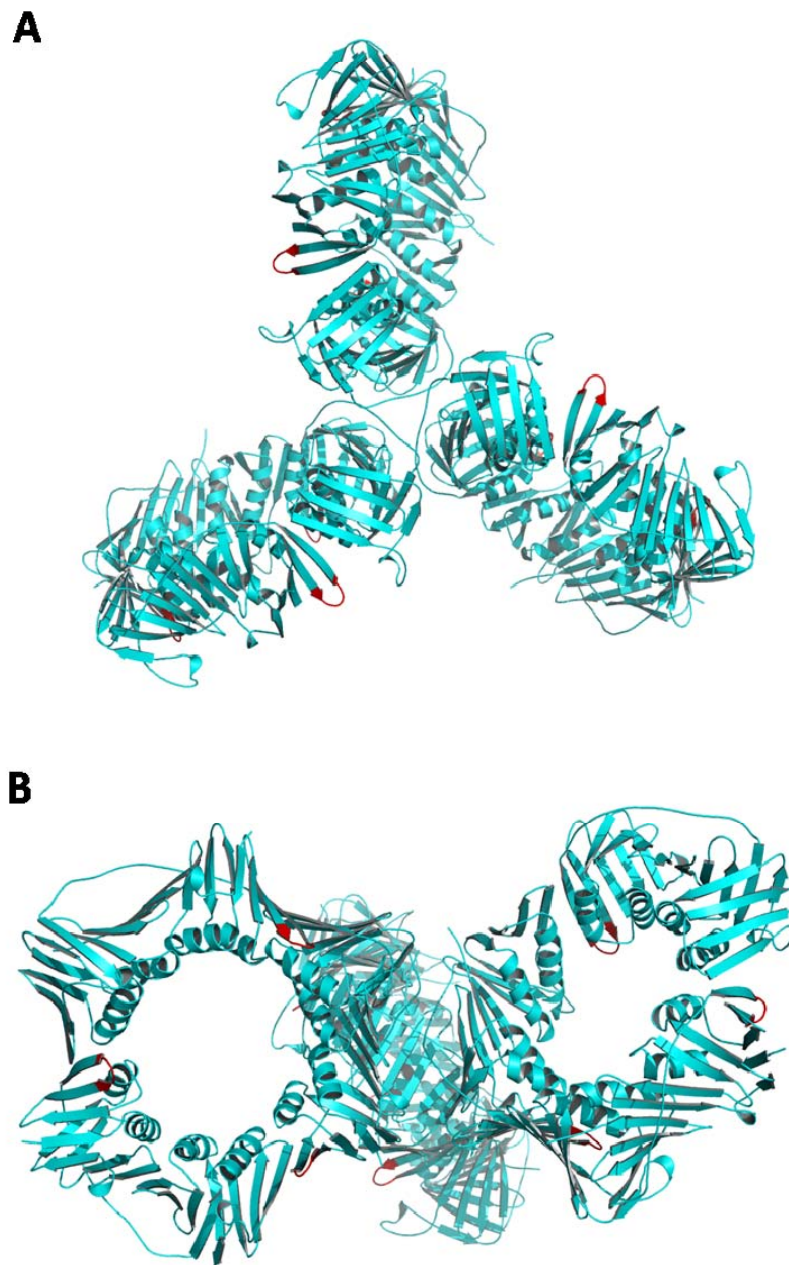


Figure 2.5 Crystal Packing of the G178S PCNA mutant protein. The crystal packing of three trimeric G178S PCNA mutant proteins is shown from the top (A) and side (B). All monomeric subunits are shown in cyan and loop J is shown in red. Both panels show the PCNA protein packing along the backside of the monomeric subunit near the inter-domain connector loop. This allows loop J to extend freely into the solvent-filled spaces of the crystal lattice.

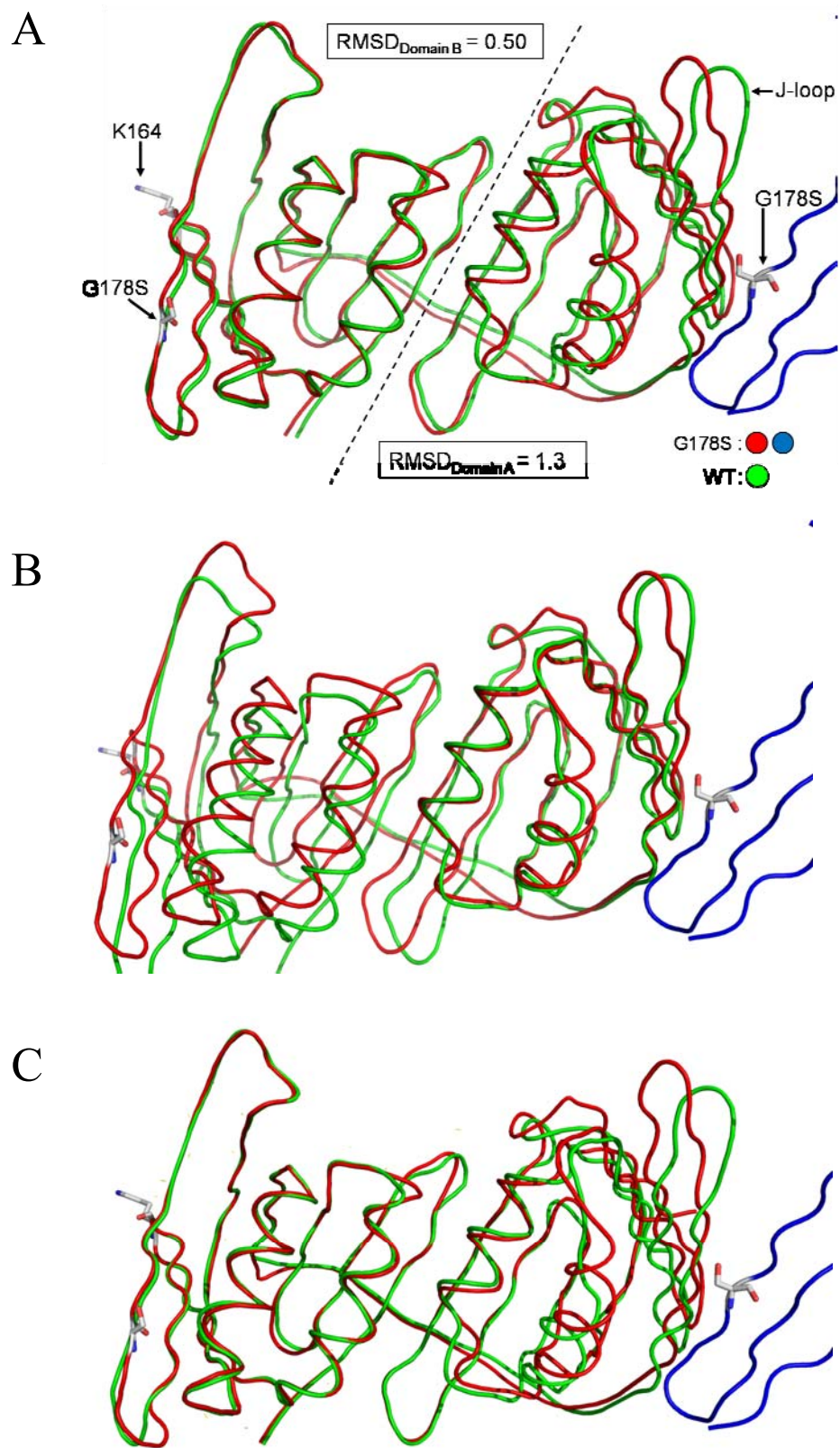


Figure 2.6 Superposition of the PCNA monomer backbone of wild type and mutant PCNA proteins.

Figure 2.6 continued. The monomeric subunit is lying on its side with the inter-domain connector loop in the back to allow the separate domains to be easily viewed. The adjacent mutant monomeric subunit is shown in blue with the G178S substitution indicated. The G178S substitution, the site of mono-ubiquitination (Lys-164), and loop J are indicated. Domains A and B of the monomeric subunit are separated by a dashed line and the RMSD values were independently determined for each domain. (A) Superposition of the entire full length wild type PCNA protein onto the entire G178S PCNA mutant protein. (B) Superposition of Domain A of the wild type PCNA protein onto Domain A of the mutant protein. (C) Superposition of Domain B of the wild type protein onto Domain B of the mutant protein.

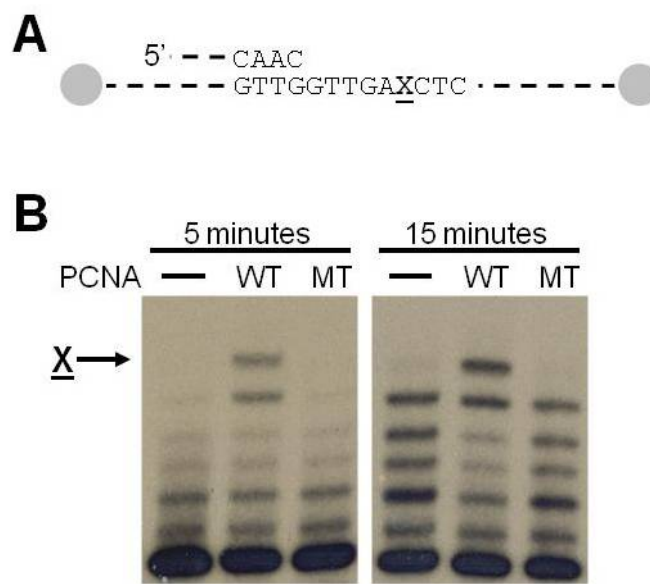


Figure 2.7 Running start experiment with pol η on an abasic site. (A) Schematic diagram of the 31/68-mer substrate used in the running start assays with the ends of the template strand containing biotin-streptavidin blocks. The X indicates the location of the abasic site (B) Autoradiograph of the synthesis products after five or fifteen minutes following the addition of pol η . The arrow indicates incorporation opposite the abasic site. Lanes labeled WT contain the wild type PCNA protein, and lanes labeled MT contain the G178S mutant PCNA protein.

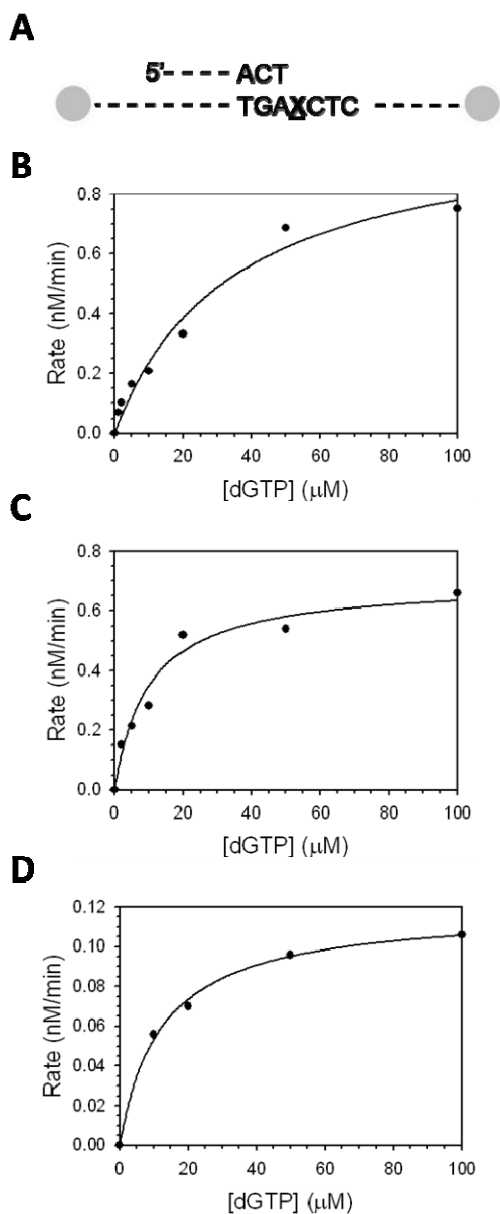


Figure 2.8 Steady state kinetics of pol η on an abasic site. (A) Schematic diagram of the substrate used in the running start assays with the ends of the template strand containing biotin-streptavidin blocks. The X indicates the location of the abasic site. The rate of nucleotide incorporation was graphed as a function of dGTP concentration for (B) pol η alone, (C) pol η with wild type PCNA protein, (D) and pol η with the G178S PCNA mutant protein. The solid lines represent the best fits of the data to the Michaelis–Menten equation, and the V_{\max} and K_m steady state parameters are given in Table 2.2 These graphs are from a single experiment and are representative of the trends that I observed over at least twenty independent experiments.

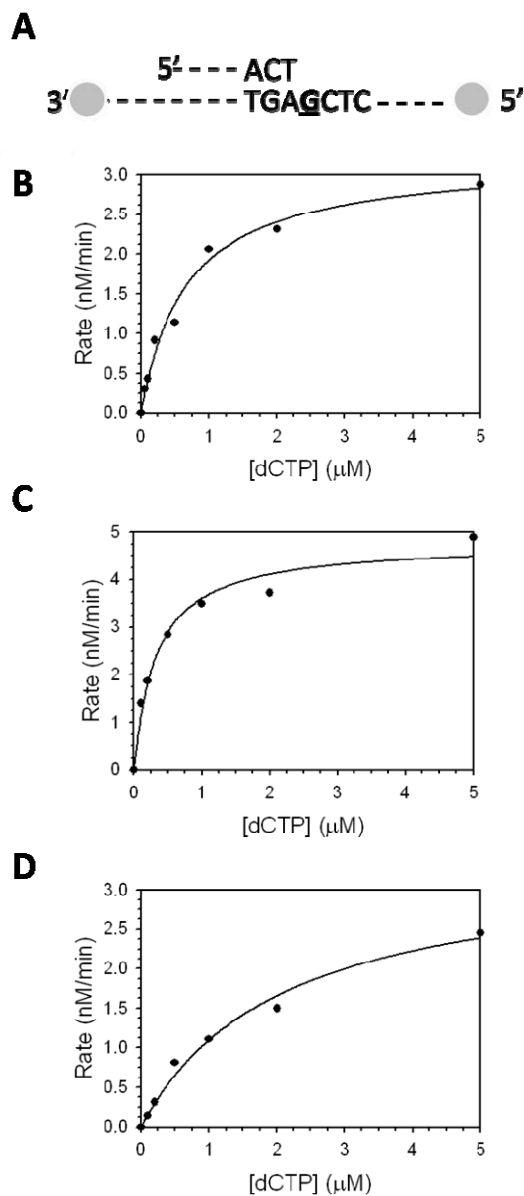


Figure 2.9 Steady state kinetics of pol η on non-damaged DNA. (A) Schematic diagram of the substrate used in the steady state kinetic assays with the ends of the template strand containing biotin-streptavidin blocks. The G indicates the location of the undamaged guanine. The rate of nucleotide incorporation was graphed as a function of dCTP concentration for (B) pol η alone, (C) pol η with wild type PCNA protein, (D) and pol η with the G178S PCNA mutant protein. The solid lines represent the best fits of the data to the Michaelis-Menten equation, and the V_{\max} and K_m steady-state parameters are given in Table 2.2 These graphs are from a single experiment and are representative of the trends that I observed over at least twenty independent experiments.

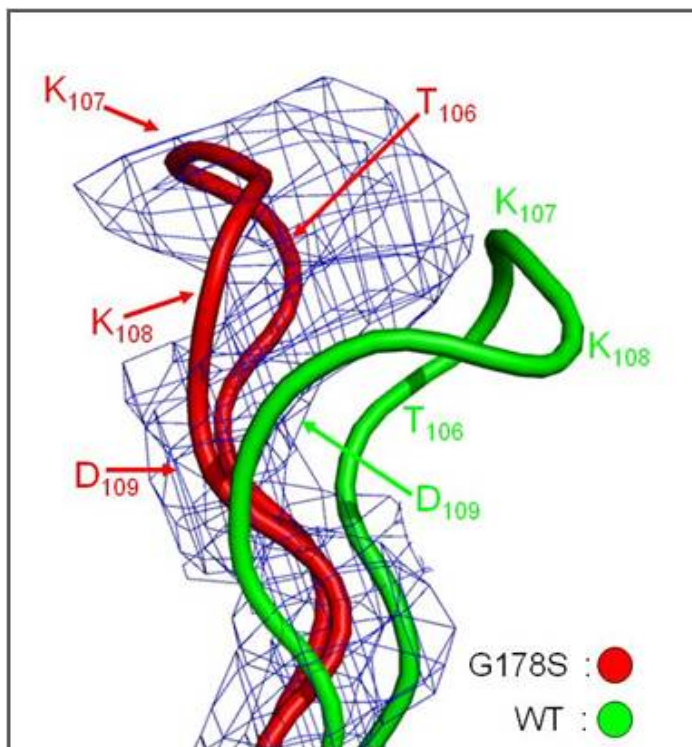


Figure 2.10 The position of loop J in the trimeric E113G mutant PCNA protein. I have obtained protein crystals of the E113G mutant PCNA protein. These crystals are in the same space group with the same unit cell dimensions as the G178S mutant protein crystals, described in Chapter 3. I have collected data on these crystals to a resolution of 3.8 Å. Shown here is the electron density (level=1.5) for the E113G mutant PCNA protein overlaid with the backbone for the wild type and G178S PCNA mutant protein in ribbon representation. The electron density for loop J of the E113G mutant protein appears much more like that of the G178S mutant protein than the wild-type PCNA protein.

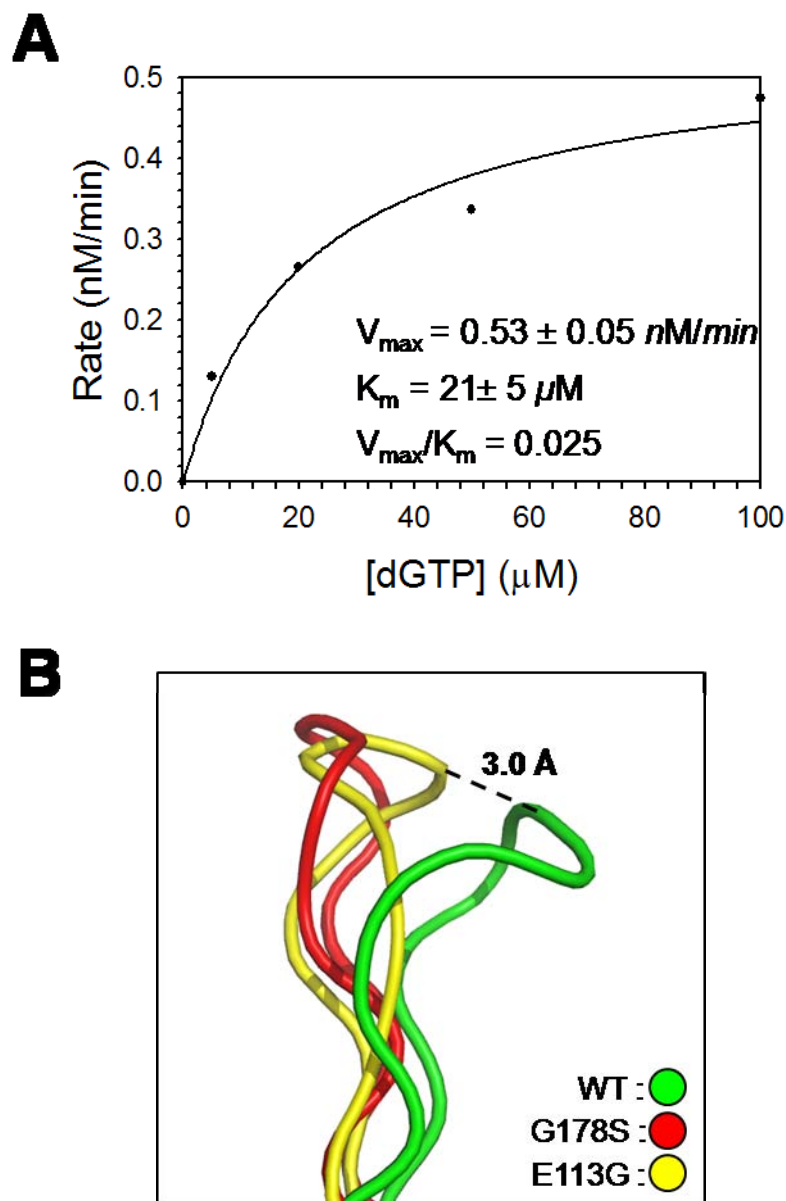


Figure 2.11 Kinetic and structural studies of the E113G PCNA mutant protein.

Steady state kinetics of pol η on an abasic site in the presence of the E113G PCNA mutant protein (A). The solid line represents the best fit of the data to the Michaelis-Menten equation with a V_{\max} and a K_m indicated. Shown in (B) are the positions of loop J in the wild-type (green), G178S mutant (red), and E113G mutant (yellow) protein structures. The distance between the αC of residue 107 in the wild-type and E113G protein structures is 3.0 Å. The analogous distance between the wild-type and G178S protein structures is 6.5 Å (see Figure 2.4).

Table 2.1 Data collection and refinement statistics for the G178S PCNA mutant protein

(A) Data collection statistics

Resolution (Å)	29.8-2.9 (3.0 – 2.9) ^a
Wavelength (Å)	1.072
Space group	P2 ₁ 3
Cell (Å)	a=123.13 b=123.13 c=123.13
Completeness (%)	100 (96.8)
Redundancy	10.79 (11.01)
I/σ _I	14.8 (2.50)
R _{merge} (%) ^b	7.3 (60.5)

(B) Refinement statistics

Resolution range (Å)	19.9 – 2.9
R (%) ^c	22.6
R _{free} (%) ^d	25.4
rms bonds (Å)	0.009
rms angles (°)	1.21
Number of water molecules	0
Number of protein atoms	1981 (254 a.a.)
Ramachandran analysis (%)	
Most favored	89.4
Allowed	10.6
PDB ID	3F1W

^a Values in parentheses relate to the highest resolution shell.

^b $R_{merge} = \frac{\sum_h \sum_i I_i(\mathbf{h}) - \langle I(\mathbf{h}) \rangle \sum_h \sum_i I_i(\mathbf{h})}{\sum_h \sum_i I_i(\mathbf{h})}$, where I_i is the i th measurement of reflection \mathbf{h} and $\langle I(\mathbf{h}) \rangle$ is a weighted mean of all measurements of \mathbf{h} .

^c $R = \frac{\sum |F_o| - |F_c|}{\sum |F_o|}$, where F_o and F_c are the observed and calculated structure factors, respectively.

^d R_{free} is defined in (Brunger 1992).

Table 2.2 Steady state kinetic parameters of pol η catalyzed nucleotide incorporation

Proteins	DNA	V_{\max} (nM/min)	K_m (μ M)	V_{\max}/K_m	Relative efficiency
Pol η alone	Abasic site	1.0 ± 0.1	34 ± 8	0.029	1.0
Pol η + wild type PCNA	Abasic site	0.70 ± 0.06	9.9 ± 3.0	0.071	2.4
Pol η + G178S PCNA	Abasic site	0.12 ± 0.01	12 ± 1	0.010	0.34
Pol η alone	Non-damaged	3.2 ± 0.2	0.67 ± 0.12	4.8	1.0
Pol η + wild type PCNA	Non-damaged	4.8 ± 0.3	0.32 ± 0.07	15	3.1
Pol η + G178S PCNA	Non-damaged	3.4 ± 0.3	2.1 ± 0.4	1.6	0.33

CHAPTER 3
A CHARGED RESIDUE AT THE SUBUNIT INTERFACE OF
PCNA PROMOTES TRIMER FORMATION BY DESTABILIZING
ALTERNATE SUBUNIT INTERACTIONS

Abstract

Eukaryotic proliferating cell nuclear antigen (PCNA) is an essential replication accessory factor that interacts with a variety of proteins involved in DNA replication and repair. Each monomer of PCNA has an N-terminal domain A and a C-terminal domain B. In the structure of the wild type PCNA protein, domain A of one monomer interacts with domain B of a neighboring monomer to form a ring-shaped trimer. Glu-113 is a conserved residue at the subunit interface in domain A. I have determined two distinct X-ray crystal structures of a mutant form of PCNA with a substitution at this position (E113G), which I previously studied because of its effect on translesion synthesis. The first structure was the expected ring-shaped trimer. The second structure was an unanticipated non-trimeric form of the protein. In this non-trimeric form, domain A of one PCNA monomer interacts with domain A of a neighboring monomer, while domain B of this monomer interacts with domain B of a different neighboring monomer. The B-B interface is stabilized by an anti-parallel β sheet and appears structurally similar to the A-B interface observed in the trimeric form of PCNA. The A-A interface, by contrast, is stabilized primarily by hydrophobic interactions. Because the E113G substitution is located at this hydrophobic surface, the A-A interface should be less favorable in the case of the wild type protein. This suggests that the side chain of Glu-113 promotes trimer formation by destabilizing these possible alternate subunit interactions. (The work described in this chapter was published in Freudenthal et al. (2009) *Acta Crystallographica Section D* **65** (Pt 6): 560-566.)

Introduction

Proliferating cell nuclear antigen (PCNA) is an essential eukaryotic replication accessory factor that interacts with and promotes DNA binding by a variety of proteins involved in DNA replication and repair^{104,121,122,203}. Normally PCNA exists as a stable, ring-shaped homotrimer with a central cavity through which double stranded DNA passes¹⁰³. The PCNA ring is loaded and unloaded from the DNA in an ATP-dependent manner by replication factor C (RFC)²⁰⁴⁻²⁰⁶. Once on the DNA, the PCNA trimer functions as a sliding clamp to enhance the processivity of DNA polymerases. In addition to serving as a processivity factor for DNA replication, PCNA also interacts with proteins functioning in a wide range of other processes including Okazaki fragment joining, base excision repair, nucleotide excision repair, mismatch repair, translesion DNA synthesis, cell cycle control, and chromatin remodeling^{104,121,122,203}.

The trimeric form of PCNA possesses a pseudo-six-fold symmetry, because each monomer is comprised of two independent domains with similar folds¹⁰³. The N-terminal domain (domain A) is linked to the C-terminal domain (domain B) through a long, flexible linker called the interdomain connector loop (IDCL). The IDCL is the binding site for many of PCNA's interacting partners, which contain a conserved PCNA-interacting protein motif (PIP motif)^{121,207}. When three PCNA monomers associate to form the trimeric ring-shaped structure, they arrange in a head-to-tail manner in which domain A of one monomer interacts with domain B of the neighboring monomer. This subunit interaction is stabilized via backbone hydrogen bonds of an anti-parallel β -sheet comprised of one β -strand from domain A of one monomer and a second β -strand from domain B on the other monomer¹⁰³.

Recently, it has been shown that yeast cells expressing a mutant form of PCNA (a glutamate-113 to glycine substitution) are unable to carry out translesion DNA synthesis¹⁸⁷. These cells have a slightly increased sensitivity to DNA-damaging agents, but have no otherwise noticeable growth defects. During my studies of the impact of this

PCNA mutant protein on translesion DNA synthesis²⁰⁸, I performed X-ray crystallographic analyses to determine the structure of the E113G PCNA mutant protein. Surprisingly, I obtained two distinct types of protein crystals and determined X-ray crystal structures of this mutant protein from both types. One structure was of the trimeric form of PCNA. The other structure was of a non-trimeric form of PCNA.

The focus of the present chapter is the structure of this non-trimeric form of PCNA. The monomers in the non-trimeric form interact in two ways. The first interaction is a tail-to-tail contact in which domain B of one monomer interacts with domain B of its neighbor. The B-B interface of this non-trimeric form of PCNA is surprisingly similar structurally to the A-B interface of the trimeric form. The second interaction is a head-to-head contact in which domain A of one monomer interacts with domain A of a different neighboring monomer. Analysis of this mutant protein structure indicates that the A-A interface would be significantly less unfavorable in the presence of the wild type Glu-113 side chain. This implies that this conserved, charged amino acid residue plays an important role in promoting trimer formation by destabilizing these possible alternate subunit interactions.

Materials and Methods

Protein Expression and Purification

Over-expression of wild type and mutant PCNA proteins from the yeast *S. cerevisiae* were carried out in *E. coli* Rosetta-2 (DE3) cells harboring pET-11a vectors, into which were cloned the wild type or mutant PCNA gene. The PCNA proteins were tagged with an N-terminal FLAG sequence for easy purification. Cells were grown in Overnight Express Instant TB Medium (Novagen) at 37 °C for 12 h. Lysis was carried out in 50 mM Tris-HCl (pH 7.5), 150mM NaCl, 1 mM PMSF, and 1 mg/mL lysozyme, with a Complete Mini Protease Inhibitor Cocktail tablet (Roche). Cell debris was removed by ultracentrifugation, and the resulting crude extract was loaded onto an Anti-

FLAG M2 Affinity Gel (Sigma) column (15 ml bed volume) and as described in the material and methods of Chapter 2. The eluted protein was then further purified using a Superose 6 HR10/30 column equilibrated with 20 mM Tris-HCl (pH 7.5), 1 mM DTT, and 250 mM NaCl. Purified PCNA was stored at -80 °C.

Crystallization of the E113G mutant PCNA protein

Crystallization was performed manually using the hanging drop method with 4 μ L drops. An initial screen utilizing conditions similar to those which produce wild type PCNA crystals¹⁰³ was used to identify ideal crystallization conditions. Crystals of the trimeric form of the E113G mutant PCNA protein that diffracted optimally were generated within 16 h by combining an equal volume of protein (20mg/ml) with a reservoir solution containing 2.03 M ammonium sulfate and 0.1 M sodium citrate (pH 5.8) at 18°C. The formation of crystals varied between protein preps and was enhanced by using a fresh prep and setting up trays immediately following gel filtration with only the peak fraction. A brown precipitant formed while setting up trays if the protein was more than a couple of days old. Crystals of the non-trimeric form of the E113G mutant PCNA protein that diffracted optimally were generated within 14 to 20 days by combining an equal volume of protein (20mg/ml) with a reservoir solution containing 1.6 M ammonium sulfate and 0.1 M sodium citrate (pH 5.8) at 18°C. These crystals were rod shaped and very reproducible in the given condition.

Data Collection and Structural Determination

PCNA protein crystals were flash-frozen at 100 K after being pre-soaked in a mother liquor containing 10% (v/v) glycerol. Data was collected from these crystals at 100 K at the 4.2.2 synchrotron beamline at the Advanced Light Source at the Ernest Orlando Lawrence Berkeley National Laboratory. Data were collected with a 150 mm crystal to detector distance. d*TREK was used to analyze and scale the data¹⁹⁹. The cubic crystals of the trimeric form of the mutant PCNA protein diffracted to a resolution of 3.8

Å, and the space group was determined to be $P2_13$, which is the same space group into which the wild type PCNA protein crystallizes¹⁰³. The orthorhombic crystals of the non-trimeric form of the mutant PCNA protein diffracted to 2.5 Å, and the space group was determined to be $C222_1$.

Molecular replacement was carried out using the structure of wild type PCNA (PDB entry 1PLQ) and PHASER²⁰⁰. Prior to refinement, simulated annealing to remove any structural bias was performed using PHENIX²⁰¹. Refinement and model building were carried out using PHENIX, REFMAC5, and Coot²⁰².

The buried surface area was determined using the program naccess with the help of Dr. Lokesh Gakhar in Dr. Ramaswamy's laboratory. This is done by calculating the solvent accessible surface area for each PCNA subunit independently and then after complex formation. By subtracting the accessible surface area for each single subunit from the accessible surface area for the complex, the buried surface area upon complex formation can be determined. This program utilizes a 1.4 Å probe to determine the accessible surface area. This was performed for the PCNA subunit alone and the PCNA complex following the A:A, B:B, or A:B interface formation. I also utilized this approach to determine the amount of surface area buried at the crystal contacts.

Size-exclusion Chromatography

Wild type and mutant PCNA proteins were diluted to a final volume of 200ul with 1xTBS (150mM NaCl, 50 mM Tris-HCl (pH 7.5) and 3ul of acetone (used as a volume marker) and were loaded onto a 24-ml Superose 6 HR10/30 column (GE Biosciences) equilibrated at 4°C with 1xTBS. Samples were eluted at 0.5 ml/min and monitored by UV absorbance using the AKTA-FPLC system (GE Biosciences). The elution volume of each protein was calculated using the Unicorn Evaluation software (Amersham Biosciences). The Stokes radius of each protein was determined using the Porath Correlation with standard proteins. The following standards were used to calibrate the column:

thyroglobulin (670 kDa, 85 Å), ferritin (440 kDa, 61 Å), catalase (232kDa, 52.2 Å), aldolase (158 kDa, 48.1 Å), bovine serum albumin (67 kDa, 35.5 Å), ovalbumin (43 kDa, 30.5 Å), and RNaseA (16.4 kDa, 14Å).

Results

Overview of the structures of two forms of the E113G

mutant PCNA protein

I obtained two distinct types of crystals of the E113G PCNA mutant protein. Crystals of the first type, which formed overnight, were cubic and diffracted to a resolution of 3.8 Å (Table 3.1). These crystals contained one PCNA monomer per asymmetric unit and had the same space group and unit cell dimensions as the crystals used to determine the structure of wild type PCNA¹⁰³. Similar to what was observed with the wild type PCNA protein, each monomer contains an N-terminal domain A (residues 1-118) and a C-terminal domain B (residues 135-240) linked by a long, flexible interdomain connector loop (IDCL, residues 119-134). The biologically relevant trimeric structure was formed by generating neighboring monomers along the 3-fold axis of the cubic symmetry as was done with the wild type protein. The three monomers form head-to-tail contacts with domain A of each monomer interacting with domain B of its neighbor (Figure 3.1). The only significant structural difference observed between the wild type protein and the E113G mutant protein is within loop J (residues 105-110), an extended loop in domain A near the subunit interface. As previously described in chapter II, the conformation of loop J is likely responsible for the inability of this mutant protein to carry out translesion DNA synthesis²⁰⁸. In the present chapter, I focus primarily on the structure of the E113G mutant protein determined with the second type of protein crystals.

Crystals of the second type, which formed over a period of two weeks, were orthorhombic and diffracted to a resolution of 2.5 Å (Table 3.1). These crystals also

contained one monomer per asymmetric unit, and generation of the symmetry-related neighbors showed that they do not pack to form the usual head-to-tail, ring-shaped trimer. Instead the monomers are arranged in a non-trimeric structure in which domain A of one monomer interacts with domain A of a neighboring monomer in a head-to-head contact and in which domain B of the original monomer interacts with domain B of a different neighboring monomer in a tail-to-tail contact (Figure 3.2). To our knowledge, this is the first structure determined for a non-trimeric form of eukaryotic PCNA.

Comparing the structures of the E113G mutant PCNA monomers in the trimeric and non-trimeric forms showed that there is flexibility between the domains within individual monomers as well as between neighboring monomers. For example, in the trimeric form of PCNA, the angle between domain A and domain B within the same monomer is 125° , (Figure 3.3A). In the non-trimeric form of PCNA, the angle between domains within the same monomer is reduced slightly to 114° (Figure 3.3B). The change in angle between the two domains is likely possible because of the inherent flexibility of the interdomain connector loop. The angles between the domains of neighboring monomers are even more variable. In the trimeric form of PCNA, the angle between domain A and domain B of the neighboring monomers (*i.e.*, the A-B interface) is 115° , (Figure 3.3A). In the non-trimeric form of PCNA, the angle between the two A domains on neighboring monomers (*i.e.*, the A-A interface) is 180° (Figure 3.3B). The angle between the two B domains on neighboring monomers (*i.e.*, the B-B interface) is 100° . As discussed below, the A-B interface of the trimeric form of PCNA and the B-B interface of the non-trimeric form of PCNA are structurally similar. At a global level, the principal difference between these two interfaces is that the angle between the interacting domains is smaller in the non-trimeric B-B interface (100°) than in the trimeric A-B interface (115°).

Subunit interactions of the nontrimeric form of the E113G mutant PCNA protein

In the trimeric form of PCNA, the A-B subunit interface consists of two anti-parallel β -strands: β -I₁ (residues 109-117) in domain A of one monomer and β -D₂ (residues 175-183) in domain B of the other monomer (Figure 3.4A). Interactions between the two monomers are stabilized by seven hydrogen bonds between the backbone carbonyl and amide groups of these two β -strands, and this interface buries a total of 1310 Å² of solvent accessible surface area. In the non-trimeric form of PCNA, the B-B interface is surprisingly similar in structure to the trimeric A-B interface. The B-B interface also consists of two anti-parallel β -strands; both are the β -D₂ strands in the two interacting B domains (Figure 3.4B). In this case, interactions between the monomers are stabilized by eight hydrogen bonds between the backbones of these two β -strands and a total of 1580 Å² of solvent accessible surface area is buried. It should be noted that the E113G substitution does not directly influence the formation of the B-B interface, because this amino acid substitution is in domain A on the opposite end of the monomers 50 Å away from the B-B interface. Thus it seems likely that the B-B interface observed with this mutant PCNA protein would be equally favorable with the wild type PCNA protein.

The A-A interface of the non-trimeric form of PCNA, by contrast, is dramatically different from the A-B interface of the trimeric form. The region of each monomer near the A-A interface is comprised of a β -sheet containing five β -strands as shown in Figure 3.5A: β -A₁ (residues 2-6), β -E₁ (residues 59-61), β -G₁ (residues 87-92), β -H₁ (residues 98-104), and β -I₁ (residues 109-117). The side of this β -sheet facing the neighboring monomer is hydrophobic, and the hydrophobic contacts between Ile-91 (in β -G₁) and Ile-100 (in β -H₁) stabilize the subunit interaction at the A-A interface (Figure 3.5B). This interface buries 1650 Å² of solvent accessible surface area. The E113G substitution plays an important role in favoring the formation of the A-A interface. As shown in Figure

3.5C, if the wild type Glu-113 (in β -I₁) residues are present, their negatively charged side chains would project toward and likely interfere with the hydrophobic contacts made by the four Ile-91 and Ile-100 residues. Therefore, the A-A interface observed with this mutant PCNA protein is in all likelihood less stable in the case of the wild type protein.

Comparison of the domains of the trimeric and nontrimeric forms of the E113G mutant PCNA protein

To determine if the novel A-A and B-B interfaces of the non-trimeric form of the mutant PCNA protein effected the structure of the individual domains of each monomer, I determined the RMSD between the C α atoms of the monomers of the trimeric form of the wild type protein and the non-trimeric form of the mutant protein. Surprisingly, there are very few differences between the structures of the protein backbones of the individual domains of PCNA in the trimeric and non-trimeric forms (Figure 3.6). In the case of domain B, which made structurally similar contacts in both the trimeric form of PCNA (the A-B interface) and the non-trimeric form of PCNA (the B-B interface), the backbone structures of the domain are very similar with an RMSD of 0.3Å over 105 C α atoms. In the case of domain A, which made dramatically different contacts in the trimer form (the A-B interface) and the non-trimeric form (the A-A interface), the backbone structures are slightly less similar with an RMSD of 0.9Å over 118 C α atoms. Overall, these results indicate that the structures of the individual domains within the PCNA monomers are not significantly impacted by the oligomeric form of PCNA.

Stability of the trimeric form of the E113G-mutant PCNA protein

Because I observed a non-trimer form of the E113G PCNA mutant protein, I carried out size exclusion chromatography at various concentrations of the wild type and mutant PCNA proteins to examine the stability of the trimeric form of this mutant protein in solution. Figure 3.7 shows the Stokes radius graphed as a function of PCNA monomer

concentration. The wild type PCNA protein was in the trimeric form at all concentrations used with a Stokes radius equal to 45 Å, which corresponds closely with its actual radius (46 Å). A comparison with molecular weight standards provided a predicted molecular weight of 109 kDa, which is in reasonable agreement with the actual molecular weight of the PCNA trimer (87 kDa) given the unusually flat shape of the PCNA ring. In the case of the E113G mutant PCNA protein, the trimeric form predominated at high monomer concentration ($> 5 \mu\text{M}$). At lower monomer concentrations ($< 0.5 \mu\text{M}$), the mutant protein appears to exist predominantly as a dimer. The Stokes radius of the dimer was 33 Å, and this corresponds to a predicted molecular weight of 54 kDa, which is in close agreement with the actual molecular weight of the PCNA dimer (58 kDa). Thus the trimeric form of the E113G mutant PCNA protein is significantly less stable than the trimeric form of the wild type protein.

Discussion

In the structure of the trimeric form of PCNA, only one type of subunit interface is observed. This is the A-B interface, which is stabilized by an anti-parallel β -sheet formed between two β -strands, one from domain A of one monomer and one from domain B of a neighboring monomer¹⁰³. In this chapter I report the structure of a non-trimeric form of the E113G PCNA mutant protein that reveals two alternate subunit interfaces. The first is the B-B interface in which an anti-parallel β -sheet is formed between two β -strands, one from domain B of one monomer and one from domain B of a neighboring monomer. Because the E113G substitutions are on the other end of the PCNA monomers from this interface, it is likely that the B-B interface observed in this mutant protein is at least as favorable in the wild type protein. The second is the A-A interface, which is stabilized primarily through hydrophobic contacts between domain A of one monomer and domain A of a neighboring monomer. Because in the wild type protein, the side chain of Glu-113 projects toward and likely interferes with these

hydrophobic interactions (see Figure 3.5C), the A-A interface observed here is in all likelihood significantly less favorable in the wild type protein.

There are compelling reasons why the A-A and B-B interfaces observed in the structure of the non-trimeric form of PCNA are not merely the result of crystal packing, but instead are actual contacts that likely occur in solution under some conditions. First, the B-B interface of the non-trimeric form and the A-B interface of the trimeric form are structurally similar. In fact, the B-B interface may be slightly more stable than the A-B interface. The B-B interface is stabilized by eight backbone hydrogen bonds, while the normal A-B interface is stabilized by seven. In addition, more surface area (1580 \AA^2) is buried at the B-B interface than at the A-B interface (1310 \AA^2). This is important because large buried surface areas are characteristics of actual subunit interfaces as opposed to crystal contacts²⁰⁹. Similarly, the A-A interface buries 1650 \AA^2 , which also implies that it is not a result of crystal packing but instead can occur in solution, at least in the case of this mutant protein. It is worth noting that in addition to the A-A and B-B contacts, there is another contact between two monomers in the crystal of the non-trimeric form of PCNA, and this contact is along the IDCL of each monomer. I believe that this contact is indeed the result of crystal packing because it has a lower buried surface area (1060 \AA^2) and is very similar to the crystal contact observed in the trimeric structure of wild type PCNA.

The stable, trimeric form of PCNA is generally believed to assemble in two steps as shown in Figure 3.8. First, two PCNA monomers come together to form the head-to-tail dimer with domain A of one monomer contacting domain B of the other monomer (see the structure in Figure 3.1 and middle schematic in Figure 3.8). Next, a third monomer comes together with the dimer with domain A and domain B of the monomer contacting the available domain B and domain A of the dimer, respectively (bottom of Figure 3.8). Our finding of possible alternative subunit interactions in PCNA complicates this scenario, because our results suggest that three distinct types of PCNA dimers can be

formed. In addition to the standard head-to-tail dimer described above, dimers can be formed when PCNA monomers come together in a head-to-head manner with domain A of one monomer contacting domain A of another (see Figure 3.2 and the middle right of Figure 3.8) or a tail-to-tail manner with domain B of one monomer contacting domain B of another (see Figure 3.2 and the middle left of Figure 3.8). In the case of the E113G mutant PCNA protein, all three types of dimers likely co-exist at low and intermediate protein concentrations ($< 1 \mu\text{M}$). In the case of the wild type PCNA protein, however, the presence of the charged Glu-113 side chain should destabilize any head-to-head A-A interfaces and greatly favor formation of the standard PCNA trimer even at lower protein concentrations.

While to my knowledge, this is the first structure that has been determined of a non-trimeric form of eukaryotic PCNA, an X-ray crystal structure has been determined of a non-trimeric form of the unrelated prokaryotic PCNA from the archaeon *Pyrococcus furiosus*. Although lacking homology in amino acid sequence to eukaryotic PCNA, prokaryotic PCNA is also normally a trimeric, ring-shaped protein generally similar in overall structure to eukaryotic PCNA¹⁰⁰. The A-B interface of the prokaryotic PCNA trimer, however, differs from that of the eukaryotic PCNA trimer in that this interface is stabilized by several electrostatic interactions between charged side chains of residues from different monomers. X-ray crystal structures have been determined for two mutant forms of this prokaryotic PCNA with substitutions of these charged residues in domain B at the subunit interface²¹⁰. The oligomeric forms of both of these mutant proteins are dimers, which are held together by a mutant B-B interface that is roughly analogous to the one I describe here for eukaryotic PCNA. Incidentally, no A-A interfaces have been observed with prokaryotic PCNA. The primary conclusion of the study of the non-trimeric form of the prokaryotic protein was that the charged residues in question promote trimer formation by directly stabilizing the trimeric structure. This is quite different from our observations regarding the role of Glu-113 in eukaryotic PCNA. Here I

conclude that the eukaryotic PCNA trimer formation is favored by Glu-113 due to destabilization of the A-A interface.

Finally, given that the tail-to-tail B-B dimer could exist at low protein concentration in the case of the wild type PCNA protein, it is tempting to speculate about a possible biological role of this species. Clearly the trimeric form of PCNA is the most important oligomeric form of this protein as it participates in DNA replication and many DNA repair processes. However, at estimated cellular concentrations of PCNA, a significant population of stable wild type PCNA dimers has been observed by several *in vitro* experimental techniques²¹¹. Given that PCNA plays a role in so many other biological processes, including cell cycle control and survival, chromatin assembly and remodeling, and regulation of transcription^{104,121,122,203}, and given that the oligomeric state of the PCNA molecules participating in these processes has not been determined, it is possible that PCNA functions in some biological contexts as a stable dimer. The alternate subunit interactions reported here suggest that a stable B-B dimer may in fact be a biologically important molecular species. Formation of a stable B-B dimer would allow for novel protein-protein interactions between the large hydrophobic surface of domain A and potential protein partners.

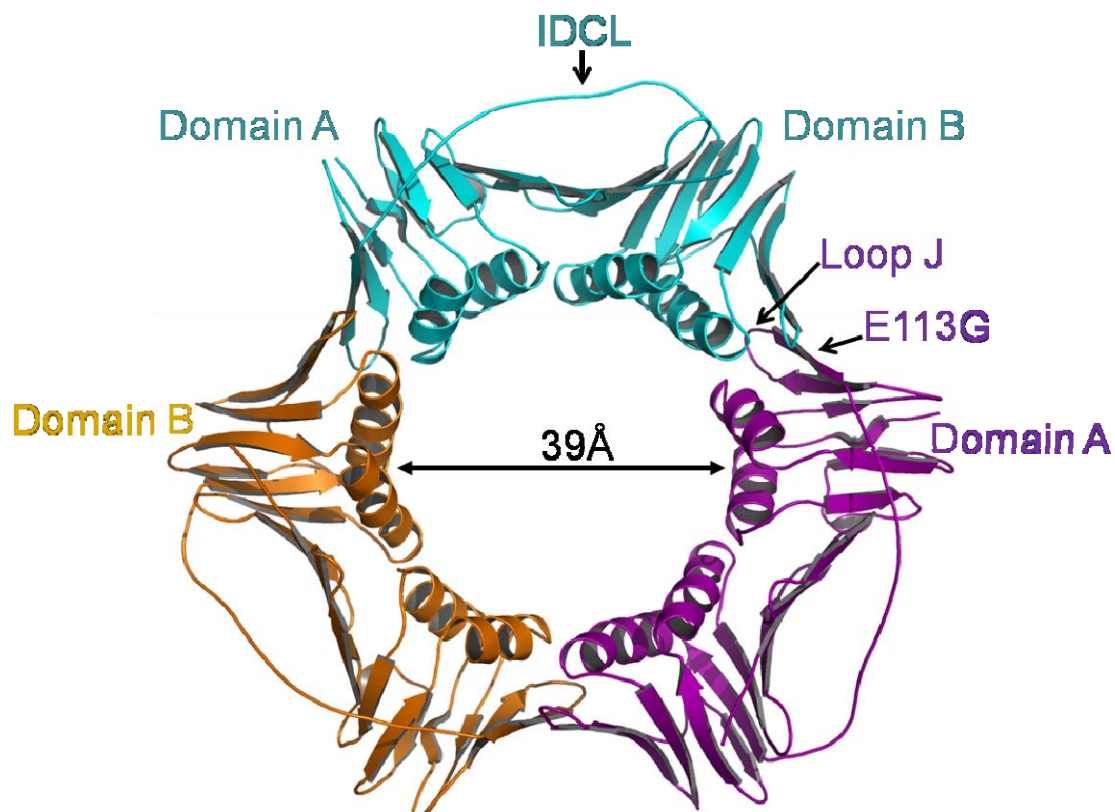


Figure 3.1 Structures of the trimeric E113G PCNA mutant protein. The monomeric subunits are shown in orange, purple, and light blue. Domains A and B, the inter-domain connecting loop (IDCL), loop J, and the E113G substitution are indicated.

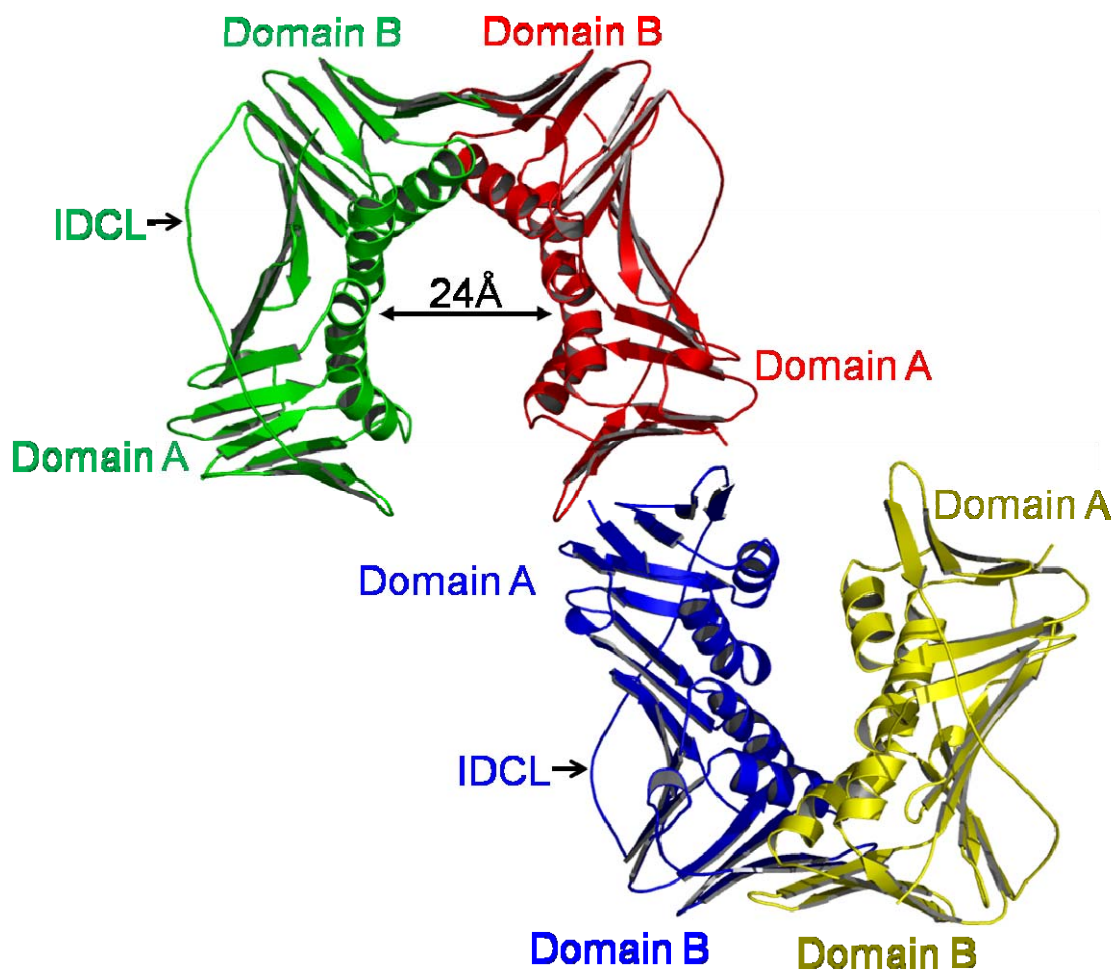


Figure 3.2 Structure of the non-trimeric E113G PCNA mutant protein. The monomers are shown in green, red, blue and yellow. Domains A and B are indicated for each monomer.

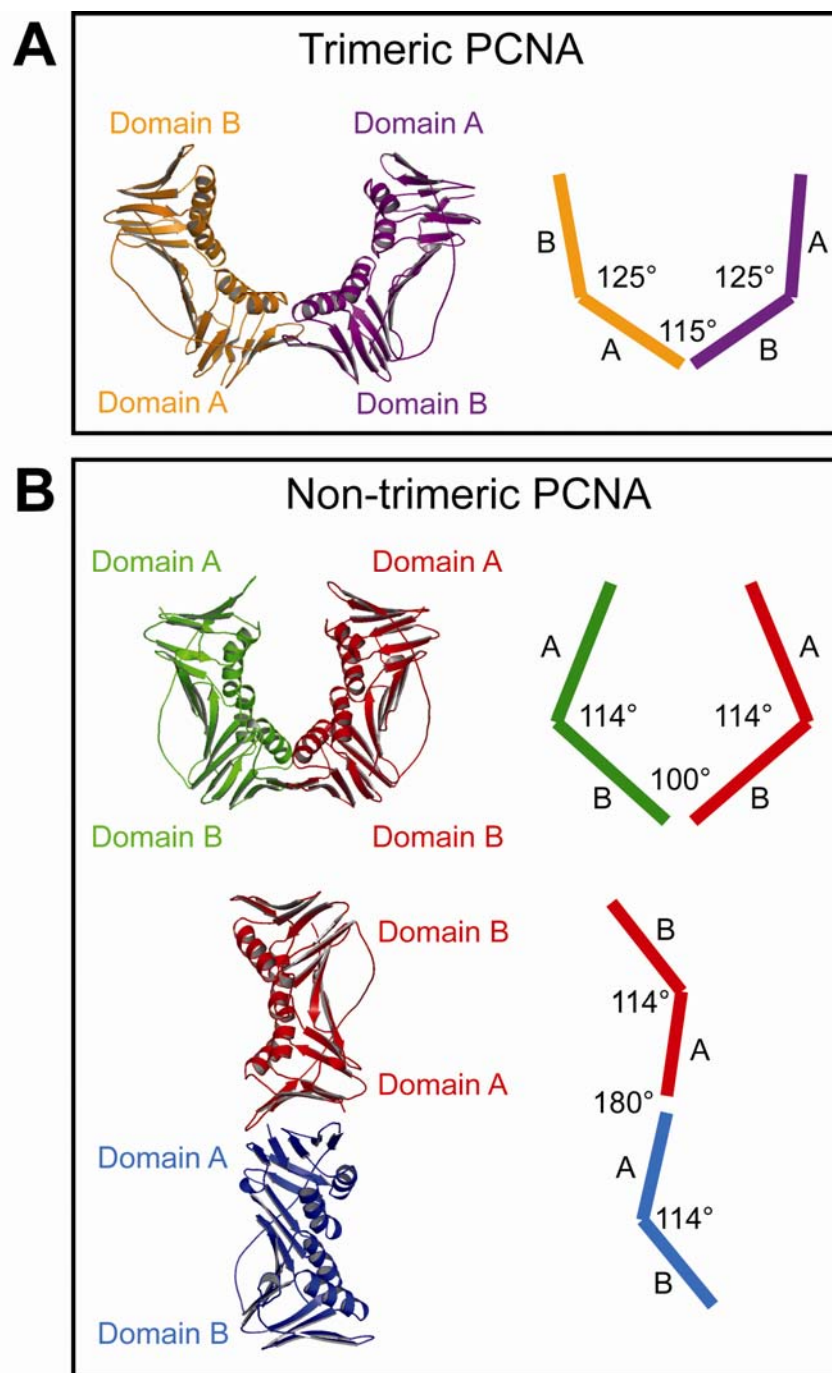


Figure 3.3 Subunit interfaces of the trimeric and non-trimeric forms of the E113G PCNA mutant protein.

Figure 3.3 continued. Interfaces of the trimeric and non-trimeric forms of the E113G mutant PCNA protein are shown. (A) The A-B interface of the trimeric form of the mutant protein is shown with a schematic indicating the values of angles within each monomer and angles between monomers. (B) The B-B interface (top structure of the panel) and the A-A interface (bottom structure of the panel) of the non-trimeric form of the mutant protein is shown with a schematic indicating the values of angles within each monomer and angles between monomers.

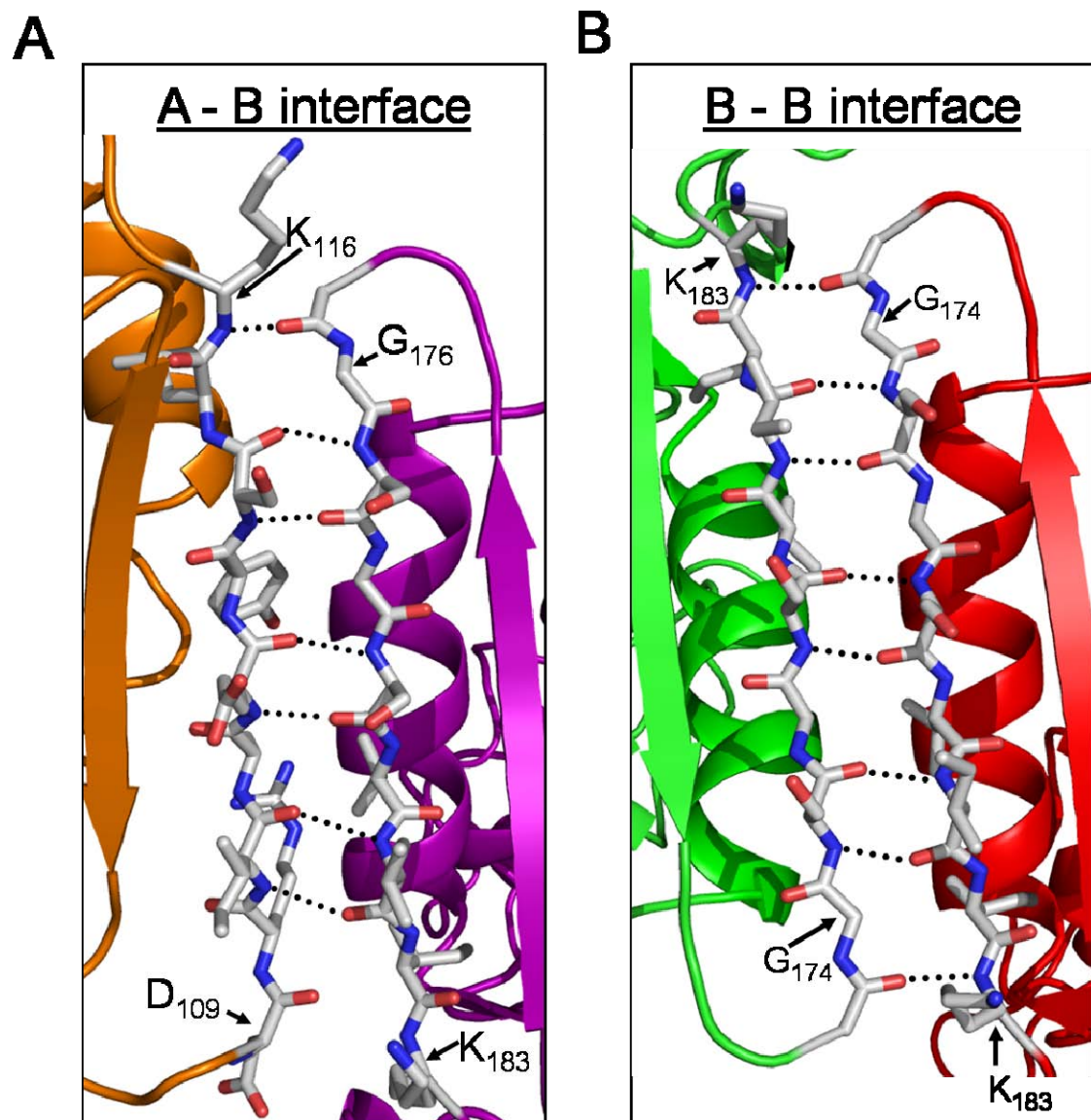


Figure 3.4 The B-B interface of the non-trimeric form of the E113G PCNA mutant protein

Figure 3.4 continued. (A) The A-B interface of the trimeric form of the mutant protein is stabilized by the β -D2 strand (residues 175-183) from domain B of one monomer forming an anti-parallel β -sheet with the β -I1 (residues 109-117) in domain A of the other monomer. (B) The B-B interface of the non-trimeric form of the mutant protein is stabilized by the β -D2 strands (residues 175-183) from domain B of each monomer forming an anti-parallel β -sheet. The positions of the hydrogen bonds are shown.

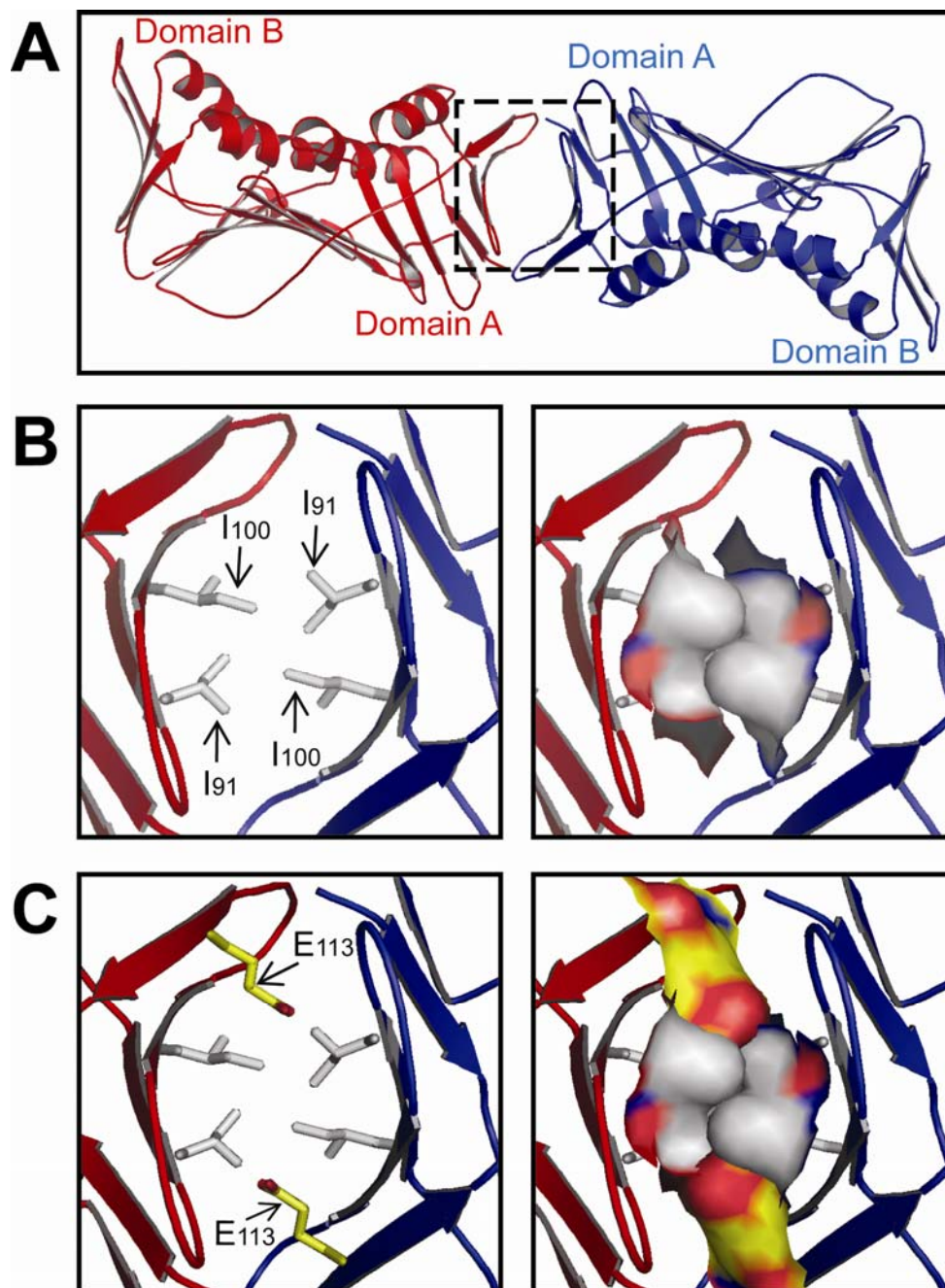


Figure 3.5 The A-A interface of the non-trimeric form of the E113G PCNA mutant protein

Figure 3.5 continued. (A) The A-A interface of the non-trimeric form of the mutant protein is stabilized by hydrophobic interactions between surfaces of each monomer comprised of five β -strands: β -A1, β -E1, β -G1, β -H1, and β -I1. These surfaces are highlighted by the dashed square. (B) Close up view of the A-A interface of the E113G mutant protein. The side chains of the hydrophobic Ile-91 and I-100 residues are shown in the stick format (left side of the panel) and in the space-fill format (right side of the panel). (C) Model of the A-A interface of the wild type protein. This panel is identical to panel B, except that the side chain of Glu-113 has been modeled and shown in yellow.

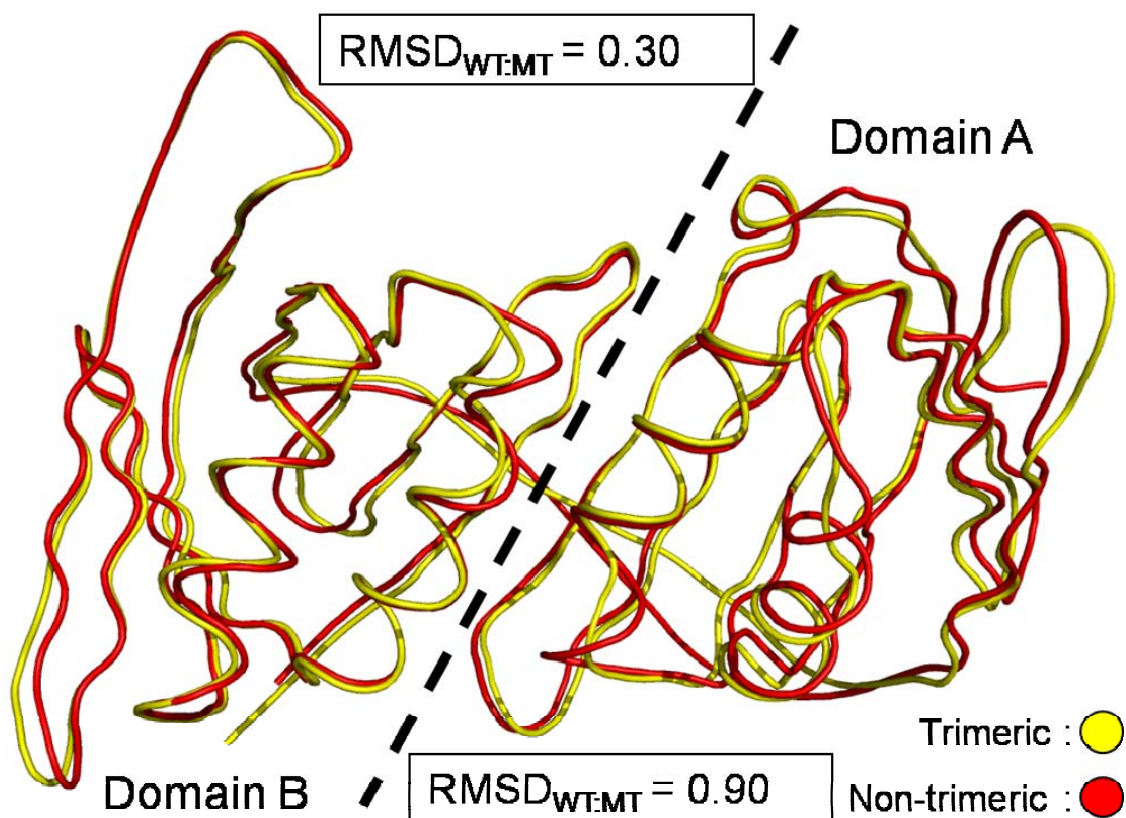


Figure 3.6 Overlay of the trimeric and non-trimer PCNA. Superimposition of the protein backbone of the trimeric form of the wild type PCNA protein and the non-trimeric form of the E113G mutant PCNA protein. Domains A and B of the monomers are separated by a dashed line and the RMSD values were independently determined for each domain.

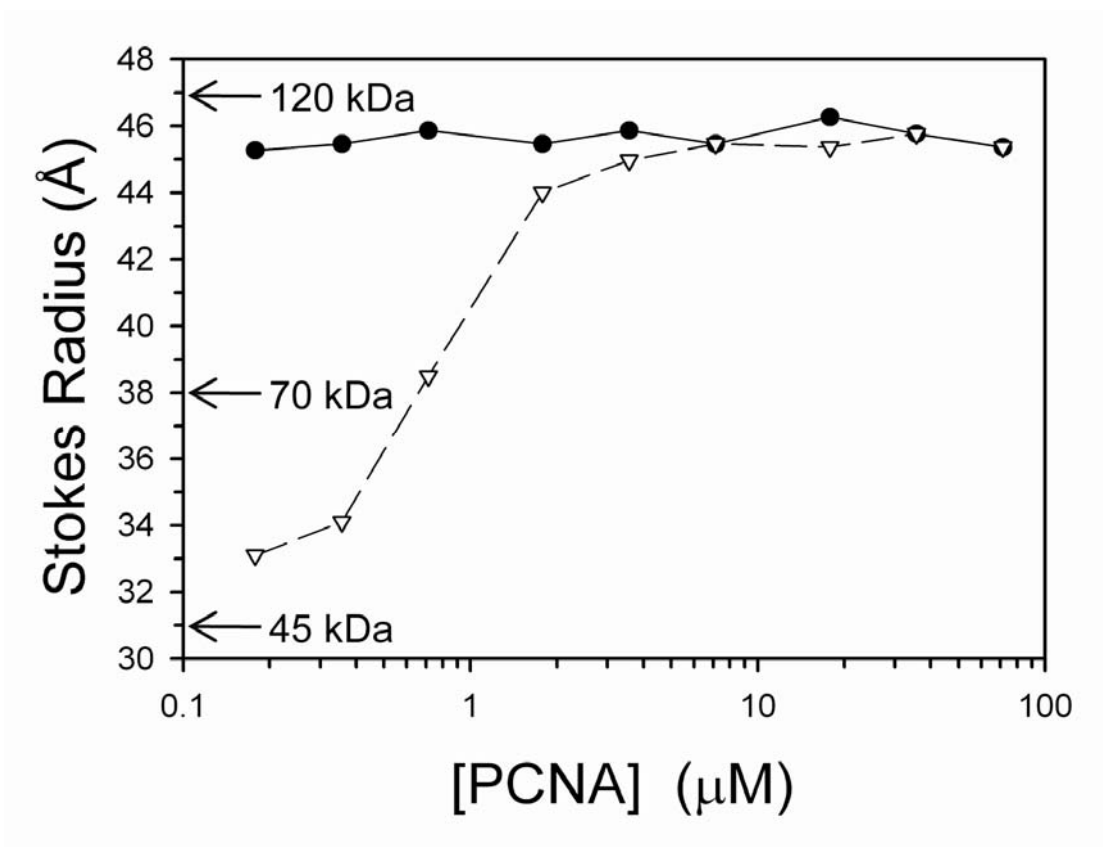


Figure 3.7 Stability of the trimeric forms of the wild type and E113G PCNA mutant proteins. Size exclusion chromatography was carried out and the Stokes radius was determined for various protein loading concentrations of the wild type PCNA (black circles) and the mutant PCNA (white triangles). Estimated molecular weights derived from protein standards are provided. The elution curves can be found in my notebook and on Dr. Marc Wold's AKTA FPLC machine for each point.

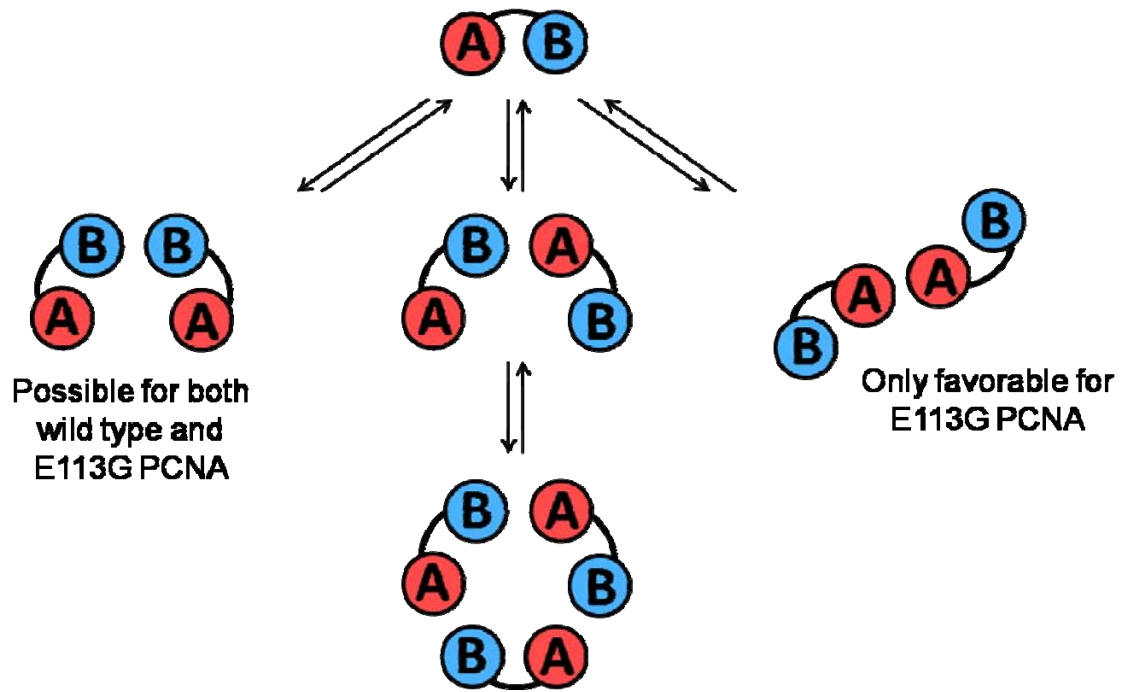


Figure 3.8 PCNA homotrimer formation. The single monomeric subunit of PCNA is shown in a dumbbell shape with domain A and domain B connected by the IDCL. The monomeric subunit is shown at the top and the final trimeric PCNA homotrimer is shown at the bottom. Alternate dimeric complexes are shown in the middle. The A-A dimer is only favorable for the E113G PCNA mutant protein, while the B-B dimer is possible for both the wild type and E113G PCNA proteins.

Table 3.1 Data collection and refinement statistics for the E113G PCNA mutant proteins.

	<i>Trimeric form</i>	<i>Non-trimeric form</i>
<i>(A) Data collection statistics</i>		
Resolution (Å)	29.61 – 3.80 (3.94 – 3.80) ^a	28.91 – 2.50 (2.59 – 2.50)
Wavelength (Å)	0.97	0.97
Space group	P2 ₁ 3	C222 ₁
Cell (Å)	a=122.09 b=122.09 c=122.09	a=74.59 b=147.51 c= 81.44
Completeness (%)	100 (100)	98.1 (96.8)
Redundancy	10.56 (9.84)	4.75 (3.79)
I/σ ₁	17.9 (6.8)	11.4 (3.2)
R _{merge} (%) ^b	7.2 (29.4)	9.0 (36.5)
<i>(B) Refinement statistics</i>		
Resolution range (Å)	29.6 – 3.80	28.9 – 2.50
R (%) ^c	27.0	23.0
R _{free} (%) ^d	31.0	27.0
rms bonds (Å)	0.011	0.017
rms angles (°)	1.5	1.7
Number of water molecules	0	0
Number of protein atoms	1981 (254 a.a.)	1967 (253 a.a.)
Ramachandran analysis (%)		
Most favored	82	93
Allowed	18	7
PDB ID	3GPM	3GPN

^a Values in parentheses relate to the highest resolution shell.

^b $R_{merge} = \frac{\sum_h \sum_i |I_i(\mathbf{h}) - \langle I(\mathbf{h}) \rangle|}{\sum_h \sum_i I_i(\mathbf{h})}$, where I_i is the i th measurement of reflection \mathbf{h} and $\langle I(\mathbf{h}) \rangle$ is a weighted mean of all measurements of \mathbf{h} .

^c $R = \frac{\sum |F_o| - |F_c|}{\sum |F_o|}$, where F_o and F_c are the observed and calculated structure factors, respectively.

^d R_{free} is defined in (Brunger 1992).

CHAPTER 4
STRUCTURE OF MONOUBIQUITINATED PCNA AND
IMPLICATIONS FOR TRANSLESION SYNTHESIS AND THE
POLYMERASE EXCHANGE

Abstract

DNA synthesis by classical polymerases is blocked by many lesions. These blocks are overcome by translesion synthesis, whereby the stalled classical polymerase is replaced by a non-classical polymerase. In eukaryotes, this polymerase exchange requires PCNA monoubiquitination. To better understand the polymerase exchange, I developed a novel means of producing monoubiquitinated PCNA by splitting the protein into two self-assembling polypeptides. I determined the X-ray crystal structure of monoubiquitinated PCNA and found that the ubiquitin moieties are located on the back face of PCNA and interact with it via their canonical hydrophobic surface. Moreover, the attachment of ubiquitin does not change PCNA's conformation. This implies that PCNA ubiquitination facilitates non-classical polymerase recruitment to the back of PCNA by forming a new binding surface for non-classical polymerases, which is consistent with a "tool belt" model of the polymerase exchange. (The work presented in this chapter is published in Freudenthal et al. (2010) *Nat. Struct. and Mol. Biol* and is currently in press.)

Introduction

DNA damage, caused by radiation and a variety of chemical agents, can lead to mutations, genomic instability, cancer, and cell death. Genetic studies in the yeast *Saccharomyces cerevisiae* have revealed three general pathways for coping with radiation-induced DNA damage in eukaryotes²¹². Proteins in the Rad3 pathway catalyze nucleotide excision repair, which removes bulky, helix-distorting lesions. Proteins in the Rad52 pathway catalyze double-strand break repair through homologous recombination.

Proteins in the Rad6 pathway catalyze post-replication repair, a multi-faceted process that includes translesion synthesis.

Post-replication repair is regulated by the monoubiquitination and polyubiquitination of proliferating cell nuclear antigen (PCNA), the eukaryotic sliding clamp processivity factor. Rad6 is an ubiquitin conjugating enzyme that associates with Rad18, a ubiquitin ligase^{163,213}. The Rad6/Rad18 complex catalyzes the monoubiquitination of PCNA on Lys-164, which promotes translesion synthesis^{150,154}. The Mms2-Ubc13 dimer is an ubiquitin conjugating enzyme that associates with Rad5, another ubiquitin ligase, and this complex catalyzes the formation of polyubiquitin chains via Lys-63 linkages¹⁶⁴⁻¹⁶⁶. These proteins convert monoubiquitinated PCNA (Ub-PCNA) to polyubiquitinated PCNA, which promotes a currently uncharacterized error-free pathway of post-replication repair^{150,154}.

Translesion synthesis is a process that occurs when a classical DNA polymerase (*i.e.*, one that synthesizes DNA during normal replication and repair) is blocked at a DNA lesion in the template strand. In translesion synthesis, the stalled classical polymerase is replaced by a non-classical DNA polymerase which then carries out replication through the damage. Eukaryotes possess several non-classical DNA polymerases, which differ from their classical counterparts in the ability to accommodate damaged DNA templates^{34,189,214}. DNA polymerase zeta (pol ζ), for example, functions in the mutagenic bypass of a wide range of lesions^{182,194,215,216}. By contrast, DNA polymerase eta (pol η) functions in the error-free translesion synthesis of thymine dimers^{75,80}. In humans, lack of pol η causes the variant form of xeroderma pigmentosum, a cancer-prone genetic disorder^{83,84}.

Several lines of evidence demonstrate that the monoubiquitination of PCNA plays a critical role in recruiting non-classical polymerases to sites of DNA damage and in orchestrating the polymerase exchange step between the classical and non-classical polymerases during translesion synthesis. First, most non-classical polymerases,

including pol η , possess ubiquitin-binding motifs, and mutations in these motifs lead to loss of protein function *in vivo*^{97,217}. Second, in human cells, pol η and Ub-PCNA co-localize to replication foci following DNA damage¹⁶⁷. Moreover, pol η specifically interacts with Ub-PCNA, but not with unmodified PCNA in these cells following DNA damage¹⁶⁷. Third, purified yeast pol η can replace the classical DNA polymerase delta (pol δ) on the DNA when it stalls *in vitro* in the presence of Ub-PCNA, but not in the presence of unmodified PCNA¹⁷⁸.

Despite the obvious importance of Ub-PCNA in facilitating the polymerase exchange step of translesion synthesis, the structural and biochemical basis by which it does this remains unknown. Efforts to better understand the polymerase exchange have been hampered by the inability to produce sufficient quantities of Ub-PCNA for structural and biochemical studies. In this chapter I report a novel strategy to produce large quantities of Ub-PCNA by splitting the protein into two polypeptides that self-assemble *in vivo*. I show that Ub-PCNA produced in this manner stimulates pol η activity *in vitro* and fully supports translesion synthesis *in vivo*. I have determined the X-ray crystal structure of Ub-PCNA and found that the ubiquitin moieties are located on the back face of the PCNA ring. Moreover, the attachment of ubiquitin to PCNA does not change the conformation of PCNA. This strongly suggests that ubiquitination of PCNA facilitates non-classical polymerase recruitment to the back face of the PCNA ring by forming a new interacting surface for the non-classical polymerases. This is consistent with a “tool belt” model of the polymerase exchange in which classical and non-classical polymerases simultaneously bind to Ub-PCNA (Figure 1.9).

Materials and Methods

Protein Expression and Purification

Non-split yeast PCNA with an N-terminal FLAGTM tag was over-expressed in *E. coli* Rosetta-2 (DE3) cells from a pET11a plasmid as described in Chapter 2²⁰⁸. To

produce split PCNA, the gene encoding the N-terminally FLAGTM tagged N fragment (residues 1-163) was cloned into multi-cloning site 2 of the pET-Duet1 plasmid. The gene encoding the C fragment (residues 164-258) was cloned into multi-cloning site 1 of the same plasmid using BamHI and HindIII. The two fragments of split PCNA were simultaneously over-expressed in *E. coli* Rosetta-2 (DE3). Cells were grown in six 1.5 liter batches inoculated with 25ml of an overnight culture. The cells were grown at 37°C to an OD ~0.400 and then transferred to a shaker at 18°C. At an OD of 0.600 the cells were induced with 1mM IPTG and harvested after 18hrs.

To produce Ub-PCNA, the gene encoding the N-terminally FLAGTM tagged N fragment (residues 1-163) was cloned into multi-cloning site 2 of the pET-Duet1 plasmid. The gene encoding the ^{Ubi}C fragment was cloned into multi-cloning site 1 of the pET-Duet1 plasmid. The ^{Ubi}C fragment contained an N-terminal His₆-tag fused to ubiquitin (residues 1-76) fused to a two-glycine linker fused to PCNA (residues 165-258). The two fragments of Ub-PCNA were simultaneously over-expressed in *E. coli* Rosetta-2 (DE3) cells. Cells were grown in twelve 1.5 liter batches inoculated with 25ml of an overnight culture. The cells were grown at 37°C to an OD ~0.400 and then transferred to a shaker at 18°C. At an OD of 0.600 the cells were induced with 1mM IPTG and harvested after 18hrs.

Cells expressing non-split PCNA, split PCNA, and Ub-PCNA were lysed in 50 mM TrisCl (pH 7.5), 150 mM NaCl, 1 mM PMSF, and 1 mg/ml lysozyme with a Complete Mini Protease Inhibitor Cocktail Tablet (Roche), and the cell lysate was subject to ultracentrifugation. Non-split PCNA and split PCNA were purified using an Anti-FLAGTM M2 affinity chromatography column (Sigma) and a Superose 6 size exclusion chromatography column (Pharmacia GE Healthcare), as described in Chapter 3. Ub-PCNA was purified the same way, except that an NTA-agarose affinity chromatography column (Qiagen) was used before the anti-FLAGTM affinity and the size exclusion columns. The NTA-agarose column was performed by loading the lysate over a

10ml bed volume by gravity. The NTA-agarose column was then washed with ten column volumes of a high salt wash consisting of 50mM TrisCl, pH 7.5, 500mM NaCl, and 10mM imidazole. The column is then further washed by a low salt condition of 50mM TrisCl, pH 7.5, 150mM NaCl, and 40mM imidazole. The protein is eluted with 3-5 column volumes of 400mM imidazole and 10ml fractions are collected. This process can also be performed on an AKTA-FPLC system (GE Bioscience) in Dr. Marc Wold's laboratory. Following elution the protein must be immediately buffer exchanged into 50mM TrisCl, pH 7.5, 150mM NaCl, 1mM DTT to remove the imidazole. The subsequent day the eluted protein was subject to the anti-FLAG affinity and size exclusion chromatography as described in Chapter 3. Purified proteins were stored in aliquots at -80 °C. Following all the purification steps the final yield was about 0.25-0.50mg of Ub-PCNA per liter.

Crystallization of Split PCNA and Ub-PCNA

Crystallization of the split PCNA protein was performed manually using the hanging drop method with 2 μ l drops. The best diffracting crystals were obtained by combining an equal volume of protein (20 mg/ml) with reservoir solution containing 1.9 M ammonium sulfate and 0.1 M sodium citrate (pH 6.0). Cubic crystals formed within 3 days at 18 °C. Crystallization of the Ub-PCNA protein was set up using a TTP LabTech Mosquito by the hanging drop method with 400 μ l drops. A wide assortment of additives (Hampton) and conditions were tested, and multiple crystal forms were obtained. The best diffracting crystals were obtained by combining an equal volume of protein (18 mg/ml) with a reservoir solution containing 2.04 M ammonium sulfate, 0.1 M sodium citrate (pH 6.2), and 3% ethanol. These cubic crystals formed within 60 days at 18 °C. I consistently observed that slowing the formation of crystals resulted in better diffracting crystals. Again the best diffracting crystals formed when the prep was only a couple days old and immediately following gel filtration.

Data Collection and Structural Determination

Both split PCNA and Ub-PCNA protein crystals were pre-soaked in a mother liquor containing 10% (v/v) ethylene-glycol prior to being flash cooled in liquid nitrogen. Mounted crystals were subsequently used for data collection at 100 K at the 4.2.2 synchrotron beamline at the Advanced Light Source in the Lawrence Berkeley National Laboratory. The data were collected with a crystal to detector distance of 150 mm. The data were processed and scaled using *d*trek*¹⁹⁹ to a resolution of 3.0 Å for split-PCNA and 2.8 Å for Ub-PCNA, and the space groups were determined to be P2₁3 for both proteins. Molecular replacement was performed using the structure of non-split PCNA (PDB ID: 1PLQ) and PHASER²⁰⁰ to produce the initial model. For split PCNA, simulated annealing was performed to remove any structural bias using PHENIX²⁰¹ prior to refinement with REFMAC5 from the CCP4 package²¹⁸. Model building was carried out using Coot²⁰².

For Ub-PCNA, I initially obtained clear electron density for only the PCNA portion of Ub-PCNA following molecular replacement with PCNA (1PLQ.pdb). I also attempted to locate the ubiquitin moiety using the molecular replacement program PHASER by inputting both the PCNA and ubiquitin ensembles and searching for them independently. This technique and other density improvement techniques did not help to determine the location of ubiquitin. With that being said I was able to identify a region with an enriched electron density following molecular replacement with only the PCNA moiety (circled in red within Figure 4.18A). A difference map between the split PCNA and Ub-PCNA revealed clear extra density further suggesting the position of the ubiquitin moiety. The difference map could be generated because the split and Ub-PCNA proteins are in the same space group. We utilized the split PCNA data as the heavy atom to generate a Patterson difference map between split and Ub-PCNA, resulting in a 20% difference between the two maps. This method allowed me to clearly identify the secondary structural elements of ubiquitin, but the density was not good enough to fully

orient the ubiquitin moiety (Figure 4.18B). To improve the maps, I first refined only the PCNA portion of the complex using REFMAC5²¹⁸ followed by maximum entropy refinement as implemented in Buster²¹⁹. Buster is ideally suited for completion of a partial structure and performs real space density refinement for both the partial structure and the missing portion independently. The resulting map was good enough to fit the ubiquitin backbone and identify all the secondary structural elements (Figure 4.18C). ESSENS²²⁰ and SOLEX were used to determine the orientation and position of the ubiquitin in this improved electron density map in a non-biased manner following the approach used previously to determine the structure of the acetylcholinesterase-fasciculin complex²²⁰. ESSENS is a docking program that docks the ubiquitin moiety into the electron density map and SOLEX extracts the top solutions from ESSENS. The top two orientations of the ubiquitin (with scores of 3.7 and 2.8, which represent the number of standard deviation above the mean) were similarly oriented and structurally possible. These two orientations were assigned equal occupancy and subjected to a final round of refinement using REFMAC5. It should be noted that there is precedent for alternative domain conformations, as a 120-amino acid domain of the ISP protein in the structure of the eleven-subunit mitochondrial cytochrome bc_1 complex showed a mixture of three different conformations²²¹.

The buried surface area was determined using the program naccess with the help of Dr. Lokesh Gakhar in Dr. Ramaswamy's laboratory. This is done by calculating the solvent accessible surface area for the PCNA and ubiquitin moiety independently, and then for the Ub-PCNA structure. By subtracting the accessible surface area for PCNA and ubiquitin from the accessible surface area for Ub-PCNA, the buried surface area was calculated between the ubiquitin and PCNA moieties in the Ub-PCNA structure. This program utilizes a 1.4 Å probe to determine the accessible surface area. I also utilized this approach to determine the amount of surface area buried at the crystal contacts.

DNA substrates

For all DNA polymerase activity assays, a synthetic 68-mer oligodeoxynucleotide with the sequence 5'- biotin-GAC GGC ATT GGA TCG ACC TCX AGT TGG TTG GAC GGG TGC GAG GCT GGC TAC CTG CGA TGA GGA CTA GC-biotin was used as the template strand (X is an abasic site). For the running start abasic bypass assays, a synthetic 26-mer oligodeoxynucleotide with the sequence 5'- GGT AGC CAG CCT CGC ACC CGT CCA AC was used as a primer. For the steady state kinetics assays, a synthetic 31-mer oligodeoxynucleotide with the sequence 5'- GGT AGC CAG CCT CGC ACC CGT CCA ACC AAC T was used as a primer. Primer strands were 5'-³²P-end-labeled and annealed by heating to 95 °C for 2 min. and slowly cooled to room temperature over several hours. Labeled DNA substrates were stored at 4° C for up to 2 weeks.

Polymerase Activity Assay

All assays were carried out in 40 mM Tris-HCl (pH 7.5), 8 mM MgCl₂, 150 mM NaCl, 1 mM DTT, and 100 µg/ml bovine serum albumin. Reaction mixtures also contained a 10-fold molar excess of streptavidin over DNA to block the ends of the DNA to prevent PCNA dissociation. Non-split PCNA, split PCNA, and Ub-PCNA proteins were loaded onto the DNA substrates by incubating 75 nM PCNA (trimer concentration), 20nM DNA, 500 µM ATP, and 20 nM replication factor C (provided by Manju Hingorani at Wesleyan University), for 30 sec at 22 °C. In the steady state kinetic assays, the reaction mixtures contained various concentrations of dATP (0 to 600 µM). Reactions were initiated by adding 1 nM pol η and were quenched after 10 min by adding 10 volumes of formamide loading buffer [80% deionized formamide, 10mM EDTA (pH 8.0), 1 mg/ml xylene cyanol, and 1 mg/ml bromophenol blue]. Extended primers and non-extended primers were separated on a 15% polyacrylamide sequencing gel containing 8 M urea. The intensities of the gel bands were determined using a

PhosphorImager (Molecular Dynamics). The rate of product formation was graphed as a function of dNTP concentration, and the V_{\max} and K_m values were obtained from the best fit of the data to the Michaelis-Menten equation using SigmaPlot 10.0. Experiments were carried out at least three times to ensure reproducibility. In the running start bypass assays, the reaction mixtures contained 20 μM of each dNTP. Reactions were quenched after 3 and 5 min. by the addition of 10 volumes of formamide loading buffer, and the products were visualized on a 15% polyacrylamide sequencing gel containing 8 M urea. The percent bypass was calculated by dividing the amount of incorporation at the lesion by the incorporation events prior to the lesion.

Genetic Complementation Assay

Because the *POL30* gene (which encodes PCNA) is essential, I carried out a plasmid shuffle. The wild type PCNA gene under control of its native promoter was subcloned into pTB366 (*URA3*) and transformed into wild type EMY74.7 yeast cells. The genomic *POL30* gene was then replaced by the *TRP1* gene through homologous recombination with a linearized piece of DNA containing the TRP1 gene flanked by the complementary 1kb upstream and 1kb downstream UTR of the *POL30* gene. Cells were then grown on synthetic complete media lacking tryptophan and uracil, and verification that the *POL30* gene was replaced by *TRP1* was carried out by PCR. Genes for wild type, non-split PCNA, the K164R mutant PCNA protein, and the N fragment of split PCNA and split Ub-PCNA were sub-cloned into the p425 GPD vector (*LEU2*). The C fragments of split PCNA or the split ^{Ubi}C fragment of Ub-PCNA were sub-cloned into the p423 GPD vector (*HIS3*). I used high expressing GPD promoters to ensure that there would be enough of each protein fragment that was soluble and could self-assemble *in vivo*. Combinations of these plasmids or empty p423 GPD vector were transformed into the *pol30Δ* cells to generate the strains producing only wild type PCNA, only the mutant K164R PCNA, only split PCNA, and only split Ub-PCNA. These strains were grown on

complete synthetic media lacking leucine, tryptophan, and histidine with the addition of FOA to select against the original wild type PCNA plasmid. Following counter-selection with FOA, the absence of full length PCNA genes in strains producing split PCNA and split Ub-PCNA were confirmed by both PCR and DNA sequencing. These strains were assayed for UV resistance as previously described²²². To ensure reproducibility, the UV resistance experiments were performed at least six times, and mean and standard error values for percent survival were determined at each UV dose. Growth rates for these strains were examined by inoculating 100 ml liquid media with 1×10^5 cells from overnight cultures. The growth rate at 30 °C was monitored by measuring absorbance at 600 nm.

Results

Production of Split PCNA and Ub-PCNA

The production of sufficient quantities of monoubiquitinated proteins for structural and biochemical studies has been very challenging. Here I report a novel strategy for easily producing large quantities of monoubiquitinated proteins. This strategy, which could be applied to a variety of systems, is (1) to split the target protein at the site of monoubiquitination into two polypeptides, (2) to fuse ubiquitin in frame at the N-terminus of the C-terminal fragment of the target protein, and (3) to co-express the two polypeptides and allow them to self-assemble *in vivo*. I have successfully used this approach to produce monoubiquitinated PCNA, and I produced a split, non-ubiquitinated form of PCNA as well.

The polypeptides used to over-express split PCNA and split Ub-PCNA are shown in Figure 4.1A,B. For production of split PCNA, the first polypeptide (the N fragment) contained amino acid residues 1 to 163 of PCNA and was N-terminally FLAGTM-tagged. The second polypeptide (the C fragment) contained residues 164 to 258 of PCNA. For production of split Ub-PCNA, the first polypeptide (the N fragment) was identical to the

one used to produce split PCNA. The second polypeptide (the ^{Ubi}C fragment) contained the entire ubiquitin sequence (residues 1-76) fused via a short linker to residues 165 to 258 of PCNA and was N-terminally His₆-tagged. The short linker consisted of two glycine residues because this is nearly isosteric with the side chain of Lys-164 and the isopeptide bond to the C-terminus of ubiquitin (Figure 4.1C).

I was able to purify milligram quantities of both split PCNA and split Ub-PCNA. In both cases, the two polypeptides fragments were present in a one-to-one ratio (Figure 4.2A). Size exclusion chromatography showed that split PCNA had a Stokes radius of 45 Å, which was identical to the Stokes radius of non-split PCNA and closely agreed with the actual radius of the PCNA trimer (46 Å). The Stokes radius of split Ub-PCNA was 50 Å, which was slightly larger than the Stokes radius of unmodified PCNA, as would be expected. This demonstrated that, like non-split PCNA, split PCNA and split Ub-PCNA formed stable, ring-shaped trimers. Furthermore, both mass spectrometry and western blotting confirmed the presence of the ubiquitin moiety in the split Ub-PCNA preparations (Figure 4.2B).

Effect of split PCNA and Ub-PCNA on DNA pol η activity

Before carrying out structural determinations, I first examined whether split PCNA and split Ub-PCNA could function *in vitro* to stimulate the catalytic activity of DNA polymerase η (pol η), a prototypical non-classical DNA polymerase. It has been shown previously that both non-split PCNA and non-split Ub-PCNA stimulate the ability of pol η to incorporate nucleotides opposite template abasic sites^{96,173,174}. Thus, I examined the ability of split PCNA and split Ub-PCNA to stimulate pol η in a running start assay (Figure 4.3). The different PCNA proteins (non-split PCNA, split PCNA, and split Ub-PCNA) were loaded onto the DNA substrate by replication factor C (the ATP-dependent clamp loading complex), and both ends of the DNA were blocked with biotin/streptavidin to prevent the PCNA proteins from sliding off the substrate. Figure

4.3B shows the incorporation of nucleotides by pol η opposite an abasic site under running start conditions. Pol η alone had very low activity in this context and incorporated opposite the lesion on 2.5% of the substrates in 5 min. In the presence of non-split PCNA, split PCNA, and split Ub-PCNA, pol η had greater activity and incorporated opposite the lesion on 11%, 12%, and 14% of the substrates in 5 min., respectively. I observed no full length, run-off products under these conditions. Although full-length products were observed previously for pol η in experiments with both unmodified PCNA and Ub-PCNA¹⁷³, the enzyme was in excess over the DNA in that study compared to the conditions used here in which the DNA was in a 10-fold excess over the enzyme.

To quantify the effects of non-split PCNA, split PCNA, and split Ub-PCNA on pol η activity, I carried out steady-state kinetic studies of nucleotide incorporation opposite a template abasic site, Figure 4.4 and Table 4.1. Non-split PCNA stimulated the catalytic efficiency (V_{\max}/K_m) of nucleotide incorporation by pol η by 2.5-fold relative to the efficiency of incorporation in the absence of PCNA. Similarly, split PCNA stimulated the catalytic efficiency of pol η by 2.7 fold. Split Ub-PCNA stimulated nucleotide incorporation opposite the abasic site to a slightly greater extent (3.8-fold) than did non-split PCNA and split PCNA. These results show that both split PCNA and Ub-PCNA retained the ability to stimulate the catalytic activity of pol η , and that Ub-PCNA stimulated the activity of pol η to a slightly greater extent than did unmodified PCNA.

Effect of split PCNA and Ub-PCNA on cell growth and UV sensitivity

I next determined whether the split PCNA and split Ub-PCNA proteins would support cell viability and normal cell growth. I generated four *pol30* Δ yeast strains (*POL30* encodes PCNA) harboring plasmids encoding different versions of PCNA. One strain produced the wild type PCNA protein; another produced the mutant K164R PCNA

protein, which served as a negative control because it cannot be monoubiquitinated by the Rad6/Rad18 complex. The other two strains produced the split PCNA and split Ub-PCNA proteins. The *POL30* gene is essential, and all four PCNA variants supported cell viability. Moreover, all four strains grew at the same rate (Figure 4.5A). Indicating no serious defects in normal DNA replication occurred in the presence of split PCNA or Ub-PCNA.

To determine whether the split PCNA and split Ub-PCNA proteins functioned in translesion synthesis *in vivo*, I examined the UV sensitivity of these four yeast strains, (Figure 4.5B). The strain producing the wild type PCNA protein was significantly more resistant to UV radiation than was the strain producing the K164R PCNA mutant protein. This was because the K164R PCNA mutant protein cannot be monoubiquitinated, and thus eliminating translesion synthesis. The strain producing the split PCNA protein, which contains Lys-164, was as sensitive to UV radiation as the strain producing the K164R mutant protein. This suggests that splitting PCNA between residues 163 and 164 prevented the monoubiquitination of PCNA by the Rad6/Rad18 complex. Interestingly, the strain producing the split Ub-PCNA protein was at least as resistant to UV radiation as the strain producing the non-split PCNA protein. These results clearly demonstrate that split Ub-PCNA fully supported translesion synthesis *in vivo*.

Structure of Split PCNA

Confident that split PCNA both stimulated the activity of pol η *in vitro* and supported cell viability *in vivo*, I proceeded to determine the X-ray crystal structure of split PCNA to a resolution of 3.0 Å (Table 4.2). There was a single PCNA subunit in the asymmetric unit, so the structure of the biologically relevant trimer was obtained by generating the symmetry related neighboring subunits as was done previously for non-split PCNA (Figure 4.6)¹⁰³. The structure of a single monomer of split PCNA with the N fragment colored blue and the C fragment colored red is shown in Figure 4.7A. Each

PCNA monomer had two domains, domain A (residues 1-118) and domain B (residues 135-258), joined by the long, flexible linker called the inter-domain connector loop (IDCL, residues 119-134). This structure shows that these two polypeptides self-assembled with the N fragment and the C fragment interdigitating in domain B. The N fragment contained all of domain A and portions of domain B, specifically β strands βA_2 (residues 135-140) and βB_2 (residues 157-163) and α helix αA_2 (residues 141-153); the C fragment contained the remainder of domain B. Three of the four α helices from each monomer that line the inside of the central cavity of the ring-shaped trimer were from the N fragment; only helix αB_2 (residues 157-163) was from the C fragment. A diagram of the protein topology is shown in Figure 4.7B

To ensure that splitting PCNA did not result in significant changes to its structure, I superimposed the backbone of split PCNA and non-split PCNA (Figure 4.8A). The root-mean-square deviation between these two structures was 0.6 Å over the 254 C α atoms showing that the break in the protein backbone between residues 163 and 164 did not significantly affect the structure of the PCNA monomer. In fact, the break in the protein backbone did not alter the structures of the β strands immediately adjacent to the break (βB_2 and βC_2), except at the position of Lys-164. This residue was disordered in split PCNA, but was not disordered in non-split PCNA (Figure 4.8B). This is probably why split PCNA does not support translesion synthesis *in vivo*; it probably cannot be ubiquitinated by Rad6/Rad18.

Structure of Ub-PCNA

Confident that split Ub-PCNA both stimulated the activity of pol η *in vitro* and supported cell viability and translesion synthesis *in vivo*, I then determined the X-ray crystal structure of Ub-PCNA to a resolution of 2.8 Å (Table 4.2). While there was a single PCNA subunit and a single ubiquitin moiety in each asymmetric unit, the ubiquitin moiety occupied two distinct, yet very similar positions within the asymmetric unit. This

means that the ubiquitin was capable of moving around somewhat in the protein crystal, but preferred to be in one of these two positions. Ubiquitin moieties in these preferred positions were both oriented the same way and were separated by only 2.5 Å (Figure 4.9). Stereo images of the electron density of the ubiquitin moiety are shown in (Figure 4.10). Thus I can safely conclude that ubiquitin is located on the back face of the PCNA ring on the opposite side from the IDCL, (Figure 4.11 and 4.12).

To determine whether the monoubiquitination of PCNA altered the conformation of the PCNA portion of the molecule, I overlaid the backbones of Ub-PCNA and non-split PCNA (Figure 4.13). The root-mean-square deviation between these two structures was 0.6 Å over the 254 C α atoms of the PCNA. In addition, I did not detect any local differences between the structures of Ub-PCNA and non-split PCNA. This shows that the attachment of ubiquitin did not alter the conformation of PCNA in any notable way.

The surface of the ubiquitin moiety that interacts with PCNA was the canonical hydrophobic surface centered on Leu-8, Ile-44, and Val-70 that interacts with a variety of other proteins^{223,224}. The regions of PCNA that interact with ubiquitin were all in domain 2 and included residues on β strand βA_2 (residues 135-140), loop P (residues 184-196), β strand βE_2 (residues 196-199), loop S (residues 222-223), and β strands βG_2 (residues 224-229). The PCNA-ubiquitin contacts are shown in (Figure 4.14). In addition to hydrophobic contacts, there were several electrostatic and hydrogen bonding interactions. For example, the backbone carbonyl oxygen of Leu-8 of ubiquitin interacted with a nitrogen atom on the side chain of Arg-224 of PCNA. Diagrams of the hydrophobic, electrostatic, and hydrogen bonding interactions for each ubiquitin moiety are shown as a lig-plot in Figure 4.15.

Discussion

Arguably the least understood step of translesion synthesis is the polymerase exchange step between the classical and the non-classical polymerase. Insight into the

structural and mechanistic basis of the polymerase exchange has come from studies of prokaryotic systems. An X-ray crystal structure of the polymerase-associated domain (PAD) of non-classical DNA polymerase IV (pol IV) from *E. coli* bound to the β sliding clamp has been determined¹⁸⁰. This structure shows that the C-terminal tail of pol IV binds to the front of the clamp in a hydrophobic pocket while the remainder of the PAD interacts with the side of the clamp at the subunit interface. Further biochemical studies showed that pol IV and the clamp form a tool belt on the DNA with classical DNA polymerase III (pol III)¹⁷⁹. In this tool belt mechanism, pol IV binds to the side of the clamp and rides piggy back while pol III synthesizes DNA in front of the clamp. When replication by pol III is blocked at a lesion in the template, these two polymerases switch places and pol IV begins synthesizing DNA.

One crucial difference between the prokaryotic and eukaryotic systems is that the polymerase exchange in eukaryotes requires the monoubiquitination of PCNA. This was shown with an *in vitro* reconstituted system comprised of classical pol δ , non-classical pol η , and PCNA or Ub-PCNA¹⁷⁸. In this system, pol η could not exchange with pol δ at the replication fork unless synthesis by pol δ was stalled. Moreover, the exchange between pol η and pol δ occurred in the presence of Ub-PCNA, but not in the presence of unmodified PCNA. Precisely how Ub-PCNA facilitated the polymerase exchange reaction in this system, however, was not clear.

To better understand the polymerase exchange in eukaryotes, I determined the X-ray crystal structure of Ub-PCNA. I found two very similar preferred positions for the ubiquitin moiety on the back side of PCNA. These preferred positions were not the result of crystal contacts, but rather formed by specific interactions between ubiquitin and PCNA. Support for this comes from the fact that there is substantially more buried surface area (1366 \AA^2) between ubiquitin and the PCNA subunit to which it is attached than there is between ubiquitin and other symmetry related molecules (460 \AA^2). Moreover, the high solvent content of the protein crystal (70%) – combined with the high

degree of flexibility of the C terminus of ubiquitin – suggests that the ubiquitin would be free to orient many different ways if there was not a specific interaction between ubiquitin and PCNA. The fact that ubiquitin has a preferred orientation shows that the interaction between ubiquitin and PCNA is specific.

Despite the fact that the interaction between ubiquitin and PCNA is specific, it appears that this interaction is rather weak. Support for this comes from the fact that there are two principal positions for the ubiquitin. I suggest that the weakness of this interaction affords ubiquitin the flexibility to re-orient itself so that it can bind other interacting partners via the same canonical hydrophobic surface with which it binds PCNA. For example, NMR titrations have shown that the UBZ motif of pol η interacts with this same surface on ubiquitin¹⁷⁵. Thus, for Ub-PCNA to bind to the UBZ of pol η , the ubiquitin moiety must undergo a rotation of approximately 60° in order to expose its binding site for the UBZ motif.

There are four general models by which the monoubiquitination of PCNA alone could facilitate the polymerase exchange reaction. These four general models are not intended to be mutually exclusive, and any combination of them is possible in principle. Model 1: ubiquitination directly reduces the binding affinity for the classical polymerase to PCNA and promotes its dissociation via interactions between the ubiquitin and the classical polymerase. Model 2: ubiquitination indirectly reduces the binding affinity for the classical polymerase via allosteric effects on PCNA. Model 3: ubiquitination directly enhances the affinity for the non-classical polymerase and promotes its recruitment via interactions between the ubiquitin and the non-classical polymerase. Model 4: ubiquitination indirectly enhances the affinity for the non-classical polymerase via allosteric effects.

The structure of Ub-PCNA provides compelling reasons to reject three of these four models of the polymerase exchange reaction. First, the attachment of ubiquitin to PCNA does not alter the conformation of PCNA. There are no detectable changes to the

structure of the hydrophobic pocket on the front face of PCNA near the IDCL to which the conserved PCNA-interacting protein (PIP) motifs of various proteins, including classical and non-classical polymerases, bind. This implies that monoubiquitination of PCNA does not induce allosteric effects resulting in either a reduction of the affinity of the classical polymerase or an enhancement of the affinity of the non-classical polymerase for PCNA as had been suggested previously¹⁵⁷. This argues against model 2 and model 4. Second, the ubiquitin is bound on the back face of the PCNA ring, presumably far away from where the classical polymerase sits in front of the PCNA ring. This strongly suggests that the ubiquitin does not promote classical polymerase dissociation by directly interacting with the classical polymerase. This argues against model 1. Consequently, the structure of Ub-PCNA supports only model 3 – namely that Ub-PCNA directly facilitates non-classical polymerase recruitment to the back face of the PCNA ring by forming a new interacting surface for the non-classical polymerase.

The structure of Ub-PCNA reported here represents the form of the protein to which pol η is recruited. Although I do not know exactly what the complex of Ub-PCNA bound to pol η and DNA looks like, I am now in an excellent position to model this complex (Figure 4.16). This model is based on the X-ray crystal structure of the catalytic core of pol η ^{50,225}, the X-ray crystal structure of the PIP motif of pol η bound to PCNA¹¹³ and the NMR structure of the UBZ motif of pol η ¹⁷⁵. In this structural model, the PIP motif of pol η at its extreme C terminus (residues 617-632) binds in the hydrophobic pocket on the front face of the Ub-PCNA ring near the IDCL. The pol η protein chain then makes its way to the back face of the Ub-PCNA ring where the UBZ motif (residues 566-577) interacts with the ubiquitin, which has been rotated 60° in order to expose its binding site for the UBZ motif. From there, the protein chain makes its way back to the front side of the PCNA ring where the catalytic core of pol η (residues 1-513) binds to the DNA primer terminus. It should be noted that the pol η protein chain, somewhere between the catalytic core and the UBZ motif, likely passes nearby and interacts with

loop J of PCNA (residues 105-110), which has previously been shown by structural and biochemical studies to be important for pol η function (see Chapter 2)²⁰⁸.

According to this structural model, with the exception of the PIP motif, the entire C-terminal region of pol η interacts exclusively with the side and back face of Ub-PCNA. This is consistent with, although does not by itself imply, a tool belt model of translesion synthesis (Figure 1.9). In essence, PCNA ubiquitination could set up the tool belt by recruiting pol η to the side and back of Ub-PCNA via the C-terminal region of pol η while pol δ synthesizes DNA in front of the Ub-PCNA ring (Figure 4.17). The catalytic core of pol η could ride piggy back on the Ub-PCNA ring because the catalytic core is connected to the C-terminal region by a long, flexible linker. When pol δ encounters a template lesion and stalls, it could be displaced by the catalytic core of pol η , which would then begin synthesizing DNA in front of the Ub-PCNA ring. Whether pol δ would dissociate at this point or remain bound to Ub-PCNA and ride piggy back while pol η synthesizes DNA – the latter option being analogous to the prokaryotic system – is unclear. While there is compelling evidence that prokaryotes utilize a tool belt mechanism to carry out translesion synthesis¹⁷⁹, it remains to be seen whether eukaryotes utilize such a mechanism.

Figure 4.1 continued. Schematic of Split and Ub-PCNA. (A) Diagram of the two polypeptides used to generate split PCNA is shown with molecular weights indicated. (B) Diagram of the two polypeptides used to generate Ub-PCNA is shown with the molecular weights indicated. (C) Schematic of the Ub-PCNA highlighting the glycine linkage with the ubiquitin moiety shown in red, the PCNA moiety shown in blue, and the glycine linker shown in black.

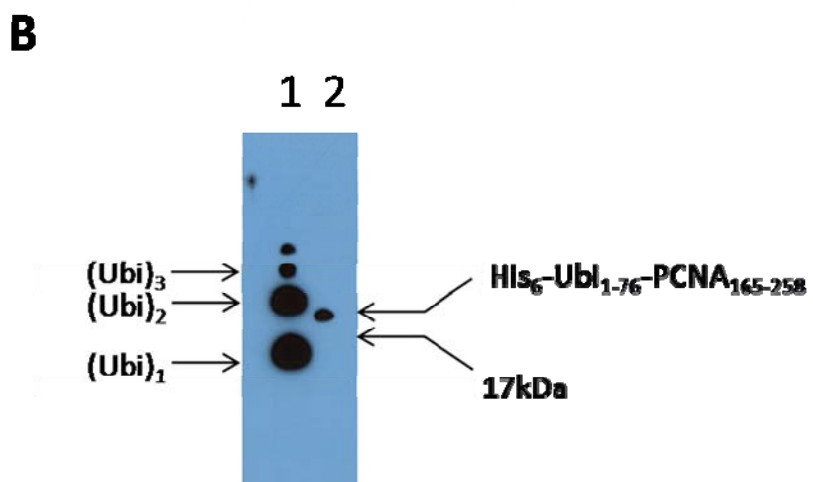
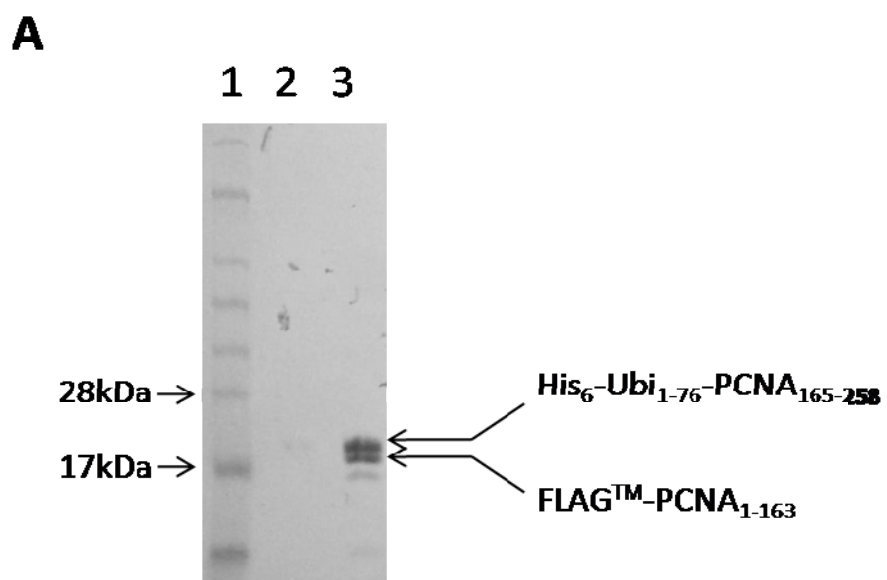


Figure 4.2 Purification of Ub-PCNA

Figure 4.2 continued. (A) SDS page analysis of the Ub-PCNA following purification and stained with commassie blue. Lane 1: Protein molecular weight standard; the molecular weights are listed next to the protein marker. Lane 2: the final fraction from the low salt wash. Lane 3: Purified Ub-PCNA with the each fragment indicated next to the protein elution lane (B) Western blot analysis using an ubiquitin antibody. Lane 1: Purified ubiquitin containing a cysteine at the C-terminus resulting in the formation of higher ordered species. Lane 2: Purified Ub-PCNA; the ^{ubi}C fragment and molecular weight marker are indicated next to the gel.

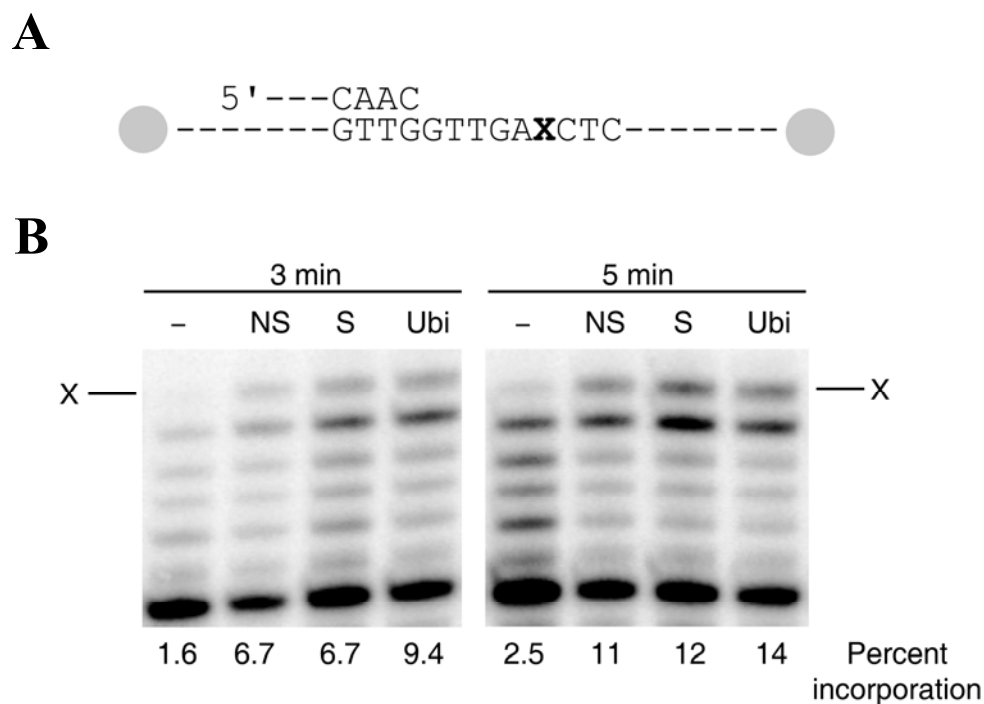


Figure 4.3 Stimulation of pol η activity by split PCNA and Ub-PCNA. (A) Diagram of the running start DNA substrate used. The 'X' represents an abasic site. Both ends of the template strand are capped with biotin-streptavidin blocks. (B) Autoradiograph of the products of the running start reaction of pol η and the indicated DNA substrate after 3 min. and 5 min. The arrow represents incorporation opposite the abasic site. Lanes labeled '-' contain no PCNA, lanes labeled 'NS' contain non-split PCNA, lanes labeled 'S' contain split PCNA, and lanes labeled 'Ubi' contain Ub-PCNA. The percent incorporation is shown below each lane.

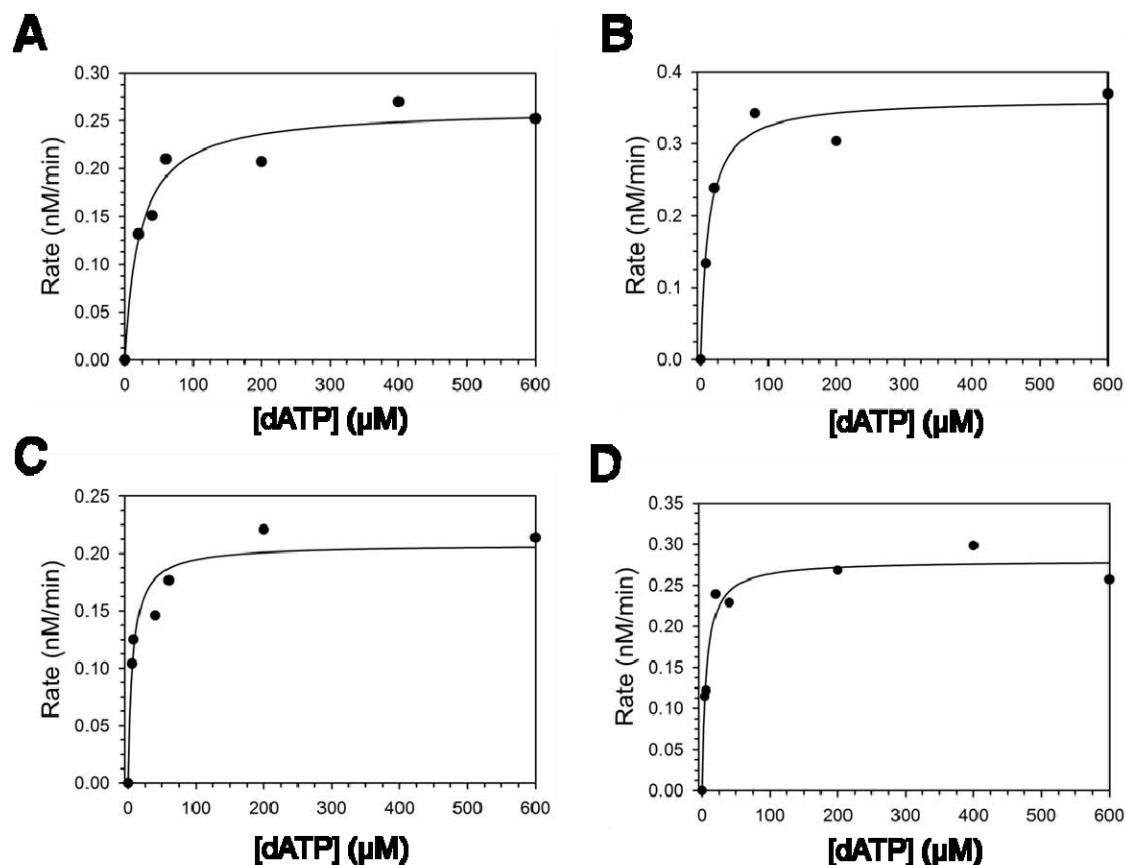


Figure 4.4 Steady state kinetics of pol η on an abasic site. The rate of nucleotide incorporation was graphed as a function of dATP concentration for (A) pol η alone, (B) pol η with wild type PCNA protein, (C) pol η with Split PCNA protein (D) and pol η with Ub-PCNA protein. The solid lines represent the best fits of the data to the Michaelis–Menten equation, and the V_{\max} and K_m steady state parameters are given in Table 4.2. These graphs are from a single experiment and are representative of the trends that I observed over at least twenty independent experiments.

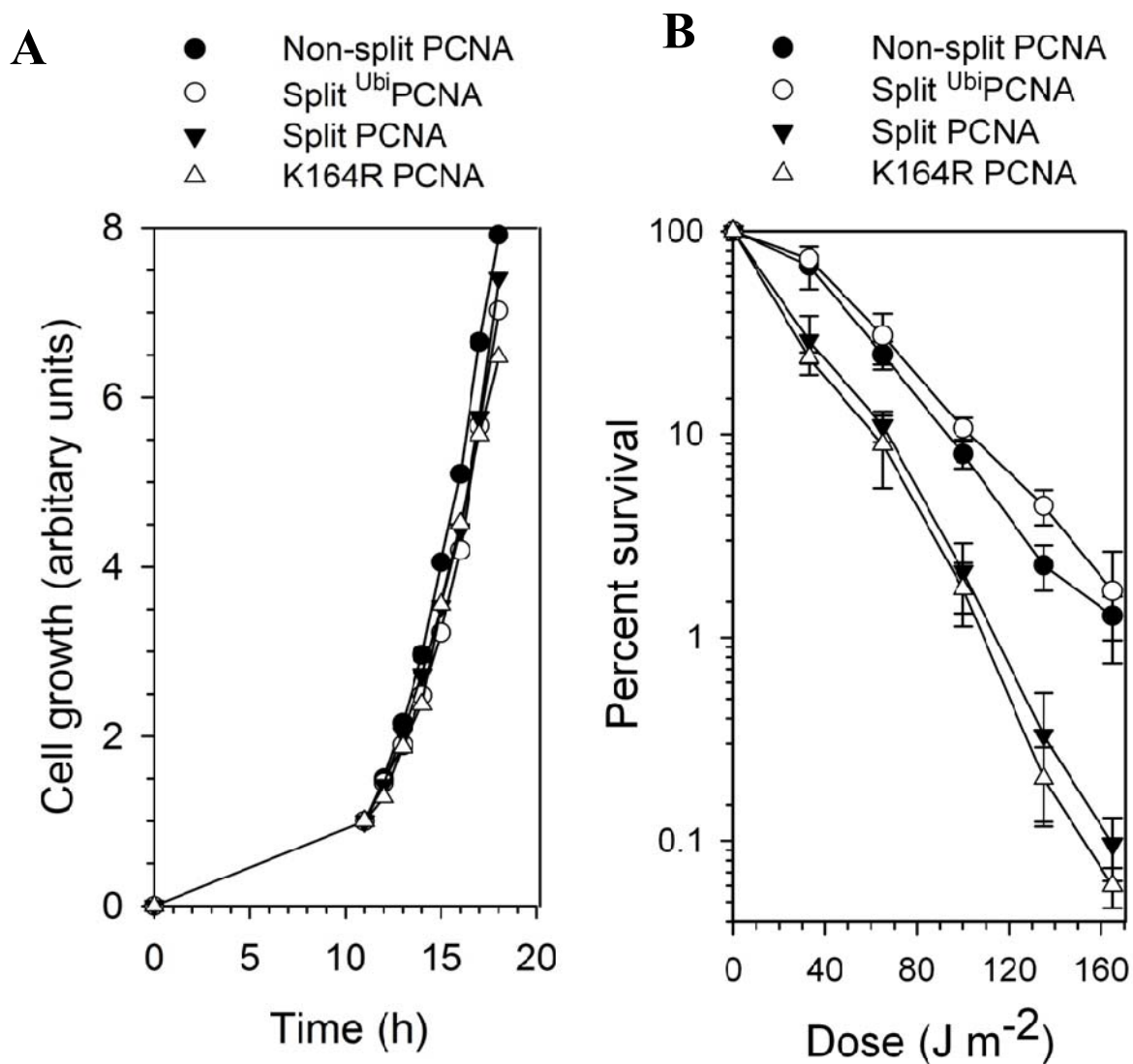


Figure 4.5 Viability and UV sensitivity of yeast cells expressing split PCNA and Ub-PCNA. (A) The growth of cells producing only non-split PCNA, the K164R mutant PCNA protein, split PCNA, or Ub-PCNA is graphed as a function of time. The plotted growth curve is an average of two experiments. (B) UV sensitivity of cells producing only non-split PCNA, the K164R mutant PCNA protein, split PCNA, or Ub-PCNA is shown by graphing the percent of surviving cells as a function of the UV dose.

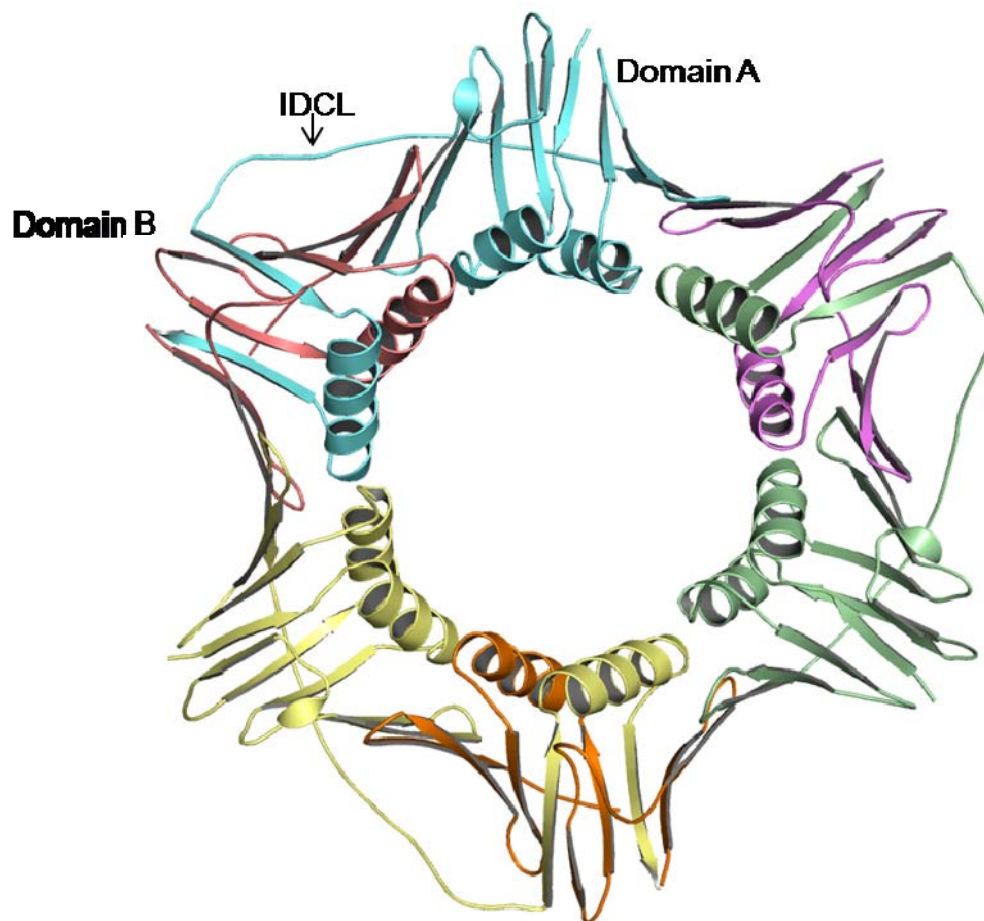


Figure 4.6 Structure of the split PCNA trimer. The three N fragments colored blue, green, and yellow and the three C fragments colored red, purple, and orange. Domain 1, domain 2, and the interdomain connector loop (IDCL) are indicated.

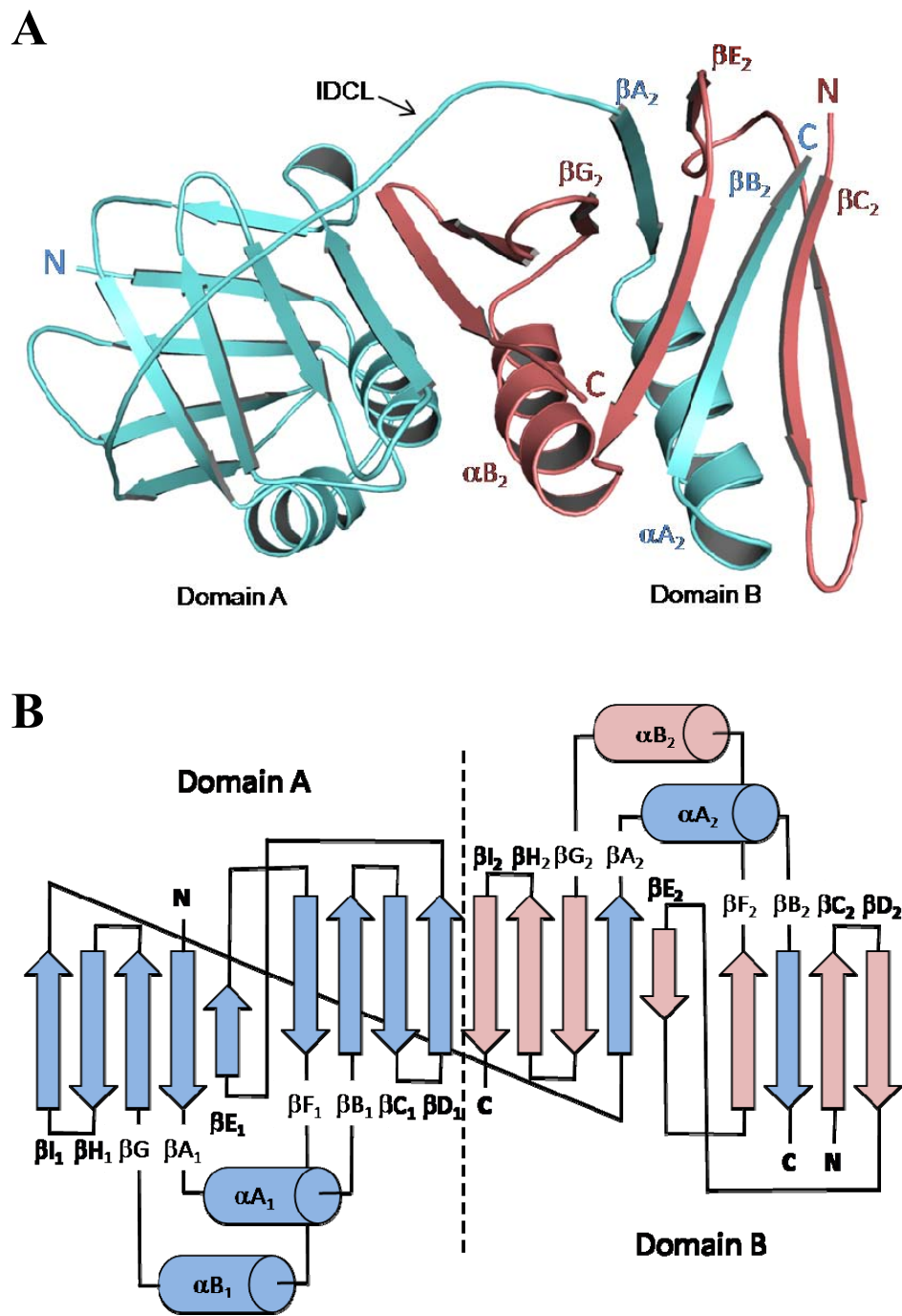
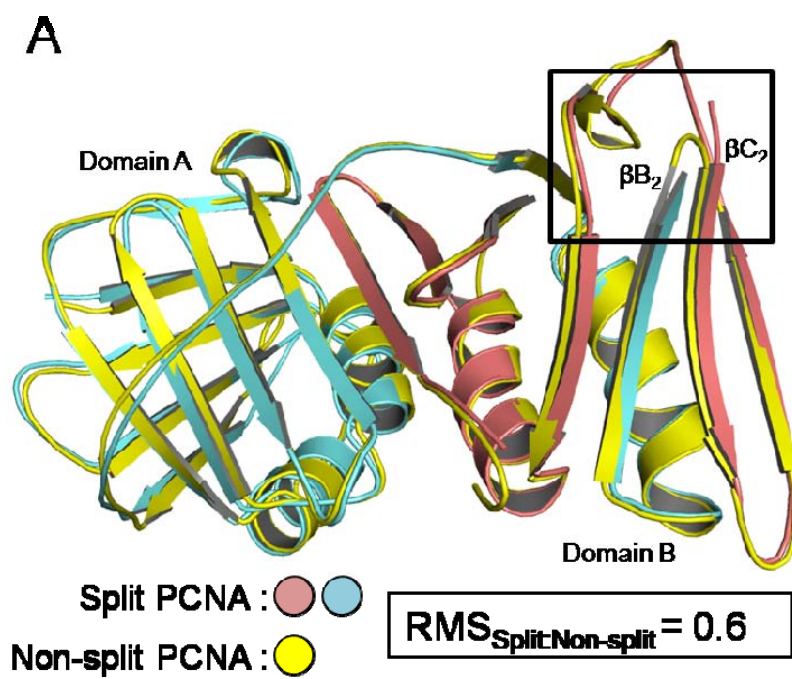


Figure 4.7 The monomeric subunit of split PCNA

Figure 4.7 continued. (A) Structure of a single split PCNA monomer is shown with the N fragment colored blue and the C fragment colored red. The interdigitating β strands of the two fragments in domain B are labeled. (B) A schematic of the single split PCNA monomer with each secondary structural element labeled.



B

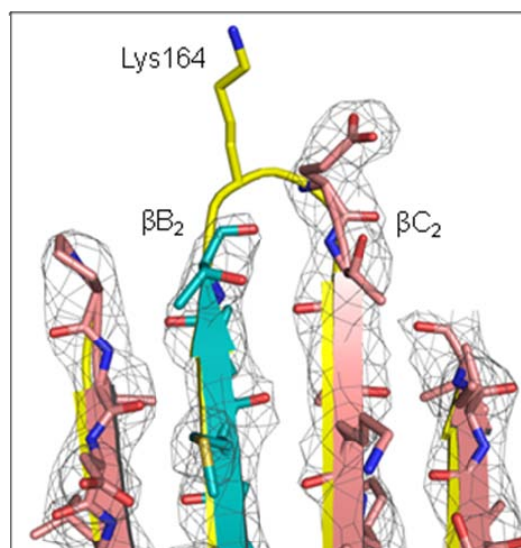


Figure 4.8 Comparison of split PCNA with non-split PCNA

Figure 4.8 continued (A) The backbone of split PCNA, which is colored blue (N fragment) and red (C fragment), is superimposed on the backbone of non-split PCNA, which is colored yellow. (B) Close up of the loop between β strands β B2 and β C2 showing the position of Lys-164 in non-split PCNA and the break in the backbone between the N fragment and C fragment of split PCNA. The electron density (level=2.0) is shown for split PCNA.

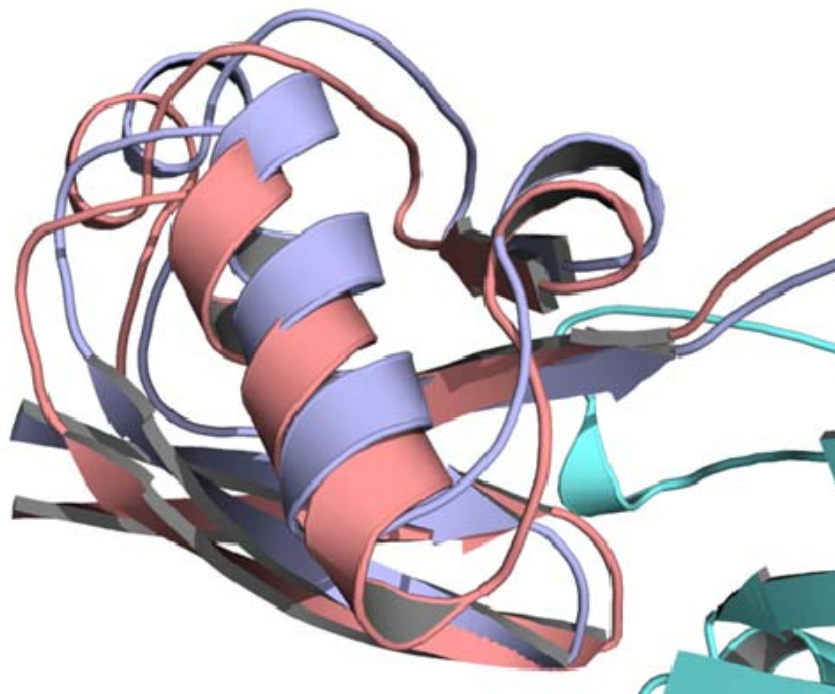


Figure 4.9 Overlay of the two preferred positions of the ubiquitin moiety. Position 1 is shown in red and position 2 is shown in blue. The corresponding atoms in these positions are separated by 2.5 Å.

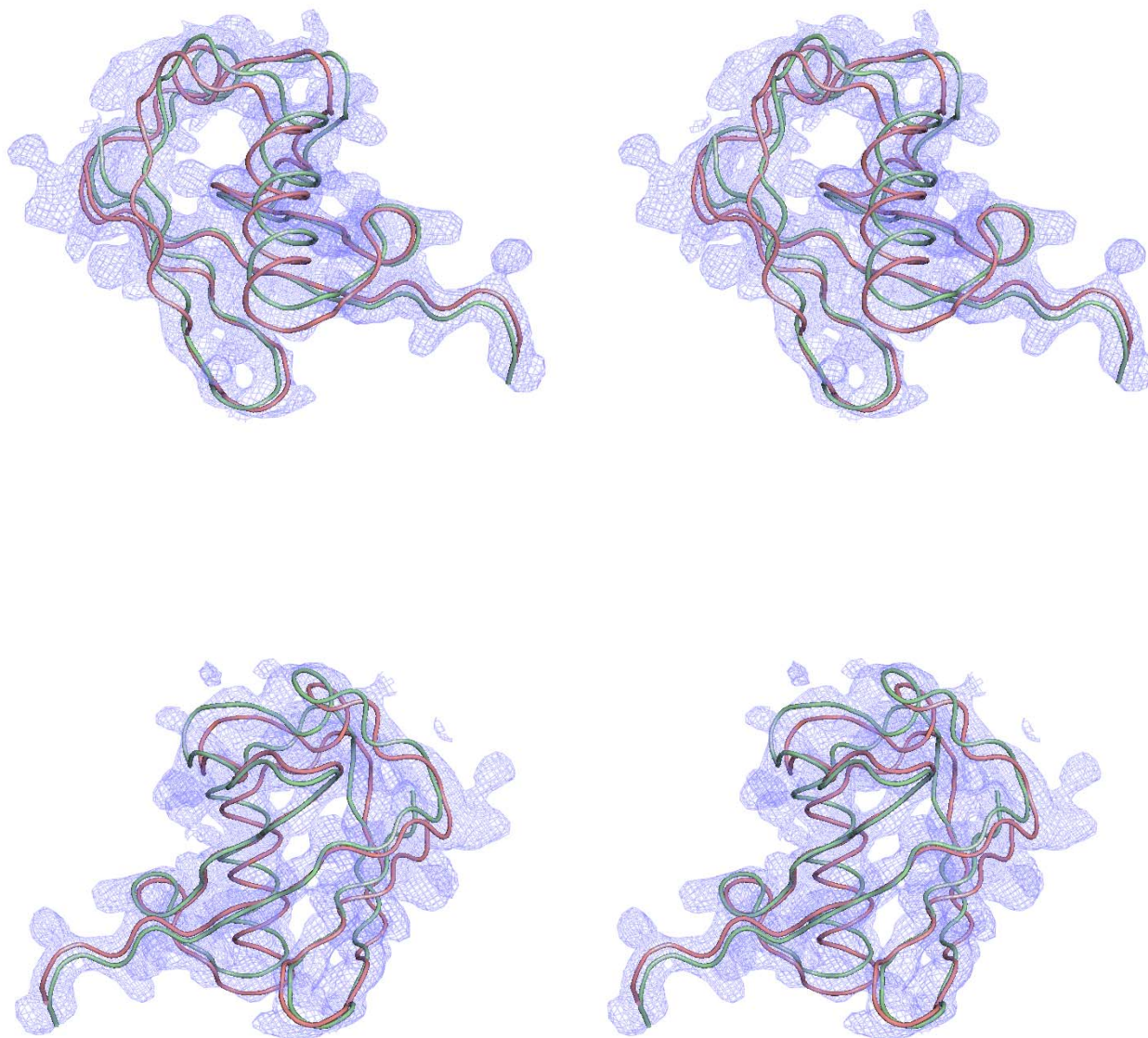


Figure 4.10 Stereo images of the electron density (level=1.2 sigma) of the ubiquitin moiety. The backbone of ubiquitin in position 1 is shown in red, and the backbone of ubiquitin in position 2 is shown in green. The bottom set of stereo images is rotated 180° relative to the top set of stereo images.

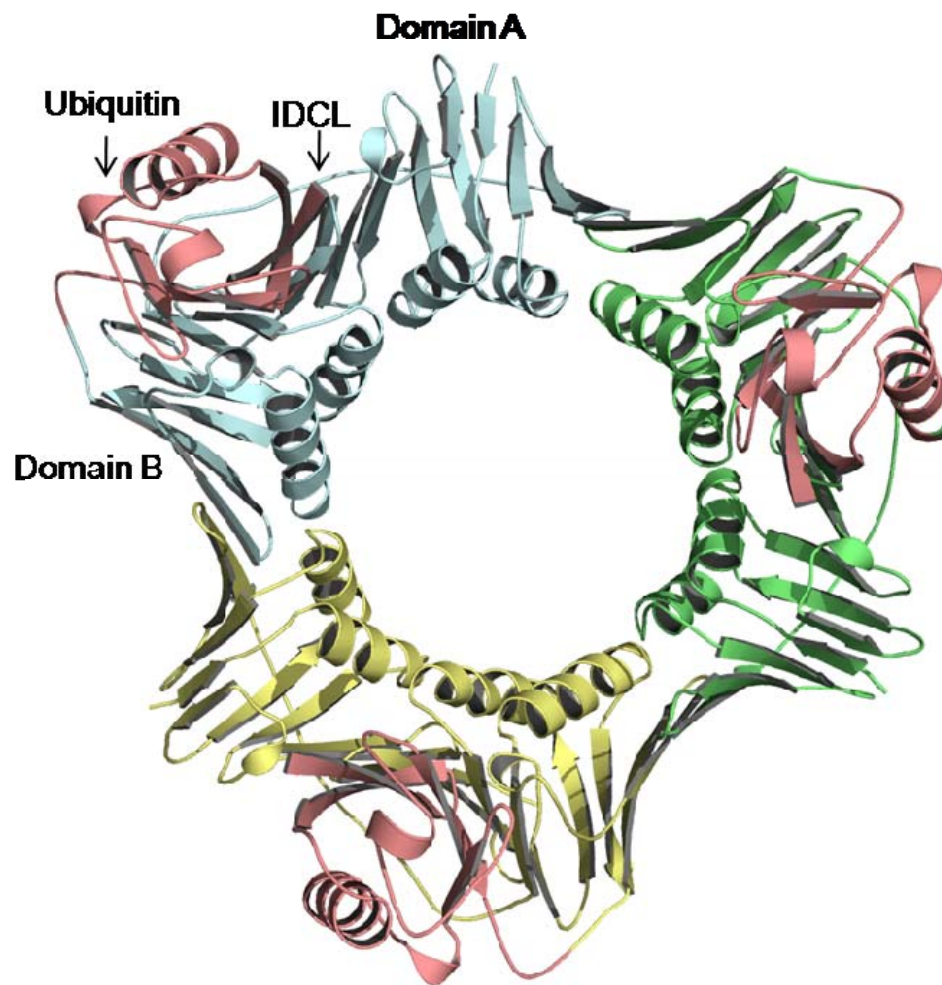


Figure 4. 11 Structure of the Ub-PCNA trimer. This is shown from the back side with the three PCNA subunits shown in blue, green, and yellow and the three ubiquitin moieties (in position 1) shown in red. Domain A, Domain B, and the IDCL are indicated for one PCNA monomer.

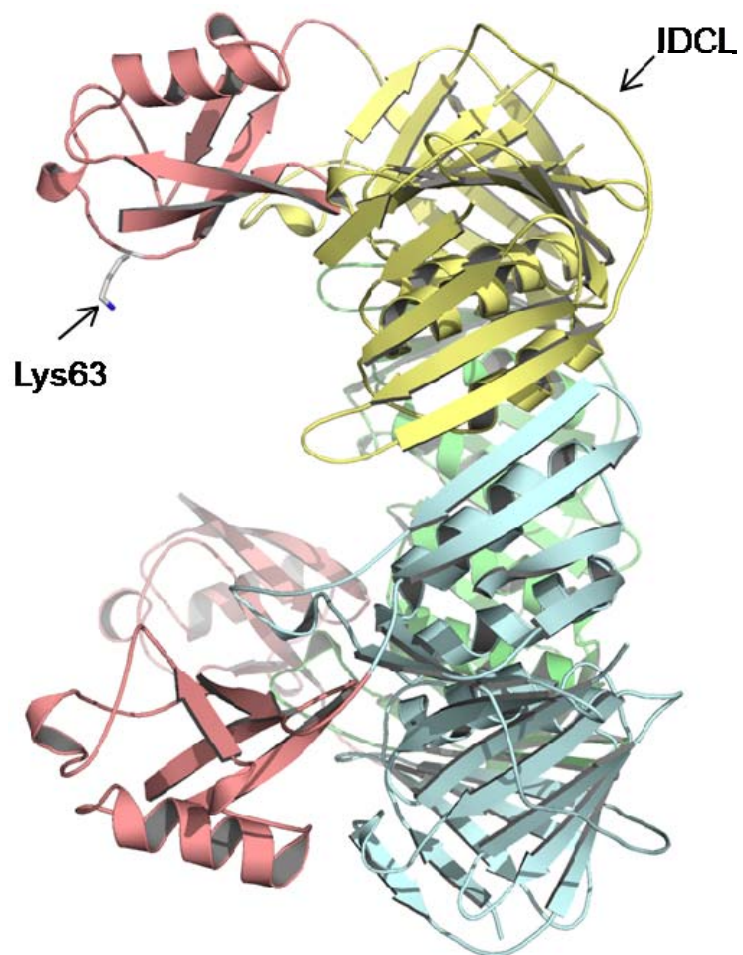


Figure 4.12 Side view of the Ub-PCNA trimer. The IDCL of PCNA and the side chain Lys-63 of ubiquitin (the site of polyubiquitination) are indicated.

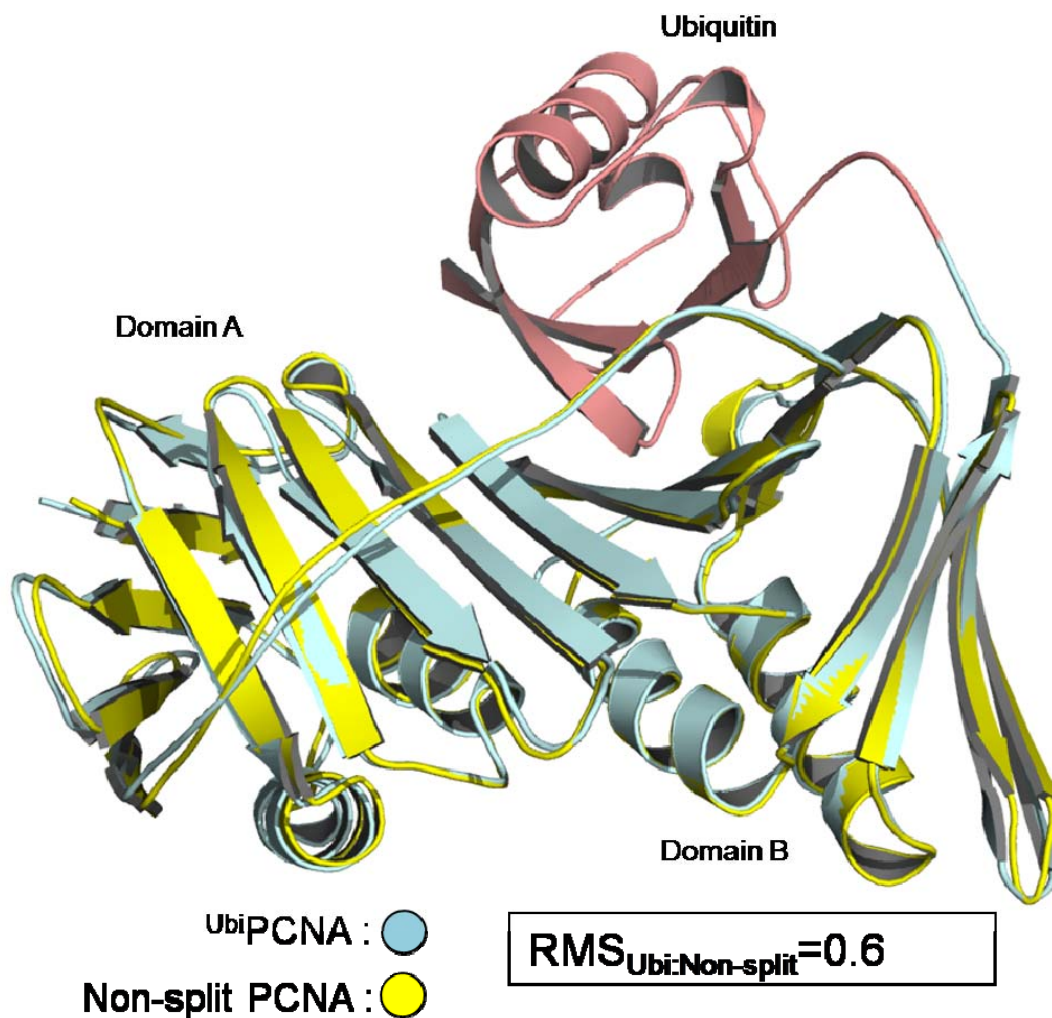


Figure 4.13 Overlay of the Ub-PCNA with non-split PCNA. The backbone of Ub-PCNA, which is colored blue (PCNA portion) and red (ubiquitin moiety), is superimposed on the backbone of non-split PCNA, which is colored yellow.

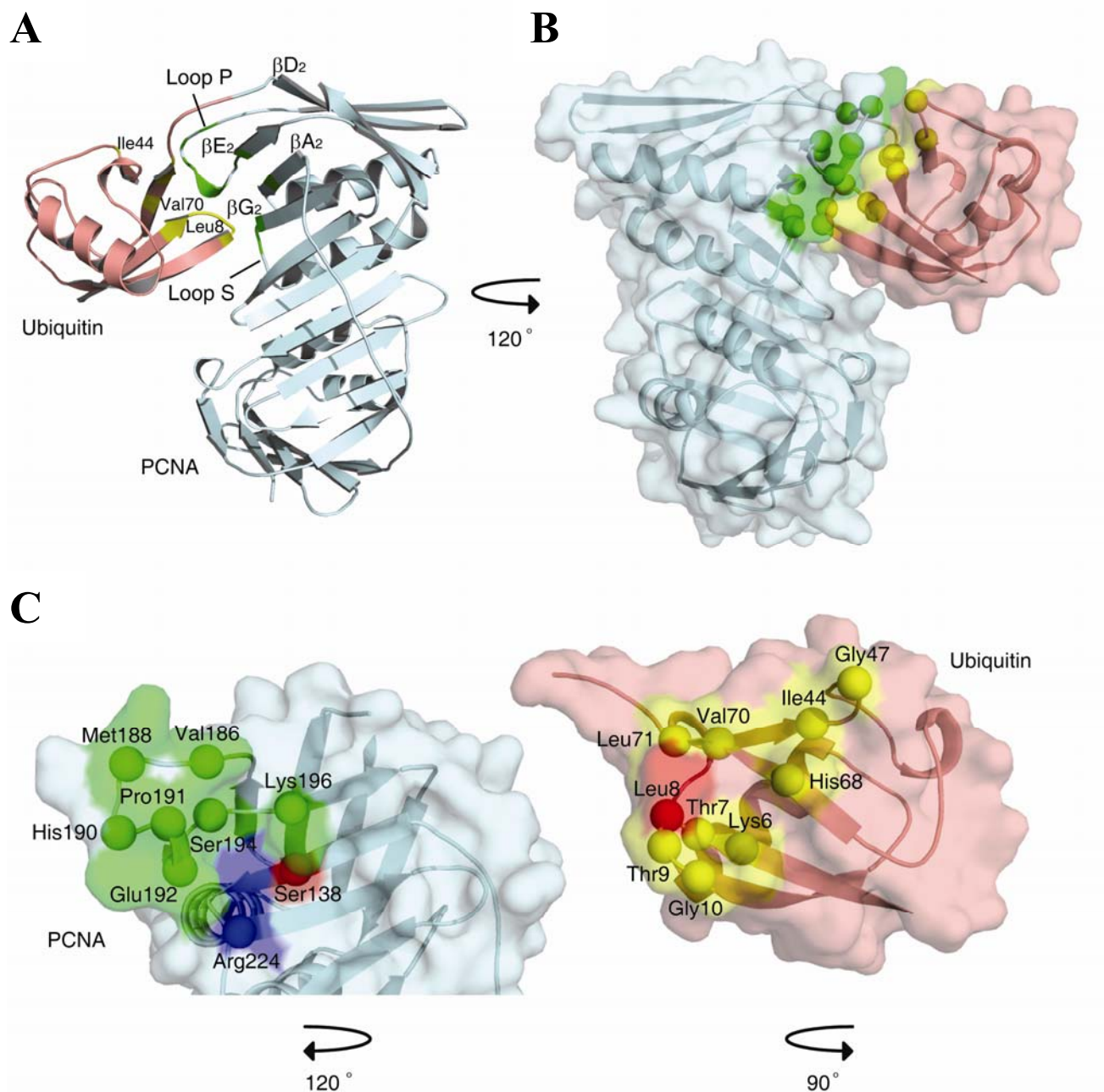


Figure 4.14 Interactions between ubiquitin and PCNA within Ub-PCNA.

Figure 4.14 continued. (A) Ribbon representation showing the ubiquitin-PCNA interface. The ubiquitin moiety is shown in red, and PCNA is shown in blue. Regions of the ubiquitin moiety contacting PCNA are shown in yellow, and regions of the PCNA contacting the ubiquitin moiety are shown in green. (B) Space filled representation of the ubiquitin-PCNA interface shown from a different angle. (C) Close up of the interfaces on the ubiquitin moiety and PCNA. The ubiquitin moiety and PCNA have been separated and rotated relative to the orientation in panel B to show the binding surfaces on each. Residues forming hydrophobic contacts are shown in green and yellow for the PCNA and ubiquitin moiety, respectively. Residues forming electrostatic contacts are shown in blue and red.

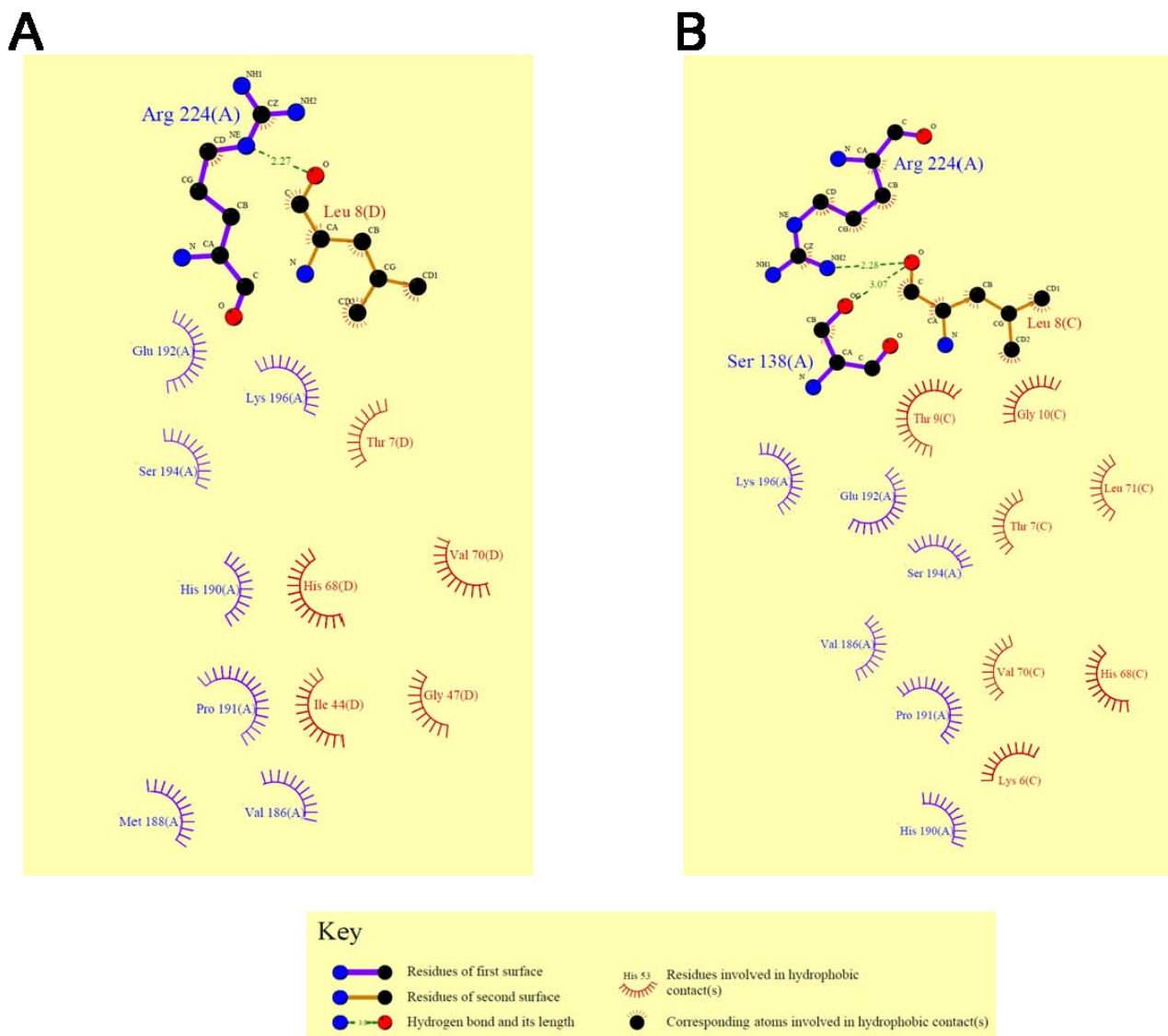


Figure 4.15 Lig-plots for the ubiquitin PCNA interactions. Diagrams of the hydrophobic, electrostatic, and hydrogen bonding interactions between ubiquitin and PCNA for both position one (A) and position two (B) of ubiquitin.

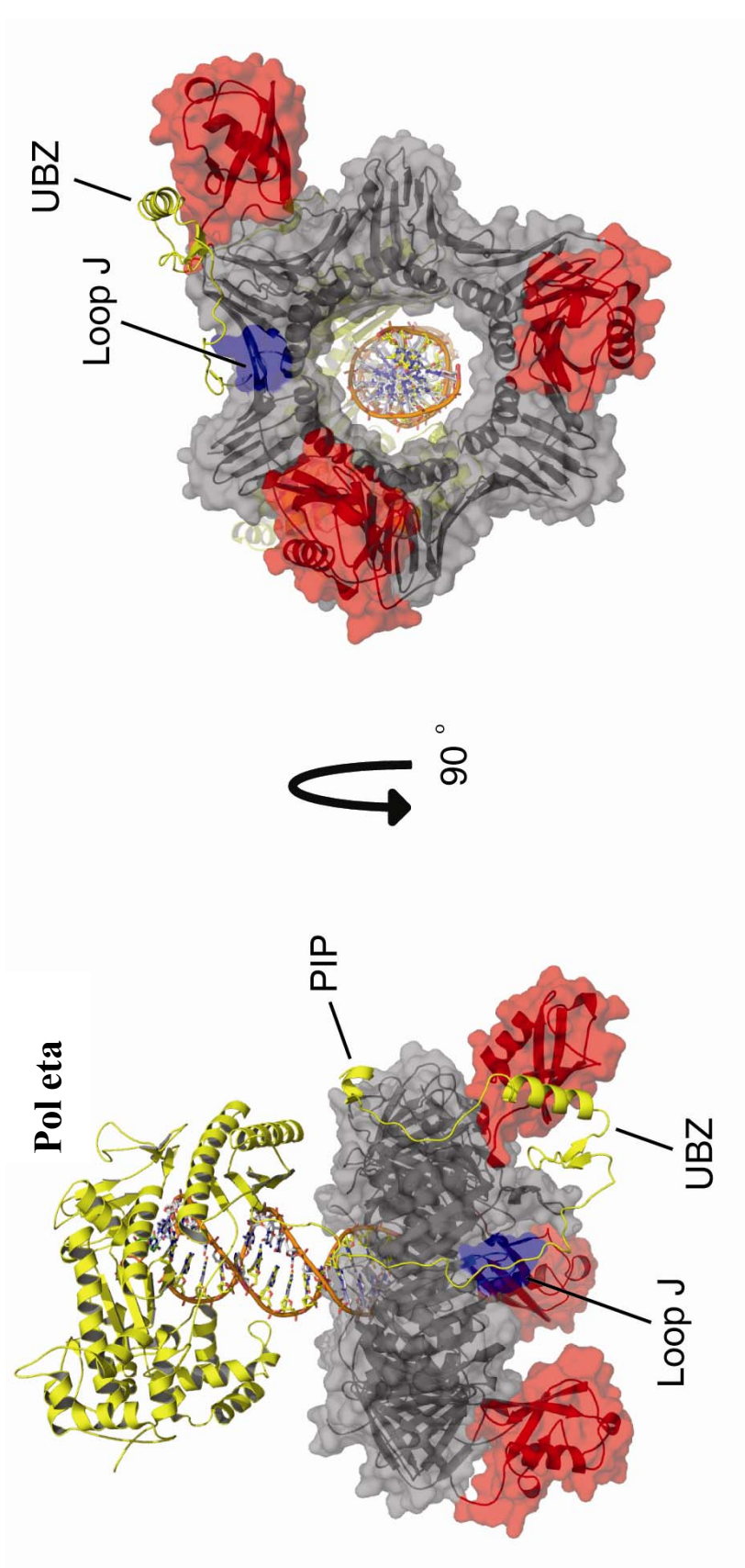


Figure 4.16 Model of the complex between Ub-PCNA and pol η

Figure 4.16 continued. Two views of the model of the Ub-PCNA-pol η complex. The PCNA portion is colored grey, loop J of PCNA is colored blue, the ubiquitin moieties are colored red, and the pol η is colored yellow. The PIP and UBZ motifs of pol η and loop J of PCNA are indicated.

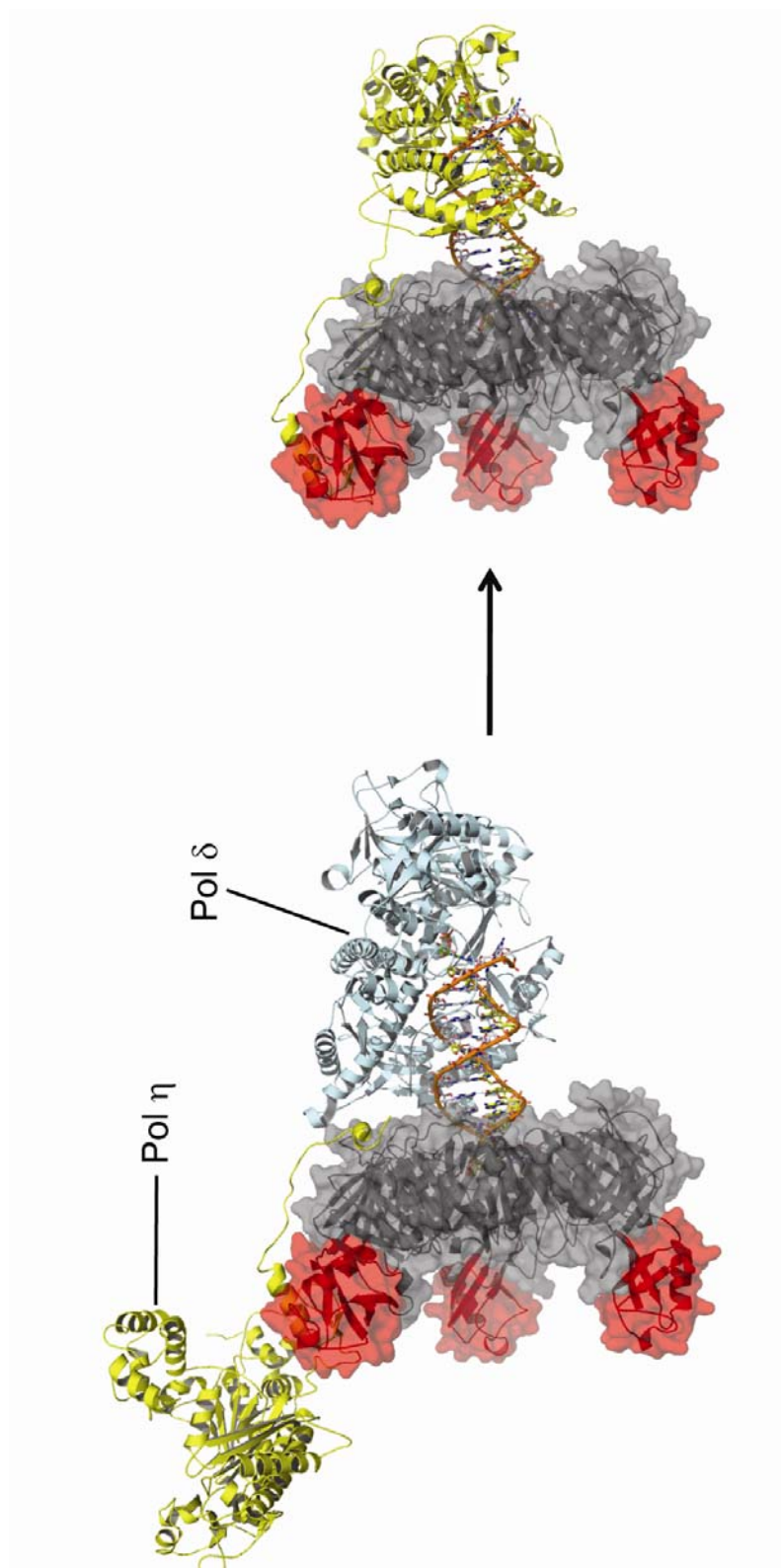


Figure 4.17 The tool-belt model

Figure 4.17 continued. A possible tool belt model showing the recruitment of pol η to the side and back face of Ub-PCNA while pol δ (colored blue) sits in front of Ub-PCNA. Eventually, pol δ is displaced from the front of Ub-PCNA by the catalytic core of pol η . For simplicity sake, pol δ is shown as dissociating from the complex, although this need not be the case.

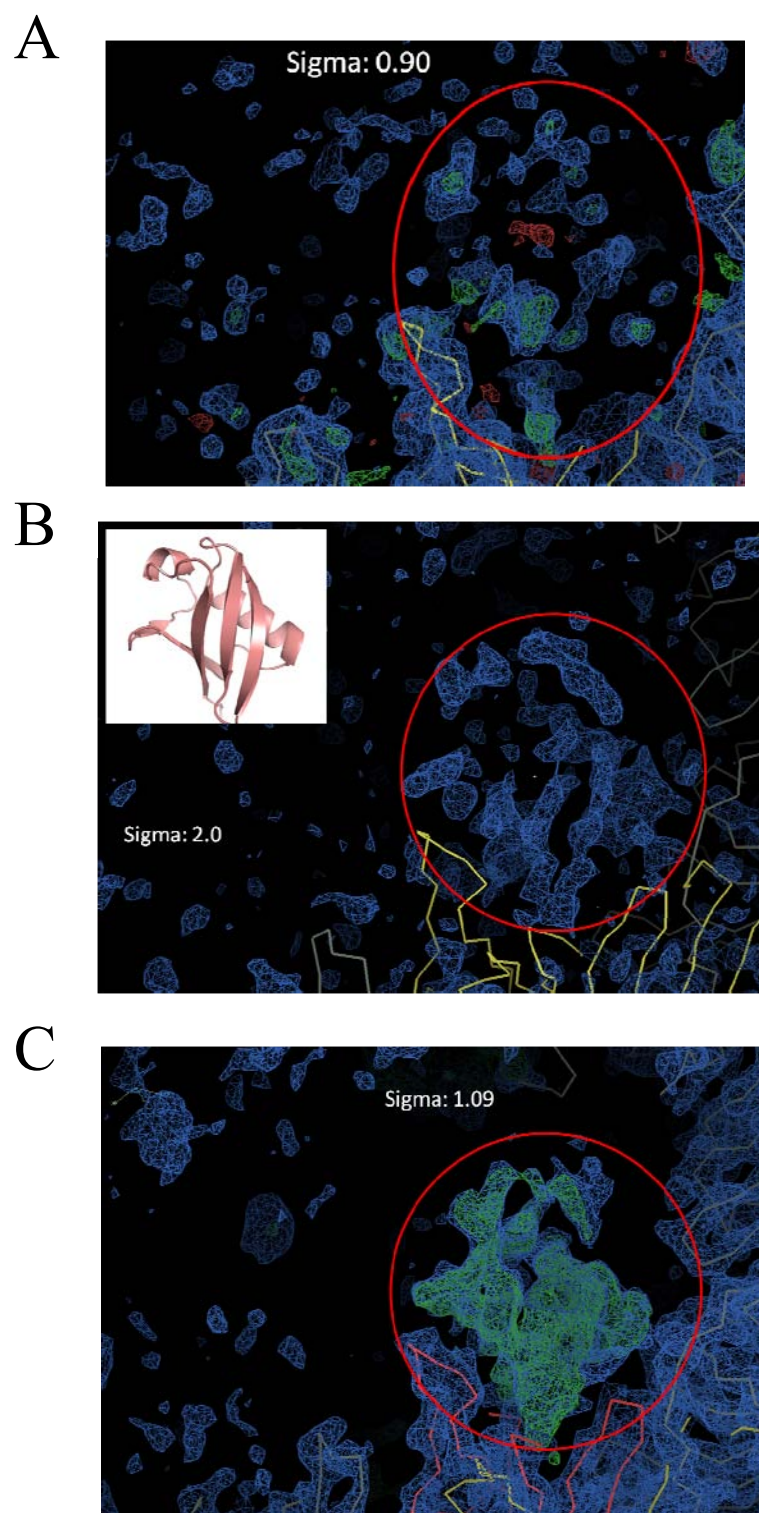


Figure 4.18 Electron density of the ubiquitin moiety at different stages of analysis.

Figure 4.18 continued. The electron density maps for the Ub-PCNA structure with PCNA shown in a backbone ribbon trace and the location of the density for the ubiquitin moiety is circled in red. Each snapshot is from the same orientation (A) The electron density (level=0.9 sigma) map following molecular replacement with only the PCNA moiety (1PLQ.pdb). (B) The Patterson difference map (level=2.0 sigma) between the split PCNA and Ub-PCNA structures with the ubiquitin structure shown in the top right corner for reference. The major secondary structural elements are becoming visible at this point with the beta strands in front and the alpha helix in back. (C) The electron density map following BUSTER refinement (level=1.09). This is the density map that was utilized during the docking stage with program ESSENS and the ubiquitin moiety.

Table 4.1 Steady state kinetic parameters of nucleotide incorporation opposite an abasic site by pol η

Proteins	V_{\max} (nM/min)	K_m (μ M)	V_{\max}/K_m	Relative efficiency
Pol η alone	0.26 ± 0.1	22 ± 5	0.012	1.0
Pol η + non-split PCNA	0.36 ± 0.01	12 ± 2.0	0.030	2.5
Pol η + split PCNA	0.21 ± 0.01	6.6 ± 2	0.032	2.7
Pol η + Ub-PCNA	0.28 ± 0.01	6.1 ± 1	0.046	3.8

Table 4.2 Data collection and refinement statistics for split and Ub-PCNA

	<i>Split PCNA</i>	<i>Ub-PCNA</i>
<i>(A) Data collection statistics</i>		
Resolution (Å)	43.5-3.0 (3.1– 3.0) ^a	43.3-2.8 (2.9 – 2.8)
Wavelength (Å)	0.97	0.97
Space group	P2 ₁ 3	P2 ₁ 3
Cell (Å)	a=b= c=123.00	a=b= c=122.52
Completeness (%)	100 (99.8)	100 (99.4)
Redundancy	9.50 (6.99)	8.74 (5.38)
I/σ _I	12.9 (3.8)	10.5 (2.4)
R _{merge} (%) ^b	10.2 (42.8)	10.9 (60.4)
<i>(B) Refinement statistics</i>		
Resolution range (Å)	43-3.0	43-2.8
R (%) ^c	24.0	28.0
R _{free} (%) ^d	25.0	29.0
rms bonds (Å)	0.007	0.009
rms angles (°)	1.0	1.18
Number of water molecules	0	0
Number of protein atoms	1994	3816
Ramachandran analysis (%)		
Most favored	89.6	85.6
Allowed	10.4	14.4
PDB ID	3L0X	3L10

^a Values in parentheses relate to the highest resolution shell.

^b $R_{merge} = \frac{\sum_h \sum_i |I_i(\mathbf{h}) - \langle I(\mathbf{h}) \rangle|}{\sum_h \sum_i I_i(\mathbf{h})}$, where I_i is the i th measurement of reflection \mathbf{h} and $\langle I(\mathbf{h}) \rangle$ is a weighted mean of all measurements of \mathbf{h} .

^c $R = \frac{\sum ||F_o| - |F_c||}{\sum |F_o|}$, where F_o and F_c are the observed and calculated structure factors, respectively.

^d R_{free} is defined in (Brunger 1992).

CHAPTER 5

DISCUSSION

The work presented in this thesis is aimed at understanding the role of PCNA during translesion synthesis. Previous work has shown that interactions between PCNA and the non-classical polymerases are essential during translesion synthesis^{34,113,156}. Subsequent cellular and biochemical studies determined that these interactions are involved in both recruiting and stimulating the non-classical DNA polymerases^{38,155}. However the regions of the proteins that are involved in the interactions between PCNA and the non-classical polymerases are not well understood. Prior to my work, only the PIP motif on the non-classical polymerases was known as a PCNA interaction site^{96,125,126,226,227}. However, not all non-classical polymerases contain a PIP motif, but all non-classical polymerases interact with and are stimulated by PCNA¹⁹⁷. This indicates that additional interaction sites between PCNA and the non-classical polymerases exist that are utilized during translesion synthesis.

The second focus of this thesis was to generate an Ub-PCNA analog and determine the structural and biochemical role of Ub-PCNA during translesion synthesis. Prior to my work, the ubiquitination of PCNA was only known to be a pre-requisite for translesion synthesis and involved in recruiting the non-classical polymerases to the replication fork *in vivo*^{38,162,228}. However, the mechanism of the polymerase switch or the impact of Ub-PCNA on the catalytic activity of the non-classical polymerases was largely undetermined. Additionally, the impact that the monoubiquitination had on the structure of PCNA was completely unknown. At the time there were two commonly discussed models: (1) the ubiquitination of PCNA induces an allosteric change to PCNA promoting the polymerase switch and (2) the ubiquitin moiety provides an additional binding site for the non-classical polymerases. The major difficulty in distinguishing between such

models was the inability to generate Ub-PCNA in sufficient quantities for biophysical and structural studies.

Role of PCNA loop J in translesion synthesis

To gain a better understanding of the interactions between PCNA and pol η , I performed structural and biochemical studies on two PCNA mutant proteins defective in translesion synthesis, which are described in Chapter 2. These two yeast PCNA mutant proteins are encoded by the *pol30-178* allele and the *pol30-113* allele^{186,197}. The *pol30-178* allele encodes the G178S PCNA mutant protein, and prior to my work, only the phenotype caused by this mutant allele had been described. The *pol30-113* allele encodes the E113G PCNA mutant protein. Glu-113 is located directly across from Gly-178 at the subunit interface, and this mutation results in the same phenotype as the G178S PCNA substitution. The work described in Chapter 2 showed that the E113G and G178S substitutions resulted in a similar localized structural change to PCNA at an extended loop, called loop J. Steady state kinetic studies showed that unlike wild type PCNA which stimulates pol η , the G178S PCNA mutant protein inhibits pol η . The E113G PCNA mutant protein also fails to stimulate pol η , but does not have any inhibitory impact. These structural and biochemical studies indicate that loop J is involved in interacting with and stimulating the non-classical polymerases during translesion synthesis.

Preliminary and ongoing PCNA loop J studies

The structural and kinetic studies presented in Chapter 2 have provided strong support for loop J being involved in translesion synthesis. To further support this, I have generated PCNA mutant proteins with the six loop J residues either mutated to alanines (Ala₆) or changed to a two-glycine hairpin loop (Gly₂). Both the Ala₆ and Gly₂ mutations were generated in a wild type PCNA background (i.e. residue 178 is a glycine).

To determine the impact these loop J mutations have on pol η , I have performed a running start assay (as described in Chapter 2) with the wild type, G178S, Ala₆, and Gly₂ PCNA proteins. As shown in Figure 5.1 pol η alone has a reduced ability to incorporate across from an abasic site. The addition of wild type PCNA stimulates the ability of pol η to incorporate across from the abasic site. In comparison the G178S and Gly₂ PCNA mutant proteins are unable to stimulate pol η incorporation opposite an abasic site. Interestingly the Ala₆ PCNA mutant protein does stimulate pol η incorporation across from an abasic site. To quantify the effects of these PCNA proteins I performed steady state kinetic studies with pol η looking at incorporation across from an abasic site (as described in Chapter 2) in the presence of wild type, G178S, Ala₆, and Gly₂ PCNA proteins. The results are presented in Table 5.1 and are consistent with the running start assay. Again, only wild type PCNA and Ala₆ PCNA stimulate the activity of pol η by 2.4 and 1.8-fold respectively.

The Gly₂ PCNA mutant protein inhibits pol η comparable to the G178S PCNA mutant protein. This result supports the notion that loop J is a site of interaction for pol η . Surprisingly, I found that the Ala₆ PCNA mutant protein does not inhibit pol η . This suggests that the backbone contacts between pol η and PCNA at loop J are sufficient to support function, indicating side chain contacts might be less important. This result is reasonable considering the low conservation of loop J between human and yeast PCNA. Together these results indicate that loop J forms backbone contacts with pol η that are required for stimulating its catalytic activity. It is important to highlight that these are preliminary results and are currently being repeated.

To correlate the kinetic effects of the PCNA mutant proteins with the position of loop J, I have determined the X-ray crystal structures of the Ala₆, and Gly₂ PCNA mutant proteins. As would be expected the Gly₂ PCNA mutant protein is clearly missing loop J. Interestingly the Ala₆ PCNA mutant protein, the one that stimulates pol η , has loop J located in nearly the same location as the wild type PCNA protein (Figure 5.2). Together,

these results further support a role of loop J in forming a functional interaction during translesion synthesis that is position dependent and is likely through backbone interactions.

An important outstanding question is whether or not the loss of translesion synthesis in yeast harboring the G178S PCNA substitution results from interference with the monoubiquitination of PCNA. While I did not directly answer this question in my current studies, the body of work presented in this thesis indicates that the G178S PCNA mutant protein is likely ubiquitinated. First the domain with the site of monoubiquitination (Lys-164) in the G178S PCNA mutant protein has the same overall structure as the wild type PCNA protein. Second, the E113G PCNA mutant protein which blocks translesion synthesis through the same mechanism as the G178S PCNA mutant protein is able to be ubiquitinated¹⁹⁷. Importantly even in the absence of ubiquitination the G178S substitution inhibits the catalytic activity of pol η , thus indicating that contacts at loop J are important during translesion synthesis. Furthermore, my additional loop J studies substantiate the role of loop J in supporting translesion synthesis independent of the ubiquitination state. With all that being said, future *in vivo* studies with a PCNA specific antibody will have to be performed to empirically address the ubiquitination state of the G178S PCNA mutant protein.

Non-trimeric form of PCNA

During our structural studies of the E113G PCNA mutant protein, I unexpectedly obtained another structure of this protein in a novel non-trimeric form. These findings are described in Chapter 3. In the normal, trimeric form of PCNA, domain A of each subunit interacts with domain B of another subunit in a head-to-tail fashion. In this novel non-trimeric form of PCNA, two alternate subunit interactions are observed. In one alternative interaction, domain A of one PCNA monomer contacts domain A of a neighboring monomer. In the other, domain B of one monomer interacts with domain B of a different

monomer. The novel B-B interface is structurally similar to the A-B interface observed in the trimeric ring structure and forms a similar hydrogen bonding pattern between two anti-parallel β -sheets on adjacent monomeric subunits. By contrast, the A-A interface is stabilized by hydrophobic interactions between neighboring monomeric subunits. Since the E113G substitution is located at the A-A interface this form is likely destabilized in the wild type PCNA protein. These findings suggest that the Glu-113 side chain in wild type PCNA promotes trimer formation by destabilizing these possible alternate subunit interactions; this is expanded upon in the discussion of Chapter 3.

While the work presented in Chapter 3 is the first reported structure of a non-trimeric form of PCNA, there are reported non-trimeric processivity factors utilized by the herpes virus family. Perhaps the best studied is the human cytomegalovirus processivity factor UL44, which both binds DNA and enhances the processivity of the viral polymerase²²⁹. Interestingly, the functional form of UL44 is a dimer in both solution and the crystal structure²³⁰. Analysis of the UL44 crystal structure shows that while it lacks homology with PCNA the monomeric subunit is strikingly similar (Figure 5.3A), with the monomeric subunit of UL44 containing two domains connected by a long flexible linker. This linker is very similar to the IDCL of PCNA and has been shown to interact with the viral replicative DNA polymerase²³⁰. The final dimeric state of UL44 forms through head-to-head interactions between monomeric subunits. This is in direct contrast to the trimeric PCNA structure that forms through head-to-tail contacts. Comparing the dimeric UL44 to my non-trimeric PCNA structure shows some striking similarity (Figure 5.3). The dimeric UL44 contacts are nearly identical to my non-trimeric PCNA tail-to-tail (B-B) interface contacts. Both of these contacts are formed through main chain hydrogen bonding interactions between two β strands from adjacent monomers. Importantly, the B-B contact in my PCNA mutant protein is not affected by the E113G substitution and could occur naturally in solution, as discussed in Chapter 3.

It is tempting to speculate that PCNA might function as a dimer in some situations given that the PCNA B-B dimer could exist at low protein concentrations and is nearly identical to the viral dimeric form, which is fully functional in viral DNA metabolism. Furthermore, PCNA was recently shown to have the ability to directly bind DNA without RFC loading, providing the possibility that it does not need to encircle the DNA to perform some metabolic functions²³¹. Interestingly, the viral dimeric processivity factors have been shown to be up regulated in lytic infected cells and show homogeneous rather than punctate distribution in replication compartments²³². It has been speculated that the viral processivity factor is protecting the newly synthesized viral DNA from nuclease attack or histone assembly by occupying the surface of the DNA. A similar phenomenon could also occur for the dimeric B-B form of PCNA that could allow for novel protein interactions. It is possible that some of the PCNA functions that are attributed to the trimeric form of PCNA during chromatin assembly and remodeling are actually being performed by a dimeric form of PCNA bound to the DNA preventing histone assembly or nuclease attack. This would provide a means of utilizing PCNA without having to load it onto the DNA in an ATP-dependent fashion by RFC.

Ub-PCNA and the Polymerase switch

PCNA is monoubiquitinated at Lys-164 in response to DNA damage¹⁵⁰. This monoubiquitinated form of PCNA has been shown to be associated with the non-classical polymerases and a pre-requisite for translesion synthesis^{154,162}. It is believed that Ub-PCNA facilitates the polymerase switch and stimulates the non-classical polymerases³⁸. However, the exact biochemical and structural role of Ub-PCNA was unclear because of difficulties in obtaining large amounts of Ub-PCNA for biochemical and structural studies. The work presented in Chapter 4 showed a novel way of generating an Ub-PCNA analog that is able to support both viability and translesion synthesis *in vivo*. Using this method, I determined that Ub-PCNA only moderately stimulates the

enzymatic activity of pol η over unmodified PCNA. The X-ray crystal structure of this Ub-PCNA analog showed that the monoubiquitination of PCNA does not induce a conformational change to PCNA and that the ubiquitin moieties are located on the back side of PCNA away from the primer terminus.

My structural and biochemical findings address multiple questions and provide some insight into the role of Ub-PCNA during translesion synthesis. (1) *Does Ub-PCNA stimulate pol η substantially more than unmodified PCNA?* Based on my steady state kinetic studies Ub-PCNA does not stimulate pol η substantially more than the unmodified form of PCNA. From a biochemical standpoint this is likely a direct result of the protein interactions between Ub-PCNA and pol η being nearly identical to interactions between unmodified PCNA and pol η . This is implied from the lack of a structural change following the ubiquitination of PCNA. From a cellular standpoint this is likely due to the cell not wanting the highly mutagenic polymerases being overly active upon having access to the replication fork. (2) *What is the function of the ubiquitin moieties during the polymerase switch if they are not inducing an allosteric change to PCNA?* Non-classical polymerases contain an ubiquitin-binding motif that is not present in the classical polymerases⁹⁷. Therefore, the ubiquitins are likely only adding an additional surface of interaction on PCNA that is specific to the non-classical polymerases during translesion synthesis. (3) *Why are the ubiquitin moieties located on the back face of PCNA away from the primer terminus?* Upon encountering DNA damage the classical polymerase would stall at the primer terminus. Placing the ubiquitin moieties on the back face of PCNA would aid in recruiting the non-classical polymerases while simultaneously not displacing the classical polymerase from the primer terminus until the non-classical polymerase is needed. (4) *How does pol η gain access to the primer terminus based on the structure of Ub-PCNA?* Upon encountering DNA damage PCNA is monoubiquitinated on the back face of PCNA while the stalled classical polymerase is likely engaging and disengaging from the DNA lesion. Pol η then binds ubiquitin through its

UBZ motif and PCNA through its PIP motif, on a different PCNA monomeric subunit than the one to which the classical polymerase is bound. If pol η were to bind the same subunit as the classical polymerase then it would likely displace the PIP motif of the classical polymerase stalled at the lesion. Upon the disengaging of the classical polymerase from the primer terminus, pol η would engage the primer terminus and bypass the DNA lesion while interacting with PCNA at multiple points.

The Ub-PCNA structure and the studies reported in Chapter 2 together suggest that the interactions between PCNA and the non-classical polymerases are significantly more complex than was anticipated. When I began these studies only the PIP motif and UBZ motifs of pol η were known to interact with Ub-PCNA^{96,97}. The model presented in Figure 4.16 indicates that regions of unknown structure surrounding these two motifs are also likely involved in interactions with PCNA at the replication fork. Furthermore, my loop J studies correlate very well with the Ub-PCNA model. This is because the C-terminal domain of pol η that is interacting with ubiquitin and PCNA must traverse to the catalytic core located at the primer terminus on the front side of PCNA. In doing so the pol η chain would likely make contacts at loop J and the monomer-monomer interface. Together my studies indicate that translesion synthesis by pol η requires that the PIP motif contacts the PCNA IDCL, the UBZ motif contacts the ubiquitin moiety, and some portion of the C-terminal domain of pol η contacts loop J of PCNA.

I have shown that Ub-PCNA stimulates the activity of pol η and the G178S PCNA mutant protein inhibits the activity of pol η . However, it would be interesting to see if the ubiquitination of PCNA can overcome the G178S inhibition of pol η or if the G178S substitution inhibits the stimulation of pol η by Ub-PCNA. Future studies will address this question by placing the G178S substitution in the Ub-PCNA analog protein. If this protein fails to support translesion synthesis it would indicate that loop J contacts are required regardless of the ubiquitination state of PCNA. This is the result I would expect based on evidence from the E113G PCNA mutant protein. The E113G PCNA

mutant protein causes a similar loss of translesion synthesis, has a similar structural change as the G178S PCNA mutant protein at loop J, and has been shown to be ubiquitinated *in vivo*¹⁹⁷. This result would indicate that although necessary, the ubiquitination of PCNA is not sufficient alone to support translesion synthesis. By contrast, if the G178S ubiquitinated PCNA analog does support translesion synthesis this would indicate at least two possible scenarios. First, the ubiquitination of PCNA is able to overcome any inhibition caused by the G178S substitution and loop J movement. Second, the G178S substitution might prevent the ubiquitination of PCNA *in vivo*. Both of these scenarios would require future experiments to determine the ubiquitination state of the G178S PCNA mutant protein *in vivo*.

Prior to my work there was no evidence that the back face of PCNA played a role in any of PCNA's known functions. The work presented here is the first evidence of the back face of PCNA being implicated in translesion synthesis. These studies could provide a possible new paradigm for the back face of PCNA playing a role in various PCNA dependent pathways. This would not be a surprise because PCNA is loaded onto the DNA with a specific orientation of the ring. Furthermore, with all the processes that PCNA must coordinate it would not be unexpected that the back face of PCNA would have evolved to recruit various factors or act as an additional scaffolding site during complex multi-protein processes.

Implications for the field and future studies

While the work present in this thesis has provided some insight into several important questions in the field, it also has provided a platform to answer more questions and perform additional studies. Specifically, the Ub-PCNA analog generated in Chapter 4 has allowed for a plethora of future structural, biochemical, and genetic studies to be performed. Here I will discuss some of these future studies and their implications for the field.

Structural studies of Ub-PCNA co-complexes

While the structure reported in Chapter 4 provides insight into the ubiquitination of PCNA it does not identify the location of ubiquitin when the polymerase is bound to Ub-PCNA. Therefore additional structural information must be obtained for the polymerase - Ub-PCNA co-complexes. One very interesting study would be the complex of pol η and Ub-PCNA bound to DNA. While this complex would be very difficult to obtain, it is feasible in light of my work presented in Chapter 4 and the stable interactions between pol η and Ub-PCNA observed in pull down assays¹⁶⁷. In addition, the X-ray structures of both pol η and PCNA bound to DNA have been determined independently, thus indicating that the interaction with DNA is stable enough for crystallography^{50,231}. Determining the crystal structure of this complex would determine if the pol η – Ub-PCNA model presented in Chapter 4 is correct. Furthermore, it would identify the key interaction sites between Ub-PCNA and the C-terminus of pol η that might be involved in mediating the loop J contacts described in Chapter 2. An alternative method to obtaining a similar result would be to determine the crystal structure of only the pol η C-terminal domain bound to Ub-PCNA.

Another structural study would be to compare the protein-protein interactions between Ub-PCNA and the various non-classical polymerases. This study would provide insight into understanding the specificity of different non-classical polymerases to Ub-PCNA during translesion synthesis. Specifically, the crystal structure of Ub-PCNA bound to the C-terminal domain of the non-classical polymerases Rev1 and pol η would be of interest. This is because Rev1 and pol η are required for different types of DNA lesions and have different functions during translesion synthesis³⁴. Furthermore, it was recently shown by NMR that pol η and Rev1 have partially non-overlapping binding sites on ubiquitin²³³. The structures of these co-complexes should be attainable because the ubiquitin-binding motifs in the C-terminal domains of both Rev1 and pol η have been shown to directly bind Ub-PCNA⁹⁷. By determining the structure of the co-complex for

each of these domains bound to Ub-PCNA, the unique interactions between Ub-PCNA and each polymerase can be identified. These interactions have the possibility of providing insight into protein-protein interactions that could be involved in providing one polymerase priority over the other during translesion synthesis. These are only a few of the possible structural studies that are feasible in the laboratory.

Polyubiquitination of PCNA

The error-free pathway of DNA damage tolerance is dependent on the polyubiquitination of PCNA through Lys-63 linkages of ubiquitin¹⁶². In contrast to translesion synthesis, this pathway is not well understood. It is believed that the polyubiquitination of PCNA promotes template switching in order to bypass DNA damage. One difficulty in studying this process has been the inability to obtain large amounts of polyubiquitinated PCNA. The method developed in Chapter 4 could circumvent this problem by generating multiple ubiquitin moieties in frame as shown in Figure 5.4B. This fusion is believed to be a good mimic to the Lys-63 linkages because of the close proximity of Lys-63 to the N-terminus of ubiquitin, and because of the extended nature of the Lys-63 linkages in the crystal structure, as shown in Figure 5.4C^{234,235}. This method of generating polyubiquitinated PCNA will allow for additional *in vitro* biochemical and structural studies similar to those reported in this thesis. For example, it would be interesting to see the impact polyubiquitinated PCNA has on the catalytic activity of the non-classical polymerases. Structural studies would also indicate if the polyubiquitin moieties are extended in solution or interact directly with PCNA. Both of these types of studies would provide mechanistic insight into the functional role of polyubiquitinated PCNA.

Another problem in studying this alternate DNA damage tolerance pathway is the capacity to specifically prevent or induce the Lys-63 linkages on PCNA *in vivo*. This problem is further complicated by the ability to dissect the monoubiquitinated and

polyubiquitinated pathways from each other during genetic studies. By utilizing a similar genetic method as that described in Chapter 4, one could study the phenotypic impact of having PCNA continually polyubiquitinated. Alternatively the phenotype of Ub-PCNA that cannot be polyubiquitinated can be characterized by using the Ub-PCNA analog with a K63R mutation in ubiquitin. These studies would allow for the interplay between the mono and polyubiquitination of PCNA to be studied *in vivo* within a tightly controlled system. Taken together this method of generating polyubiquitinated PCNA would allow for a more thorough analysis both *in vitro* and *in vivo* of the poorly understood DNA damage tolerance error-free pathway.

Sumolyated PCNA

The novel method of severing the PCNA backbone into self assembling peptides could also be utilized to study the impact of sumolyating PCNA. This is because PCNA is sumolyated at Lys-164 and this modification is similar to ubiquitin¹⁵⁰. The sumo protein is attached to the target protein through an isopeptide linkage between its C-terminal glycine residue and an acceptor lysine on the target protein, which occurs in a very similar enzymatic cascade as ubiquitination. While both sumoylation and ubiquitination modifications are very similar, they have drastically different impacts on the function of PCNA. In general the ubiquitination of PCNA is involved in the DNA damage tolerance pathway and the sumoylation of PCNA is a DNA damage independent process involved in preventing homologous recombination during classical replication^{151,161}. The prevention of homologous recombination by sumolyated PCNA occurs through interactions with the Srs2 helicase like enzyme, which strips the recombinase Rad51 off the DNA¹⁵².

It should be possible to generate large amounts of sumolyated PCNA using a similar technique to the one described in Chapter 4. Obviously structural studies of this modification would be interesting to determine its relative location in comparison to the

ubiquitin modification. Also biochemical studies could be performed to determine if the sumoylation of PCNA stimulates the catalytic activity of the Srs2 helicase, while inhibiting the catalytic activity of the non-classical polymerases involved in translesion synthesis. Perhaps the most interesting studies would be genetic assays using this sumoylated protein analog, similar to those described in Chapter 4. It would be interesting to see if all ubiquitin dependent DNA damage tolerance pathways are inhibited and if homologous recombinatorial repair is reduced. Characterizing the phenotype of this strain under various conditions could provide insight into the interplay between homologous recombination repair and the ubiquitin dependent DNA damage tolerance pathway.

Recruitment Studies

The studies presented in this document have provided valuable insight into the role of PCNA during translesion synthesis, but did not directly address the recruitment of the non-classical polymerases to the stalled replication fork. There are currently two general hypotheses for the recruitment of non-classical polymerases to the replication fork: (1) the recruitment of the non-classical polymerase occurs because of direct binding to Ub-PCNA and requires no accessory proteins, (2) the non-classical polymerase is directly shuttled to the replication fork through protein-protein interactions with an accessory protein. Support for either of these models is limited. However, it has been hypothesized that Rad18 shuttles pol η to the replication fork based on pull down and co-localization assays²³⁶. Nevertheless this model has been difficult to test because of the well established fact that Rad18 is needed to ubiquitinate PCNA.

The methods and genetic studies developed in Chapter 4 allow one to directly look at the factors involved in the recruitment of pol η to Ub-PCNA. Specifically one can test if Rad18 is required for any processes independent of its role in ubiquitinating PCNA, such as shuttling the non-classical polymerase to the replication fork. Using the

Ub-PCNA yeast strain developed in Chapter 4, one can knockout the Rad18 gene in the presence of the constitutively ubiquitinated PCNA analog and assay the impact this has on translesion synthesis. No phenotypic difference between the Rad18 knockout and the wild type strain would indicate that Rad18 is not involved in shuttling the non-classical polymerases to Ub-PCNA, this result would favor model 1. In comparison, a loss of translesion synthesis in the Rad18 knockout (with the Ub-PCNA analog present) would indicate that it plays an additional role during translesion synthesis independent of ubiquitinating PCNA, this results would favor model 2. One could further look at other proteins involved in translesion synthesis that could be involved in shuttling the non-classical polymerases to Ub-PCNA, such as Rev1²³⁷. This type of assay would not be possible without the Ub-PCNA analog and yeast strains developed in this thesis.

Concluding Remarks and Implications for the field

In conclusion the work presented in this thesis has made substantial contributions to our understanding of the role of PCNA during translesion synthesis by utilizing PCNA mutant proteins defective in translesion synthesis and an Ub-PCNA analog. Perhaps the largest implications for the field as a result of these studies are yet to come. This is because future studies can take advantage of the Ub-PCNA analog instead of spending time and energy generating Ub-PCNA. For example, the tool belt and polymerase switch mechanisms can be more rigorously tested using sophisticated *in vitro* techniques such as single molecule imaging and surface plasmon resonance.

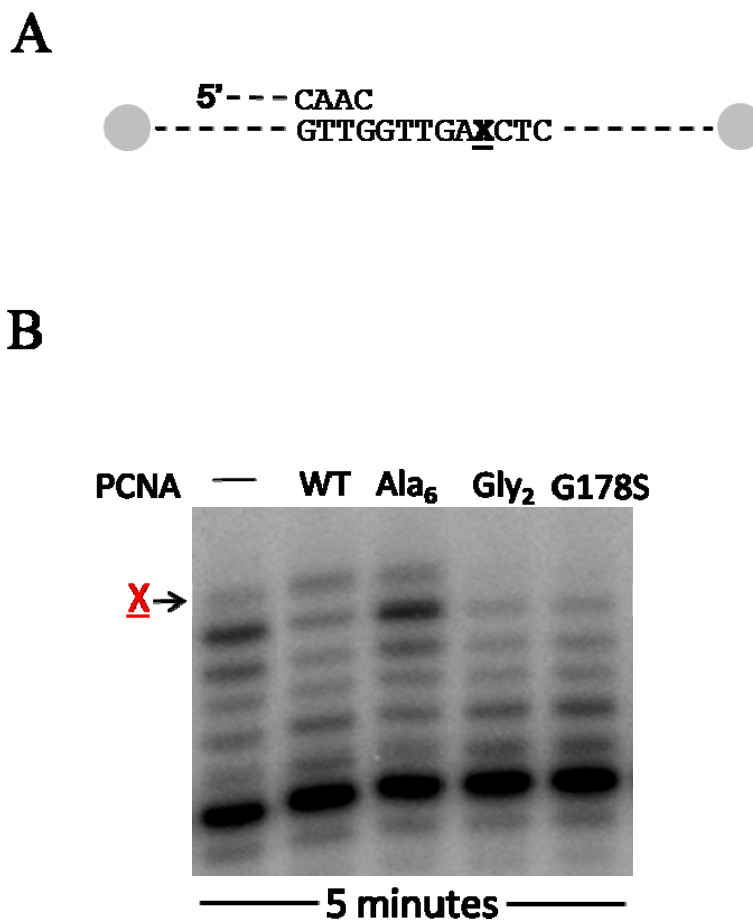


Figure 5.1 Running start experiment with pol η on an abasic site. (A) Schematic diagram of the 31/68-mer substrate used in the running start assays with the ends of the template strand containing biotin-streptavidin blocks. The X indicates the location of the abasic site. (B) Autoradiograph of the synthesis products five minutes following the addition of pol η . Lanes labeled with a (–) contain only pol η . Lanes labeled with a WT contain the wild type PCNA protein, and lanes labeled G178S contain the G178S PCNA mutant protein. Lanes labeled Ala₆ contain the loop J Ala₆ PCNA mutant protein, and lanes labeled Gly₂ have loop J replaced by a two glycine hairpin loop.

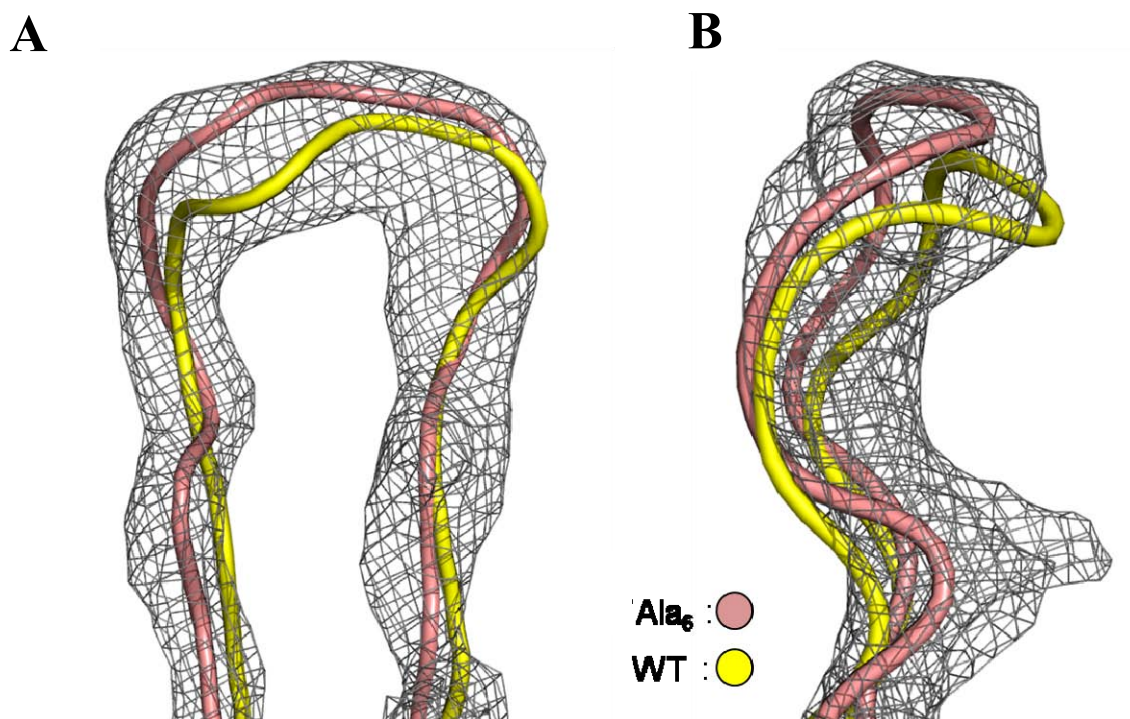


Figure 5.2 Close up view of loop J. The superimposition of the wild type (WT) and wild type Ala₆ (Ala₆) PCNA proteins was performed and only loop J is shown. (A) Electron density (level=2.0 sigma) for the Ala₆ PCNA mutant protein is shown with the backbone of the wild type and mutant PCNA proteins shown in ribbon representation. (B) Side view of loop J.

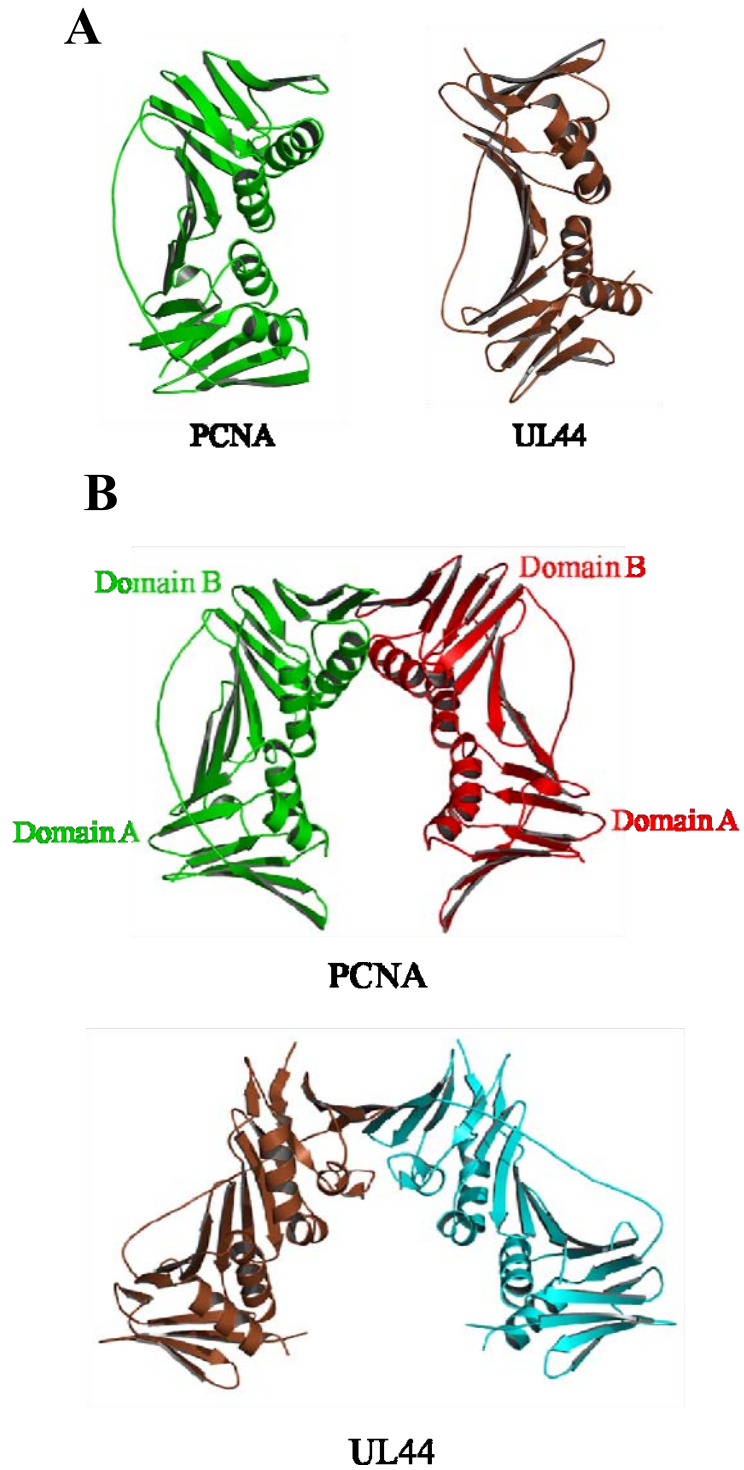


Figure 5.3 Eukaryotic (PCNA) and viral (UL44) processivity factors

Figure 5.3 continued. (A) The monomeric subunits for the eukaryotic, PCNA, and viral, UL44, processivity factors are shown in green and brown respectively. (B) Both the non-trimeric E113G B-B interface (top structure of panel) for PCNA and the viral dimeric processivity factors are shown (bottom structure of panel). (PDB ID codes: 1T6L and 3GPN)

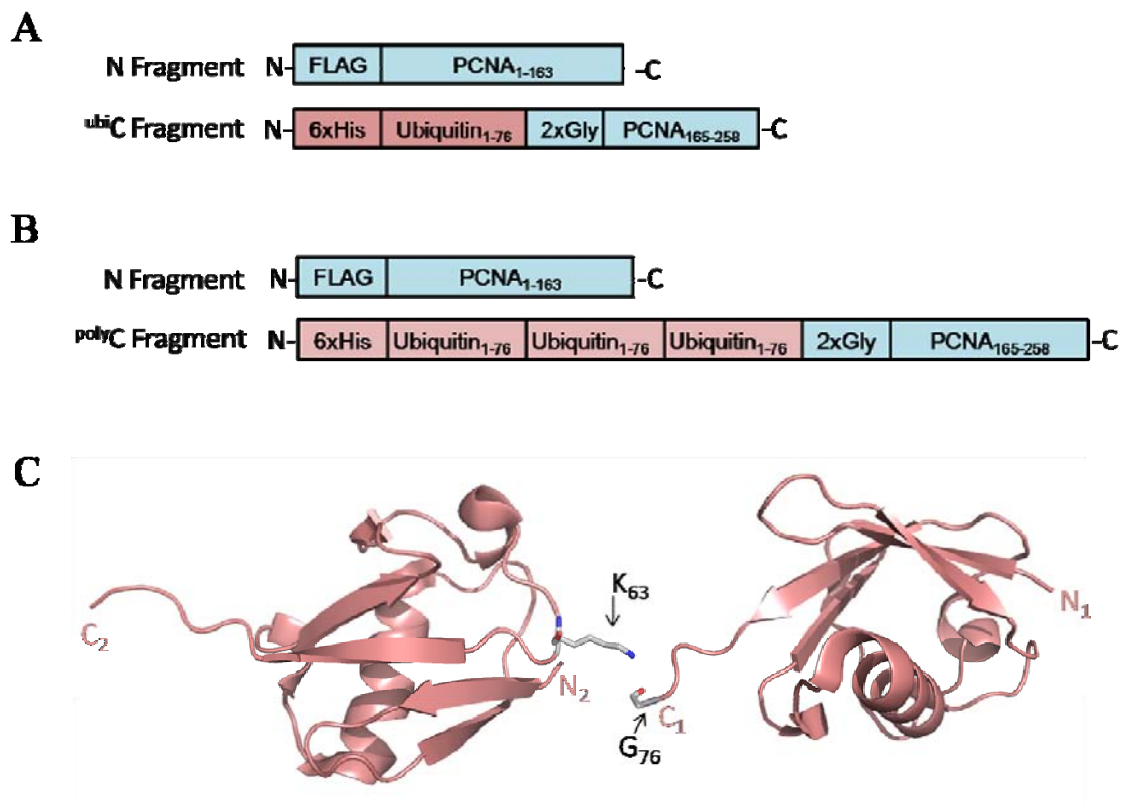


Figure 5.4 Generation of polyubiquitinated PCNA. Schematic of the two polypeptides used to generate monoubiquitinated PCNA (A) and polyubiquitinated PCNA (B). (C) X-ray crystal structure of K63 linked polyubiquitins. (PDB ID: 3H7P)

Table 5.1 Steady state kinetic parameters of pol η catalyzed nucleotide incorporation

<i>Proteins</i>	<i>DNA</i>	V_{max} (<i>nM/min</i>)	K_m (μM)	V_{max}/K_m	<i>Relative efficiency</i>
Pol η alone	Abasic site	1.0 ± 0.1	34 ± 8	0.029	1.0
Pol η + wild type PCNA	Abasic site	0.70 ± 0.06	9.9 ± 3.0	0.071	2.4
Pol η + G178S PCNA	Abasic site	0.12 ± 0.01	12 ± 1	0.010	0.34
Pol η + Gly ₂	Abasic site	0.12 ± 0.03	10 ± 2	0.011	0.37
Pol η + Ala ₆	Abasic site	0.43 ± 0.02	8.1 ± 1	0.053	1.8

REFERENCES

1. Bruce Alberts, A.J., Julian Lewis, Martin Raff, Keith Roberts, Peter Walter. *The Cell*, (Garland Science, 2002).
2. Garg, P. & Burgers, P.M.J. DNA polymerases that propagate the eukaryotic DNA replication fork. *Critical Reviews in Biochemistry and Molecular Biology* **40**, 115-128 (2005).
3. Hamdan, S.M. & Richardson, C.C. Motors, Switches, and Contacts in the Replisome. *Annual Review of Biochemistry* **78**, 205-243 (2009).
4. Wold, M.S. Replication protein A: A heterotrimeric, single-stranded DNA-binding protein required for eukaryotic DNA metabolism. *Annual Review of Biochemistry* **66**, 61-92 (1997).
5. Kunkel, T.A. & Burgers, P.M. Dividing the workload at a eukaryotic replication fork. *Trends in Cell Biology* **18**, 521-527 (2008).
6. Langston, L.D. & O'Donnell, M. DNA Polymerase delta Is Highly Processive with Proliferating Cell Nuclear Antigen and Undergoes Collision Release upon Completing DNA. *Journal of Biological Chemistry* **283**, 29522-29531 (2008).
7. Chen, S.Y., Levin, M.K., Sakato, M., Zhou, Y.Y. & Hingorani, M.M. Mechanism of ATP-Driven PCNA Clamp Loading by *S. cerevisiae* RFC. *Journal of Molecular Biology* **388**, 431-442 (2009).
8. Mitchell, D.L., Jin, J. & Cleaver, J.E. Relative Induction of Cyclobutane Dimers and Cytosine Photohydrates in DNA Irradiated In Vitro and In Vivo with Ultraviolet-C and Ultraviolet-B Light. *Photochemistry and Photobiology* **54**, 741-746 (1991).
9. Setlow, R.B. & Carrier, W.L. Pyrimidine Dimers in Ultraviolet-Irradiated Dnas. *Journal of Molecular Biology* **17**, 237-& (1966).
10. Taylor, J.S., Garrett, D.S., Brockie, I.R., Svoboda, D.L. & Telser, J. H-1-Nmr Assignment and Melting Temperature Study of Cis-Syn and Trans-Syn Thymine Dimer Containing Duplexes of D(Cgtattatgc).D(Gcataatagc). *Biochemistry* **29**, 8858-8866 (1990).
11. Ward, J.F. The Yield of DNA Double-Strand Breaks Produced Intracellularly by Ionizing-Radiation - a Review. *International Journal of Radiation Biology* **57**, 1141-1150 (1990).

12. Lindahl, T. Instability and Decay of the Primary Structure of DNA. *Nature* **362**, 709-715 (1993).
13. Barnes, D.E. & Lindahl, T. Repair and genetic consequences of endogenous DNA base damage in mammalian cells. *Annu Rev Genet* **38**, 445-76 (2004).
14. Lindahl, T. & Barnes, D.E. Repair of endogenous DNA damage. *Cold Spring Harb Symp Quant Biol* **65**, 127-33 (2000).
15. Shibutani, S., Takeshita, M. & Grollman, A.P. Insertion of Specific Bases During DNA-Synthesis Past the Oxidation-Damaged Base 8-Oxodg. *Nature* **349**, 431-434 (1991).
16. Cheng, K.C., Cahill, D.S., Kasai, H., Nishimura, S. & Loeb, L.A. 8-Hydroxyguanine, an Abundant Form of Oxidative DNA Damage, Causes G-JT and a-JC Substitutions. *Journal of Biological Chemistry* **267**, 166-172 (1992).
17. Sancar, A. No "End of History" for photolyases. *Science* **272**, 48-9 (1996).
18. Takeuchi, Y. et al. Induction and inhibition of cyclobutane pyrimidine dimer photolyase in etiolated cucumber (*Cucumis sativus*) cotyledons after ultraviolet irradiation depends on wavelength. *Journal of Plant Research* **120**, 365-374 (2007).
19. Yasui, A. et al. A New Class of DNA Photolyases Present in Various Organisms Including Aplacental Mammals. *Embo Journal* **13**, 6143-6151 (1994).
20. Sancar, A. DNA excision repair. *Annu Rev Biochem* **65**, 43-81 (1996).
21. Parikh, S.S. et al. Base excision repair initiation revealed by crystal structures and binding kinetics of human uracil-DNA glycosylase with DNA. *Embo J* **17**, 5214-26 (1998).
22. Fuxreiter, M., Luo, N., Jedlovsky, P., Simon, I. & Osman, R. Role of base flipping in specific recognition of damaged DNA by repair enzymes. *J Mol Biol* **323**, 823-34 (2002).
23. Guillet, M. & Boiteux, S. Origin of endogenous DNA abasic sites in *Saccharomyces cerevisiae*. *Mol Cell Biol* **23**, 8386-94 (2003).
24. Wilson, D.M. & Barsky, D. The major human abasic endonuclease: formation, consequences and repair of abasic lesions in DNA. *Mutation Research-DNA Repair* **485**, 283-307 (2001).

25. Wilson, S.H. Mammalian base excision repair and DNA polymerase beta. *Mutat Res* **407**, 203-15 (1998).
26. Caldecott, K.W. XRCC1 and DNA strand break repair. *DNA Repair (Amst)* **2**, 955-69 (2003).
27. Dalhus, B., Laerdahl, J.K., Backe, P.H. & Bjoras, M. DNA base repair - recognition and initiation of catalysis. *Fems Microbiology Reviews* **33**, 1044-1078 (2009).
28. Fousteri, M. & Mullenders, L.H. Transcription-coupled nucleotide excision repair in mammalian cells: molecular mechanisms and biological effects. *Cell Res* **18**, 73-84 (2008).
29. Modrich, P. Mechanisms in eukaryotic mismatch repair. *Journal of Biological Chemistry* **281**, 30305-30309 (2006).
30. Weterings, E. & Chen, D.J. The endless tale of non-homologous end-joining. *Cell Res* **18**, 114-24 (2008).
31. Huertas, P. DNA resection in eukaryotes: deciding how to fix the break. *Nature Structural & Molecular Biology* **17**, 11-16.
32. Budzowska, M. & Kanaar, R. Mechanisms of Dealing with DNA Damage-Induced Replication Problems. *Cell Biochemistry and Biophysics* **53**, 17-31 (2009).
33. McCulloch, S.D. & Kunkel, T.A. The fidelity of DNA synthesis by eukaryotic replicative and translesion synthesis polymerases. *Cell Research* **18**, 148-161 (2008).
34. Prakash, S., Johnson, R.E. & Prakash, L. Eukaryotic translesion synthesis DNA polymerases: Specificity of structure and function. *Annual Review of Biochemistry* **74**, 317-353 (2005).
35. Guo, C., Kosarek-Stancel, J.N., Tang, T.-S. & Friedberg, E.C. Y-family DNA polymerases in mammalian cells. *Cellular and Molecular Life Sciences* **66**, 2363-2381 (2009).
36. Washington, M.T., Carlson, K.D., Freudenthal, B.D. & Pryor, J.M. Variations on a theme: Eukaryotic Y-family DNA polymerases. *Biochim Biophys Acta* (2009).
37. de Saro, F.J.L. Regulation of Interactions with Sliding Clamps During DNA Replication and Repair. *Current Genomics* **10**, 206-215 (2009).

38. Lehmann, A.R. et al. Translesion synthesis: Y-family polymerases and the polymerase switch. *DNA Repair* **6**, 891-899 (2007).
39. Burgers, P.M.J. et al. Eukaryotic DNA polymerases: Proposal for a revised nomenclature. *Journal of Biological Chemistry* **276**, 43487-43490 (2001).
40. O'Donnell, M. Replisome architecture and dynamics in Escherichia coli. *Journal of Biological Chemistry* **281**, 10653-10656 (2006).
41. Guo, D.Y., Wu, X.H., Rajpal, D.K., Taylor, J.S. & Wang, Z.G. Translesion synthesis by yeast DNA polymerase zeta from templates containing lesions of ultraviolet radiation and acetylaminofluorene. *Nucleic Acids Research* **29**, 2875-2883 (2001).
42. Sobol, R.W. & Wilson, S.H. Mammalian DNA beta-polymerase in base excision repair of alkylation damage. *Prog Nucleic Acid Res Mol Biol* **68**, 57-74 (2001).
43. Doublet, S. & Ellenberger, T. The mechanism of action of T7 DNA polymerase. *Current Opinion in Structural Biology* **8**, 704-712 (1998).
44. Doublet, S., Tabor, S., Long, A.M., Richardson, C.C. & Ellenberger, T. Crystal structure of a bacteriophage T7 DNA replication complex at 2.2 angstrom resolution. *Nature* **391**, 251-258 (1998).
45. Kiefer, J.R., Mao, C., Braman, J.C. & Beese, L.S. Visualizing DNA replication in a catalytically active Bacillus DNA polymerase crystal. *Nature* **391**, 304-307 (1998).
46. Li, Y., Korolev, S. & Waksman, G. Crystal structures of open and closed forms of binary and ternary complexes of the large fragment of Thermus aquaticus DNA polymerase I: structural basis for nucleotide incorporation. *Embo Journal* **17**, 7514-7525 (1998).
47. Doublet, S., Sawaya, M.R. & Ellenberger, T. An open and closed case for all polymerases. *Structure with Folding & Design* **7**, R31-R35 (1999).
48. Franklin, M.C., Wang, J. & Steitz, T.A. Structure of the replicating complex of a pol alpha family DNA polymerase. *Cell* **105**, 657-67 (2001).
49. Hogg, M., Wallace, S.S. & Doublet, S. Crystallographic snapshots of a replicative DNA polymerase encountering an abasic site. *Embo Journal* **23**, 1483-1493 (2004).

50. Trincão, J. et al. Structure of the catalytic core of *S-cerevisiae* DNA polymerase ϵ : Implications for translesion DNA synthesis. *Molecular Cell* **8**, 417-426 (2001).
51. Brautigam, C.A. & Steitz, T.A. Structural and functional insights provided by crystal structures of DNA polymerases and their substrate complexes. *Current Opinion in Structural Biology* **8**, 54-63 (1998).
52. Hubscher, U., Maga, G. & Spadari, S. Eukaryotic DNA polymerases. *Annual Review of Biochemistry* **71**, 133-163 (2002).
53. Frick, D.N. & Richardson, C.C. DNA primases. *Annual Review of Biochemistry* **70**, 39-80 (2001).
54. Burgers, P.M.J. Eukaryotic DNA polymerases in DNA replication and DNA repair. *Chromosoma* **107**, 218-227 (1998).
55. Burgers, P.M.J. & Gerik, K.J. Structure and processivity of two forms of *Saccharomyces cerevisiae* DNA polymerase δ . *Journal of Biological Chemistry* **273**, 19756-19762 (1998).
56. Pursell, Z.F., Isoz, I., Lundstrom, E.B., Johansson, E. & Kunkel, T.A. Yeast DNA polymerase ϵ participates in leading-strand DNA replication. *Science* **317**, 127-130 (2007).
57. Swan, M.K., Johnson, R.E., Prakash, L., Prakash, S. & Aggarwal, A.K. Structural basis of high-fidelity DNA synthesis by yeast DNA polymerase δ . *Nature Structural & Molecular Biology* **16**, 979-U107 (2009).
58. Johnson, S.J. & Beese, L.S. Structures of mismatch replication errors observed in a DNA polymerase. *Cell* **116**, 803-816 (2004).
59. Hsu, G.W., Huang, X.W., Luneva, N.P., Geacintov, N.E. & Beese, L.S. Structure of a high fidelity DNA polymerase bound to a benzo[a]pyrene adduct that blocks replication. *Journal of Biological Chemistry* **280**, 3764-3770 (2005).
60. Hsu, G.W., Ober, M., Carell, T. & Beese, L.S. Error-prone replication of oxidatively damaged DNA by a high-fidelity DNA polymerase. *Nature* **431**, 217-221 (2004).
61. Hsu, G.W. et al. Observing translesion synthesis of an aromatic amine DNA adduct by a high-fidelity DNA polymerase. *Journal of Biological Chemistry* **279**, 50280-50285 (2004).

62. Li, Y. et al. Nucleotide insertion opposite a cis-syn thymine dimer by a replicative DNA polymerase from bacteriophage T7. *Nature Structural & Molecular Biology* **11**, 784-790 (2004).
63. Warren, J.J., Forsberg, L.J. & Beese, L.S. The structural basis for the mutagenicity of O-6-methyl-guanine lesions. *Proceedings of the National Academy of Sciences of the United States of America* **103**, 19701-19706 (2006).
64. Brieba, L.G. et al. Structural basis for the dual coding potential of 8-oxoguanosine by a high-fidelity DNA polymerase. *Embo Journal* **23**, 3452-3461 (2004).
65. Washington, M.T. et al. Efficient and error-free replication past a minor-groove DNA adduct by the sequential action of human DNA polymerases iota and kappa. *Molecular and Cellular Biology* **24**, 5687-5693 (2004).
66. Haracska, L. et al. Roles of yeast DNA polymerases delta and zeta and of Rev1 in the bypass of abasic sites. *Genes & Development* **15**, 945-954 (2001).
67. Nair, D.T., Johnson, R.E., Prakash, L., Prakash, S. & Aggarwal, A.K. Rev1 employs a novel mechanism of DNA synthesis using a protein template. *Science* **309**, 2219-2222 (2005).
68. Ogi, T., Shinkai, Y., Tanaka, K. & Ohmori, H. Pol kappa protects mammalian cells against the lethal and mutagenic effects of benzo[a]pyrene. *Proceedings of the National Academy of Sciences of the United States of America* **99**, 15548-15553 (2002).
69. Takenaka, K. et al. Involvement of vertebrate Pol kappa in translesion DNA synthesis across DNA monoalkylation damage. *Journal of Biological Chemistry* **281**, 2000-2004 (2006).
70. Avkin, S. et al. Quantitative analysis of translesion DNA synthesis across a benzo[a] pyrene-guanine adduct in mammalian cells - The role of DNA polymerase kappa. *Journal of Biological Chemistry* **279**, 53298-53305 (2004).
71. Washington, M.T. et al. Efficient and error-free replication past a minor-groove N-2-guanine adduct by the sequential action of yeast Rev1 and DNA polymerase zeta. *Molecular and Cellular Biology* **24**, 6900-6906 (2004).

72. Washington, M.T., Johnson, R.E., Prakash, L. & Prakash, S. Human DINB1-encoded DNA polymerase kappa is a promiscuous extender of mispaired primer termini. *Proceedings of the National Academy of Sciences of the United States of America* **99**, 1910-1914 (2002).
73. Haracska, L., Prakash, L. & Prakash, S. Role of human DNA polymerase kappa as an extender in translesion synthesis. *Proceedings of the National Academy of Sciences of the United States of America* **99**, 16000-16005 (2002).
74. Haracska, L., Prakash, S. & Prakash, L. Yeast DNA polymerase xi is an efficient extender of primer ends opposite from 7,8-dihydro-8-oxoguanine and O-6-methylguanine. *Molecular and Cellular Biology* **23**, 1453-1459 (2003).
75. Washington, M.T., Johnson, R.E., Prakash, S. & Prakash, L. Accuracy of thymine-thymine dimer bypass by *Saccharomyces cerevisiae* DNA polymerase eta. *Proceedings of the National Academy of Sciences of the United States of America* **97**, 3094-3099 (2000).
76. Washington, M.T., Johnson, R.E., Prakash, S. & Prakash, L. Fidelity and processivity of *Saccharomyces cerevisiae* DNA polymerase eta. *Journal of Biological Chemistry* **274**, 36835-36838 (1999).
77. Lone, S. et al. Human DNA polymerase kappa encircles DNA: Implications for mismatch extension and lesion bypass. *Molecular Cell* **25**, 601-614 (2007).
78. Nair, D.T., Johnson, R.E., Prakash, S., Prakash, L. & Aggarwal, A.K. Replication by human DNA polymerase-iota occurs by Hoogsteen base-pairing. *Nature* **430**, 377-380 (2004).
79. Yu, S.L., Johnson, R.E., Prakash, S. & Prakash, L. Requirement of DNA polymerase eta for error-free bypass of UV-induced CC and TC photoproducts. *Molecular and Cellular Biology* **21**, 185-188 (2001).
80. Johnson, R.E., Prakash, S. & Prakash, L. Efficient bypass of a thymine-thymine dimer by yeast DNA polymerase, Pol eta. *Science* **283**, 1001-1004 (1999).
81. McDonald, J.P., Levine, A.S. & Woodgate, R. The *Saccharomyces cerevisiae* RAD30 gene, a homologue of *Escherichia coli* dinB and umuC, is DNA damage inducible and functions in a novel error-free postreplication repair mechanism. *Genetics* **147**, 1557-1568 (1997).

82. Roush, A.A., Suarez, M., Friedberg, E.C., Radman, M. & Siede, W. Deletion of the *Saccharomyces cerevisiae* gene RAD30 encoding an *Escherichia coli* DinB homolog confers UV radiation sensitivity and altered mutability. *Molecular and General Genetics* **257**, 686-692 (1998).
83. Masutani, C. et al. The XPV (xeroderma pigmentosum variant) gene encodes human DNA polymerase eta. *Nature* **399**, 700-704 (1999).
84. Johnson, R.E., Kondratyck, C.M., Prakash, S. & Prakash, L. hRAD30 mutations in the variant form of xeroderma pigmentosum. *Science* **285**, 263-265 (1999).
85. Pabla, R., Rozario, D. & Siede, W. Regulation of *Saccharomyces cerevisiae* DNA polymerase eta transcript and protein. *Environmental and Molecular Mutagenesis* **48**, 601-601 (2007).
86. Skoneczna, A., McIntyre, J., Skoneczny, M., Policinska, Z. & Sledziewska-Gojska, E. Polymerase eta is a short-lived, proteasomally degraded protein that is temporarily stabilized following UV irradiation in *Saccharomyces cerevisiae*. *Journal of Molecular Biology* **366**, 1074-1086 (2007).
87. Bassett, E. et al. The role of DNA polymerase eta in translesion synthesis past platinum-DNA adducts in human fibroblasts. *Cancer Research* **64**, 6469-6475 (2004).
88. Lee, D.H. & Pfeifer, G.P. Translesion synthesis of 7,8-dihydro-8-oxo-2'-deoxyguanosine by DNA polymerase eta in vivo. *Mutation Research-Fundamental and Molecular Mechanisms of Mutagenesis* **641**, 19-26 (2008).
89. Haracska, L., Yu, S.L., Johnson, R.E., Prakash, L. & Prakash, S. Efficient and accurate replication in the presence of 7,8-dihydro-8-oxoguanine by DNA polymerase eta. *Nature Genetics* **25**, 458-461 (2000).
90. Carlson, K.D. & Washington, A.T. Mechanism of efficient and accurate nucleotide incorporation opposite 7,8-dihydro-8-oxoguanine by *Saccharomyces cerevisiae* DNA polymerase eta. *Molecular and Cellular Biology* **25**, 2169-2176 (2005).
91. Minko, I.G., Washington, M.T., Prakash, L., Prakash, S. & Lloyd, R.S. Translesion DNA synthesis by yeast DNA polymerase eta on templates containing N-2-guanine adducts of 1,3-butadiene metabolites. *Journal of Biological Chemistry* **276**, 2517-2522 (2001).

92. Rechko, O. et al. trans-lesion synthesis past bulky benzo[a]pyrene diol epoxide N-2-dG and N-6-dA lesions catalyzed by DNA bypass polymerases. *Journal of Biological Chemistry* **277**, 30488-30494 (2002).
93. Johnson, R.E., Haracska, L., Prakash, S. & Prakash, L. Role of DNA polymerase eta in the bypass of a (6-4) TT photoproduct. *Molecular and Cellular Biology* **21**, 3558-3563 (2001).
94. Moran, S., Ren, R.X.F. & Kool, E.T. A thymidine triphosphate shape analog lacking Watson-Crick pairing ability is replicated with high sequence selectivity. *Proceedings of the National Academy of Sciences of the United States of America* **94**, 10506-10511 (1997).
95. Kondratyck, C.M., Washington, M.T., Prakash, S. & Prakash, L. Acidic residues critical for the activity and biological function of yeast DNA polymerase eta. *Molecular and Cellular Biology* **21**, 2018-2025 (2001).
96. Haracska, L., Kondratyck, C.M., Unk, I., Prakash, S. & Prakash, L. Interaction with PCNA is essential for yeast DNA polymerase eta function. *Molecular Cell* **8**, 407-415 (2001).
97. Bienko, M. et al. Ubiquitin-binding domains in Y-family polymerases regulate translesion synthesis. *Science* **310**, 1821-1824 (2005).
98. Zhuang, Z. & Ai, Y. Processivity factor of DNA polymerase and its expanding role in normal and translesion DNA synthesis. *Biochim Biophys Acta* (2009).
99. Kong, X.P., Onrust, R., O'Donnell, M. & Kuriyan, J. 3-Dimensional Structure of the Beta-Subunit of Escherichia-Coli DNA Polymerase-Iii Holoenzyme - a Sliding DNA Clamp. *Cell* **69**, 425-437 (1992).
100. Matsumiya, S., Ishino, Y. & Morikawa, K. Crystal structure of an archaeal DNA sliding clamp: Proliferating cell nuclear antigen from *Pyrococcus furiosus*. *Protein Science* **10**, 17-23 (2001).
101. Williams, G.J. et al. Structure of the heterotrimeric PCNA from *Sulfolobus solfataricus*. *Acta Crystallographica Section F-Structural Biology and Crystallization Communications* **62**, 944-948 (2006).
102. Gulbis, J.M., Kelman, Z., Hurwitz, J., O'Donnell, M. & Kuriyan, J. Structure of the C-terminal region of p21(WAF1/CIP1) complexed with human PCNA. *Cell* **87**, 297-306 (1996).

103. Krishna, T.S.R., Kong, X.P., Gary, S., Burgers, P.M. & Kuriyan, J. Crystal-Structure of the Eukaryotic DNA-Polymerase Processivity Factor PcnA. *Cell* **79**, 1233-1243 (1994).
104. Naryzhny, S.N. Proliferating cell nuclear antigen: a proteomics view. *Cellular and Molecular Life Sciences* **65**, 3789-3808 (2008).
105. Miyachi, K., Fritzler, M.J. & Tan, E.M. Autoantibody to a Nuclear Antigen in Proliferating Cells. *Journal of Immunology* **121**, 2228-2234 (1978).
106. Bravo, R., Fey, S.J., Bellatin, J., Larsen, P.M. & Celis, J.E. Identification of a nuclear polypeptide ("cyclin") whose relative proportion is sensitive to changes in the rate of cell proliferation and to transformation. *Prog Clin Biol Res* **85 Pt A**, 235-48 (1982).
107. Ayyagari, R., Impellizzeri, K.J., Yoder, B.L., Gary, S.L. & Burgers, P.M.J. A Mutational Analysis of the Yeast Proliferating Cell Nuclear Antigen Indicates Distinct Roles in DNA-Replication and DNA-Repair. *Molecular and Cellular Biology* **15**, 4420-4429 (1995).
108. Prelich, G. et al. Functional Identity of Proliferating Cell Nuclear Antigen and a DNA Polymerase-Delta Auxiliary Protein. *Nature* **326**, 517-520 (1987).
109. Tanno, M., Ogihara, M. & Taguchi, T. Age-related changes in proliferating cell nuclear antigen levels. *Mechanisms of Ageing and Development* **92**, 53-66 (1996).
110. Bravo, R. & Celis, J.E. Up-Dated Catalog of HeLa-Cell Proteins - Percentages and Characteristics of the Major Cell Polypeptides Labeled with a Mixture of 16 C-14-Labeled Amino-Acids. *Clinical Chemistry* **28**, 766-& (1982).
111. Sakurai, S. et al. Structural basis for recruitment of human flap endonuclease 1 to PCNA. *Embo Journal* **24**, 683-693 (2005).
112. Bruning, J.B. & Shamo, Y. Structural and thermodynamic analysis of human PCNA with peptides derived from DNA polymerase-delta p66 subunit and flap endonuclease-1. *Structure* **12**, 2209-2219 (2004).
113. Hishiki, A. et al. Structural Basis for Novel Interactions between Human Translesion Synthesis Polymerases and Proliferating Cell Nuclear Antigen. *Journal of Biological Chemistry* **284**, 10552-10560 (2009).

114. Schmidt, S.L.G., Gomes, X.V. & Burgers, P.M.J. ATP utilization by yeast replication factor C III. The ATP-binding domains of Rfc2, Rfc3, and Rfc4 are essential for DNA recognition and clamp loading. *Journal of Biological Chemistry* **276**, 34784-34791 (2001).
115. Bowman, G.D., O'Donnell, M. & Kuriyan, J. Structural analysis of a eukaryotic sliding DNA clamp-clamp loader complex. *Nature* **429**, 724-730 (2004).
116. Johnson, A., Yao, N.Y., Bowman, G.D., Kuriyan, J. & O'Donnell, M. The replication factor C clamp loader requires arginine finger sensors to drive DNA binding and proliferating cell nuclear antigen loading. *Journal of Biological Chemistry* **281**, 35531-35543 (2006).
117. Miyata, T. et al. Open clamp structure in the clamp-loading complex visualized by electron microscopic image analysis. *Proceedings of the National Academy of Sciences of the United States of America* **102**, 13795-13800 (2005).
118. Zhuang, Z.H., Yoder, B.L., Burgers, P.M.J. & Benkovic, S.J. The structure of a ring-opened proliferating cell nuclear antigen-replication factor C complex revealed by fluorescence energy transfer. *Proceedings of the National Academy of Sciences of the United States of America* **103**, 2546-2551 (2006).
119. Kazmirski, S.L., Zhao, Y.X., Bowman, G.D., O'Donnell, M. & Kuriyan, J. Out-of-plane motions in open sliding clamps: Molecular dynamics simulations of eukaryotic and archaeal proliferating cell nuclear antigen. *Proceedings of the National Academy of Sciences of the United States of America* **102**, 13801-13806 (2005).
120. Jonsson, Z.O., Hindges, R. & Hubscher, U. Regulation of DNA replication and repair proteins through interaction with the front side of proliferating cell nuclear antigen. *Embo Journal* **17**, 2412-2425 (1998).
121. Maga, G. & Hubscher, U. Proliferating cell nuclear antigen (PCNA): a dancer with many partners. *Journal of Cell Science* **116**, 3051-3060 (2003).
122. Moldovan, G.L., Pfander, B. & Jentsch, S. PCNA, the maestro of the replication fork. *Cell* **129**, 665-679 (2007).
123. Castrec, B. et al. Binding to PCNA in Euryarchaeal DNA Replication Requires Two PIP Motifs for DNA Polymerase D and One PIP Motif for DNA Polymerase B. *Journal of Molecular Biology* **394**, 209-218 (2009).

124. Ben-Shahar, T.R. et al. Two Fundamentally Distinct PCNA Interaction Peptides Contribute to Chromatin Assembly Factor 1 Function. *Molecular and Cellular Biology* **29**, 6353-6365 (2009).
125. Haracska, L. et al. Physical and functional interactions of human DNA polymerase eta with PCNA. *Molecular and Cellular Biology* **21**, 7199-7206 (2001).
126. Haracska, L. et al. Targeting of human DNA polymerase iota to the replication machinery via interaction with PCNA. *Proceedings of the National Academy of Sciences of the United States of America* **98**, 14256-14261 (2001).
127. Vidal, A.E. et al. Proliferating cell nuclear antigen-dependent coordination of the biological functions of human DNA polymerase iota. *Journal of Biological Chemistry* **279**, 48360-48368 (2004).
128. Ogi, T., Kannouche, P. & Lehmann, A.R. Localisation of human Y-family DNA polymerase kappa: relationship to PCNA foci. *Journal of Cell Science* **118**, 129-136 (2005).
129. Lopez de Saro, F.J. Regulation of Interactions with Sliding Clamps During DNA Replication and Repair. *Current Genomics* **10**, 206-215 (2009).
130. Chilkova, O. et al. The eukaryotic leading and lagging strand DNA polymerases are loaded onto primer-ends via separate mechanisms but have comparable processivity in the presence of PCNA. *Nucleic Acids Res* **35**, 6588-97 (2007).
131. Niimi, A., Suka, N., Harata, M., Kikuchi, A. & Mizuno, S. Co-localization of chicken DNA topoisomerase II alpha, but not beta, with sites of DNA replication and possible involvement of a C-terminal region of alpha through its binding to PCNA. *Chromosoma* **110**, 102-114 (2001).
132. Burgers, P.M.J. Polymerase Dynamics at the Eukaryotic DNA Replication Fork. *Journal of Biological Chemistry* **284**, 4041-4045 (2009).
133. Gomes, X.V. & Burgers, P.M.J. Two modes of FEN1 binding to PCNA regulated by DNA. *Embo Journal* **19**, 3811-3821 (2000).
134. Montecucco, A. et al. DNA ligase I is recruited to sites of DNA replication by an interaction with proliferating cell nuclear antigen: identification of a common targeting mechanism for the assembly of replication factories. *Embo Journal* **17**, 3786-3795 (1998).

135. Pascal, J.M., O'Brien, P.J., Tomkinson, A.E. & Ellenberger, T. Human DNA ligase I completely encircles and partially unwinds nicked DNA. *Nature* **432**, 473-478 (2004).
136. Chapados, B.R. et al. Structural basis for FEN-1 substrate specificity and PCNA-mediated activation in DNA replication and repair. *Cell* **116**, 39-50 (2004).
137. de Saro, F.J.L., Marinus, M.G., Modrich, P. & O'Donnell, M. The beta sliding clamp binds to multiple sites within MutL and MutS. *Journal of Biological Chemistry* **281**, 14340-14349 (2006).
138. Kleczkowska, H.E., Marra, G., Lettieri, T. & Jiricny, J. hMSH3 and hMSH6 interact with PCNA and colocalize with it to replication foci. *Genes & Development* **15**, 724-736 (2001).
139. Lee, S.D. & Alani, E. Analysis of interactions between mismatch repair initiation factors and the replication processivity factor PCNA. *Journal of Molecular Biology* **355**, 175-184 (2006).
140. Ko, R. & Bennett, S.E. Physical and functional interaction of human nuclear uracil-DNA glycosylase with proliferating cell nuclear antigen. *DNA Repair* **4**, 1421-1431 (2005).
141. Unk, I. et al. Stimulation of 3' \rightarrow 5' exonuclease and 3' \rightarrow 5' phosphodiesterase activities of yeast Apn2 by proliferating cell nuclear antigen. *Molecular and Cellular Biology* **22**, 6480-6486 (2002).
142. Kedar, P.S. et al. Direct interaction between mammalian DNA polymerase beta and proliferating cell nuclear antigen. *Journal of Biological Chemistry* **277**, 31115-31123 (2002).
143. Gary, R., Ludwig, D.L., Cornelius, H.L., MacInnes, M.A. & Park, M.S. The DNA repair endonuclease XPG binds to proliferating cell nuclear antigen (PCNA) and shares sequence elements with the PCNA binding regions of FEN-1 and cyclin-dependent kinase inhibitor p21. *Journal of Biological Chemistry* **272**, 24522-24529 (1997).
144. Waga, S., Hannon, G.J., Beach, D. & Stillman, B. The P21 Inhibitor of Cyclin-Dependent Kinases Controls DNA-Replication by Interaction with PcnA. *Nature* **369**, 574-578 (1994).
145. Zheleva, D.I. et al. A quantitative study of the in vitro binding of the C-terminal domain of p21 to PCNA: Affinity, stoichiometry, and thermodynamics. *Biochemistry* **39**, 7388-7397 (2000).

146. Rousseau, D. et al. Growth inhibition by CDK-cyclin and PCNA binding domains of p21 occurs by distinct mechanisms and is regulated by ubiquitin-proteasome pathway. *Oncogene* **18**, 4313-4325 (1999).
147. Prives, C. & Gottifredi, V. The p21 and PCNA partnership A new twist for an old plot. *Cell Cycle* **7**, 3840-3846 (2008).
148. Naryzhny, S.N. & Lee, H. The post-translational modifications of proliferating cell nuclear antigen - Acetylation, not phosphorylation, plays an important role in the regulation of its function. *Journal of Biological Chemistry* **279**, 20194-20199 (2004).
149. Haracska, L., Torres-Ramos, C.A., Johnson, R.E., Prakash, S. & Prakash, L. Opposing effects of ubiquitin conjugation and SUMO modification of PCNA on replicational bypass of DNA lesions in *Saccharomyces cerevisiae*. *Molecular and Cellular Biology* **24**, 4267-4274 (2004).
150. Hoegge, C., Pfander, B., Moldovan, G.L., Pyrowolakis, G. & Jentsch, S. RAD6-dependent DNA repair is linked to modification of PCNA by ubiquitin and SUMO. *Nature* **419**, 135-141 (2002).
151. Watts, F.Z. Sumoylation of PCNA: Wrestling with recombination at stalled replication forks. *DNA Repair* **5**, 399-403 (2006).
152. Papouli, E. et al. Crosstalk between SUMO and ubiquitin on PCNA is mediated by recruitment of the helicase Srs2p. *Molecular Cell* **19**, 123-133 (2005).
153. Parker, J.L. et al. SUMO modification of PCNA is controlled by DNA. *Embo Journal* **27**, 2422-2431 (2008).
154. Stelter, P. & Ulrich, H.D. Control of spontaneous and damage-induced mutagenesis by SUMO and ubiquitin conjugation. *Nature* **425**, 188-191 (2003).
155. Lehmann, A.R. Clubbing together on clamps: The key to translesion synthesis. *DNA Repair* **5**, 404-407 (2006).
156. Kannouche, P. et al. Domain structure, localization, and function of DNA polymerase eta, defective in xeroderma pigmentosum variant cells. *Genes & Development* **15**, 158-172 (2001).
157. Acharya, N. et al. Roles of PCNA-binding and ubiquitin-binding domains in human DNA polymerase eta in translesion DNA synthesis. *Proceedings of the National Academy of Sciences of the United States of America* **105**, 17724-17729 (2008).

158. McCulloch, S.D., Wood, A., Garg, P., Burgers, P.M.J. & Kunkel, T.A. Effects of accessory proteins on the bypass of a cis-syn thymine-thymine dimer by *Saccharomyces cerevisiae* DNA polymerase η . *Biochemistry* **46**, 8888-8896 (2007).
159. Maga, G. et al. 8-oxo-guanine bypass by human DNA polymerases in the presence of auxiliary proteins. *Nature* **447**, 606-+ (2007).
160. Kerscher, O., Felberbaum, R. & Hochstrasser, M. Modification of proteins by ubiquitin and ubiquitin-like proteins. *Annual Review of Cell and Developmental Biology* **22**, 159-180 (2006).
161. Bergink, S. & Jentsch, S. Principles of ubiquitin and SUMO modifications in DNA repair. *Nature* **458**, 461-467 (2009).
162. Lee, K.Y. & Myung, K.J. PCNA modifications for regulation of post-replication repair pathways. *Molecules and Cells* **26**, 5-11 (2008).
163. Jentsch, S., McGrath, J.P. & Varshavsky, A. The Yeast DNA-Repair Gene Rad6 Encodes a Ubiquitin-Conjugating Enzyme. *Nature* **329**, 131-134 (1987).
164. Broomfield, S., Chow, B.L. & Xiao, W. MMS2, encoding a ubiquitin-conjugating-enzyme-like protein, is a member of the yeast error-free postreplication repair pathway. *Proceedings of the National Academy of Sciences of the United States of America* **95**, 5678-5683 (1998).
165. Hofmann, R.M. & Pickart, C.M. Noncanonical MMS2-encoded ubiquitin-conjugating enzyme functions in assembly of novel polyubiquitin chains for DNA repair. *Cell* **96**, 645-653 (1999).
166. Ulrich, H.D. & Jentsch, S. Two RING finger proteins mediate cooperation between ubiquitin-conjugating enzymes in DNA repair. *Embo Journal* **19**, 3388-3397 (2000).
167. Kannouche, P.L., Wing, J. & Lehmann, A.R. Interaction of human DNA polymerase η with monoubiquitinated PCNA: A possible mechanism for the polymerase switch in response to DNA damage. *Molecular Cell* **14**, 491-500 (2004).
168. Soria, G., Podhajcer, O., Prives, C. & Gottifredi, V. P21(Cip1/WAF1) downregulation is required for efficient PCNA ubiquitination after UV irradiation. *Oncogene* **25**, 2829-2838 (2006).

169. Huttner, D. & Ulrich, H.D. Cooperation of replication protein A with the ubiquitin ligase Rad18 in DNA damage bypass. *Cell Cycle* **7**, 3629-3633 (2008).
170. Huang, T.T. et al. Regulation of monoubiquitinated PCNA by DUB autocleavage. *Nature Cell Biology* **8**, 339-U13 (2006).
171. Carlile, C.M., Pickart, C.M., Matunis, M.J. & Cohen, R.E. Synthesis of Free and Proliferating Cell Nuclear Antigen-bound Polyubiquitin Chains by the RING E3 Ubiquitin Ligase Rad5. *Journal of Biological Chemistry* **284**, 29326-29334 (2009).
172. Parker, J.L., Bielen, A.B., Dikic, I. & Ulrich, H.D. Contributions of ubiquitin- and PCNA-binding domains to the activity of polymerase ϵ in *Saccharomyces cerevisiae*. *Nucleic Acids Research* **35**, 881-889 (2007).
173. Garg, P. & Burgers, P.M. Ubiquitinated proliferating cell nuclear antigen activates translesion DNA polymerases ϵ and REV1. *Proceedings of the National Academy of Sciences of the United States of America* **102**, 18361-18366 (2005).
174. Haracska, L., Unk, I., Prakash, L. & Prakash, S. Ubiquitylation of yeast proliferating cell nuclear antigen and its implications for translesion DNA synthesis. *Proceedings of the National Academy of Sciences of the United States of America* **103**, 6477-6482 (2006).
175. Bomar, M.G., Pai, M.T., Tzeng, S.R., Li, S.S.C. & Zhou, P. Structure of the ubiquitin-binding zinc finger domain of human DNA γ -polymerase ϵ . *Embo Reports* **8**, 247-251 (2007).
176. Plosky, B.S. et al. Controlling the subcellular localization of DNA polymerases ι and ϵ via interactions with ubiquitin. *Embo Journal* **25**, 2847-2855 (2006).
177. van der Kemp, P.A., de Padula, M., Burguiere-Slezak, G., Ulrich, H.D. & Boiteux, S. PCNA monoubiquitylation and DNA polymerase ubiquitin-binding domain are required to prevent 8-oxoguanine-induced mutagenesis in *Saccharomyces cerevisiae*. *Nucleic Acids Research* **37**, 2549-2559 (2009).
178. Zhuang, Z.H. et al. Regulation of polymerase exchange between Pol ϵ and Pol δ by monoubiquitination of PCNA and the movement of DNA polymerase holoenzyme. *Proceedings of the National Academy of Sciences of the United States of America* **105**, 5361-5366 (2008).

179. Indiani, C., McInerney, P., Georgescu, R., Goodman, M.F. & O'Donnell, M. A sliding-clamp toolbelt binds high-and low-fidelity DNA polymerases simultaneously. *Molecular Cell* **19**, 805-815 (2005).
180. Bunting, K.A., Roe, S.M. & Pearl, L.H. Structural basis for recruitment of translesion DNA polymerase Pol IV/DinB to the beta-clamp. *Embo Journal* **22**, 5883-5892 (2003).
181. Lemontt, J.F. Mutants of Yeast Defective in Mutation Induced by Ultraviolet Light. *Genetics* **68**, 21-& (1971).
182. Nelson, J.R., Lawrence, C.W. & Hinkle, D.C. Deoxycytidyl transferase activity of yeast REV1 protein. *Nature* **382**, 729-731 (1996).
183. Morrison, A. et al. REV3, a *Saccharomyces cerevisiae* gene whose function is required for induced mutagenesis, is predicted to encode a nonessential DNA polymerase. *J Bacteriol* **171**, 5659-67 (1989).
184. Lawrence, C.W., Krauss, B.R. & Christensen, R.B. New mutations affecting induced mutagenesis in yeast. *Mutat Res* **150**, 211-6 (1985).
185. Lawrence, C.W., Das, G. & Christensen, R.B. REV7, a new gene concerned with UV mutagenesis in yeast. *Mol Gen Genet* **200**, 80-5 (1985).
186. Zhang, H.S., Gibbs, P.E.M. & Lawrence, C.W. The *Saccharomyces cerevisiae* rev6-1 mutation, which inhibits both the lesion bypass and the recombination mode of DNA damage tolerance, is an allele of POL30, encoding proliferating cell nuclear antigen. *Genetics* **173**, 1983-1989 (2006).
187. Northam, M.R., Garg, P., Baitin, D.M., Burgers, P.M.J. & Shcherbakova, P.V. A novel function of DNA polymerase zeta regulated by PCNA. *Embo Journal* **25**, 4316-4325 (2006).
188. Goodman, M.F. Error-prone repair DNA polymerases in prokaryotes and eukaryotes. *Annual Review of Biochemistry* **71**, 17-50 (2002).
189. Prakash, S. & Prakash, L. Translesion DNA synthesis in eukaryotes: A one- or two-polymerase affair. *Genes & Development* **16**, 1872-1883 (2002).
190. Washington, M.T., Prakash, L. & Prakash, S. Mechanism of nucleotide incorporation opposite a thymine-thymine dimer by yeast DNA polymerase eta. *Proceedings of the National Academy of Sciences of the United States of America* **100**, 12093-12098 (2003).

191. Johnson, R.E., Prakash, S. & Prakash, L. Requirement of DNA polymerase activity of yeast Rad30 protein for its biological function. *Journal of Biological Chemistry* **274**, 15975-15977 (1999).
192. Nelson, J.R., Lawrence, C.W. & Hinkle, D.C. Thymine-thymine dimer bypass by yeast DNA polymerase zeta. *Science* **272**, 1646-9 (1996).
193. Johnson, R.E., Washington, M.T., Haracska, L., Prakash, S. & Prakash, L. Eukaryotic polymerases iota and zeta act sequentially to bypass DNA lesions. *Nature* **406**, 1015-1019 (2000).
194. Lawrence, C.W. Cellular roles of DNA polymerase zeta and Rev1 protein. *DNA Repair* **1**, PII S1568-7864(02)00038-1 (2002).
195. Gibbs, P.E.M., McGregor, W.G., Maher, V.M., Nisson, P. & Lawrence, C.W. A human homolog of the *Saccharomyces cerevisiae* REV3 gene, which encodes the catalytic subunit of DNA polymerase zeta. *Proceedings of the National Academy of Sciences of the United States of America* **95**, 6876-6880 (1998).
196. Hingorani, M.M. & O'Donnell, M. Sliding clamps: A (tail)ored fit. *Current Biology* **10**, R25-R29 (2000).
197. Garg, P., Stith, C.M., Majka, J. & Burgers, P.M.J. Proliferating cell nuclear antigen promotes translesion synthesis by DNA polymerase zeta. *Journal of Biological Chemistry* **280**, 23446-23450 (2005).
198. Washington, M.T., Prakash, L. & Prakash, S. Yeast DNA polymerase eta utilizes an induced-fit mechanism of nucleotide incorporation. *Cell* **107**, 917-927 (2001).
199. Pflugrath, J.W. The finer things in X-ray diffraction data collection. *Acta Crystallographica Section D-Biological Crystallography* **55**, 1718-1725 (1999).
200. Read, R.J. Pushing the boundaries of molecular replacement with maximum likelihood. *Acta Crystallographica Section D-Biological Crystallography* **57**, 1373-1382 (2001).
201. Adams, P.D. et al. PHENIX: building new software for automated crystallographic structure determination. *Acta Crystallographica Section D-Biological Crystallography* **58**, 1948-1954 (2002).
202. Emsley, P. & Cowtan, K. Coot: model-building tools for molecular graphics. *Acta Crystallographica Section D-Biological Crystallography* **60**, 2126-2132 (2004).

203. Tsurimoto, T. PCNA binding proteins. *Frontiers in Bioscience* **4**, d849-858 (1999).
204. Mossi, R. & Hubscher, U. Clamping down on clamps and clamp loaders - The eukaryotic replication factor C. *European Journal of Biochemistry* **254**, 209-216 (1998).
205. Majka, J. & Burgers, P.M.J. The PCNA-RFC families of DNA clamps and clamp loaders. *Progress in Nucleic Acid Research and Molecular Biology, Vol 78* **78**, 227-260 (2004).
206. Indiani, C. & O'Donnell, M. The replication clamp-loading machine at work in the three domains of life. *Nature Reviews Molecular Cell Biology* **7**, 751-761 (2006).
207. Hingorani, M.M. & O'Donnell, M. DNA polymerase structure and mechanisms of action. *Current Organic Chemistry* **4**, 887-913 (2000).
208. Freudenthal, B.D., Ramaswamy, S., Hingorani, M.M. & Washington, M.T. Structure of a Mutant Form of Proliferating Cell Nuclear Antigen That Blocks Translesion DNA Synthesis. *Biochemistry* **47**, 13354-13361 (2008).
209. Dasgupta, S., Iyer, G.H., Bryant, S.H., Lawrence, C.E. & Bell, J.A. Extent and nature of contacts between protein molecules in crystal lattices and between subunits of protein oligomers. *Proteins-Structure Function and Genetics* **28**, 494-514 (1997).
210. Matsumiya, S., Ishino, S., Ishino, Y. & Morikawa, K. Intermolecular ion pairs maintain the toroidal structure of *Pyrococcus furiosus* PCNA. *Protein Science* **12**, 823-831 (2003).
211. Zhang, P., Zhang, S.J., Zhang, Z., Woessner, J.F. & Lee, M. Expression and Physicochemical Characterization of Human Proliferating Cell Nuclear Antigen. *Biochemistry* **34**, 10703-10712 (1995).
212. Prakash, S., Sung, P. & Prakash, L. DNA-Repair Genes and Proteins of *Saccharomyces-Cerevisiae*. *Annual Review of Genetics* **27**, 33-70 (1993).
213. Bailey, M.A. et al. ETA receptor-mediated Ca²⁺ signaling in thin descending limbs of Henle's loop: Impairment in genetic hypertension. *Kidney International* **63**, 1276-1284 (2003).
214. Freudenthal, B.D., Gakhar, L., Ramaswamy, S. & Washington, M.T. A charged residue at the subunit interface of PCNA promotes trimer formation by destabilizing alternate subunit interactions. *Acta Crystallographica Section D-Biological Crystallography* **65**, 560-566 (2009).

215. Nelson, J.R., Lawrence, C.W. & Hinkle, D.C. Thymine-thymine dimer bypass by yeast DNA polymerase zeta. *Science* **272**, 1646-1649 (1996).
216. Lawrence, C.W. Cellular functions of DNA polymerase zeta and Rev1 protein. *DNA Repair and Replication* **69**, 167-203 (2004).
217. Guo, C.X. et al. Ubiquitin-binding motifs in REV1 protein are required for its role in the tolerance of DNA damage. *Molecular and Cellular Biology* **26**, 8892-8900 (2006).
218. Bailey, S. The Ccp4 Suite - Programs for Protein Crystallography. *Acta Crystallographica Section D-Biological Crystallography* **50**, 760-763 (1994).
219. Blanc, E. et al. Refinement of severely incomplete structures with maximum likelihood in BUSTER-TNT. *Acta Crystallographica Section D-Biological Crystallography* **60**, 2210-2221 (2004).
220. Harel, M., Kleywegt, G.J., Ravelli, R.B.G., Silman, I. & Sussman, J.L. Crystal structure of an acetylcholinesterase-fasciculin complex: Interaction of a three-fingered toxin from snake venom with its target. *Structure* **3**, 1355-1366 (1995).
221. Iwata, S. et al. Complete structure of the 11-subunit bovine mitochondrial cytochrome bc(1) complex. *Science* **281**, 64-71 (1998).
222. Howell, C.A., Kondratyck, C.M. & Washington, M.T. Substitution of a residue contacting the triphosphate moiety of the incoming nucleotide increases the fidelity of yeast DNA polymerase zeta. *Nucleic Acids Research* **36**, 1731-1740 (2008).
223. Hurley, J.H., Lee, S. & Prag, G. Ubiquitin-binding domains. *Biochemical Journal* **399**, 361-372 (2006).
224. Hicke, L., Schubert, H.L. & Hill, C.P. Ubiquitin-binding domains. *Nature Reviews Molecular Cell Biology* **6**, 610-621 (2005).
225. Alt, A. et al. Bypass of DNA lesions generated during anticancer treatment with cisplatin by DNA polymerase. *Science* **318**, 967-970 (2007).
226. Haracska, L. et al. A single domain in human DNA polymerase iota mediates interaction with PCNA: implications for translesion DNA synthesis. *Molecular and Cellular Biology* **25**, 1183-1190 (2005).

227. Haracska, L. et al. Stimulation of DNA synthesis activity of human DNA polymerase kappa by PCNA. *Molecular and Cellular Biology* **22**, 784-791 (2002).
228. Kannouche, P. & Lehmann, A. Localization of Y-family polymerases and the DNA polymerase switch in mammalian cells. in *DNA Repair, Pt A*, Vol. 408 407-415 (Elsevier Academic Press Inc, San Diego, 2006).
229. Strang, B.L., Sinigalia, E., Silva, L.A., Coen, D.M. & Loregian, A. Analysis of the Association of the Human Cytomegalovirus DNA Polymerase Subunit UL44 with the Viral DNA Replication Factor UL84. *Journal of Virology* **83**, 7581-7589 (2009).
230. Appleton, B.A., Loregian, A., Filman, D.J., Coen, D.M. & Hogle, J.M. The cytomegalovirus DNA polymerase subunit UL44 forms a C clamp-shaped dimer. *Molecular Cell* **15**, 233-244 (2004).
231. McNally, R., Bowman, G.D., Goedken, E.R., O'Donnell, M. & Kuriyan, J. Analysis of the role of PCNA-DNA contacts during clamp loading. *BMC Struct Biol* **10**, 3.
232. Daikoku, T. et al. Architecture of replication compartments formed during Epstein-Barr virus lytic replication. *J Virol* **79**, 3409-18 (2005).
233. Bomar, M.G. et al. Unconventional ubiquitin recognition by the ubiquitin-binding motif within the Y family DNA polymerases iota and Rev1. *Mol Cell* **37**, 408-17.
234. Komander, D. et al. Molecular discrimination of structurally equivalent Lys 63-linked and linear polyubiquitin chains. *EMBO Rep* **10**, 466-73 (2009).
235. Weeks, S.D., Grasty, K.C., Hernandez-Cuebas, L. & Loll, P.J. Crystal structures of Lys-63-linked tri- and di-ubiquitin reveal a highly extended chain architecture. *Proteins* **77**, 753-9 (2009).
236. Notenboom, V. et al. Functional characterization of Rad18 domains for Rad6, ubiquitin, DNA binding and PCNA modification. *Nucleic Acids Research* **35**, 5819-5830 (2007).
237. Ohashi, E. et al. Interaction of hREV1 with three human Y-family DNA polymerases. *Genes to Cells* **9**, 523-531 (2004).